ENHANCED TOOLS TO MODEL PRELEUKEMIA TO LEUKEMIA TRANSFORMATION

by

Vinothkumar Rajan

Submitted in partial fulfilment of the requirements
for the degree of Doctor of Philosophy

at

Dalhousie University
Halifax, Nova Scotia
October 2019

Dedication

To my beloved Grandpa Veeraraghavan, who still continues to exist in my memory an inspiration and motivation.

This work will stay as an illustration of his inspiration.

Table of Contents

List of Tables

List of Figures

Abstract

Preleukemia to leukemia transformation is one of the least well-understood processes in the hematopoiesis field, which is in no small part due to the lack of models that faithfully recapitulate this phenomenon. In this thesis, I provide three novel model systems that help to elucidate crucial factors that contribute to leukemia progression.

First, I developed a zebrafish model that expresses human hematopoietic cytokines, which critically preserves the clonal diversity present in the original patient-derived leukemia. These human cytokine fish enhance the self-renewal capacity of transplanted human hematopoietic stem cells and also lead to multi-lineage differentiation.

Secondly, I developed a *tet2* loss-of-function zebrafish to mimic clonal hematopoiesis. TET2 mutations are seen in older individuals and significantly increases the chance of acquiring leukemia. I observed that tet2-deficient zebrafish had restrictive hematopoiesis resulting in fewer cells across multiple blood lineages. Induction of emergency hematopoiesis in these zebrafish resulted in a proliferative phenotype with increased blasts and progenitors. A key translational finding from the tet2 zebrafish is that growth factor treatment may accelerate leukemia in the subset of patients with acute myeloid leukemia and a TET2 mutation.

Finally, I examined the KIT D816V mutation commonly seen in a preleukemic neoplasm called systemic mastocytosis, which can evolve into aggressive mast cell leukemia. Upon examination of the mutant D816V KIT receptor, I discovered that dimerization does not occur as it does in the wild type in the presence of ligand and downstream signalling is activated independently of dimerization. Phosphoproteome analysis highlighted increased activity of the pro-survival mTOR axis, revealing that mTOR inhibiting agents (rapamycin and its analogues) may have a previously unrecognized therapeutic benefit in preleukemic conditions associated with mutant KIT.

These models will provide useful preclinical tools for a future candidate and unbiased drug screens to identify prospective drugs and effective drug combinations to improve the outcome of human preleukemic diseases.

List of Abbreviations Used

Abbreviations

7AAD	Amino actinomycin D
AGM	aorta gonad-mesonephros
ALL	acute lymphoblastic leukemia
ALM	anterior lateral mesoderm
AML	acute myeloid leukemia
ANOVA	analysis of variance
araC	cytarabine
BSA	bovine serum albumin
Cas9	CRISPR associated protein 9
ChIP	chromatin immunoprecipitation
CHT	caudal hematopoietic tissue
CML	chronic myelogenous leukemia
CMP	common myeloid progenitor
CMTMR	Cell Tracker Orange dye
COG	Children's Oncology Group
CRISPR	clustered regularly interspersed short palindromic repeats
DA	dorsal aorta
DNA	deoxyribonucleic acid
DNMT	DNA (cytosine-5)-methyltransferase
DMSO	Dimethyl sulfoxide
eGFP	Enhanced green fluorescent protein

EMP	erythro-myeloid progenitor
FACS	fluorescently activated cell sorting
FBS	fetal bovine serum
FDR	false discovery rate
FITC	fluorescein isothiocyanate
FL	fetal liver
FSC	forward scatter
gDNA	genomic DNA
GMP	granulocyte monocyte progenitor
HOX	homeobox
HSC	hematopoietic stem cell
ICM	intermediate cell mass
KIT	KIT proto-oncogene receptor tyrosine kinase
KO	knockout
MDS	myelodysplastic syndrome
MEP	megakaryocyte erythroid progenitor
ML-DS	Myeloid leukemia of Down Syndrome
MPN	myeloproliferative neoplasm
MPP	multi-potent progenitor
mRNA	messenger RNA
PB	peripheral blood
PBI	posterior blood island

PBS	phosphate-buffered saline
PCR	polymerase chain reaction
polyA	polyadenylation
qRT-PCR	quantitative reverse transcriptase PCR
RBC	red blood cell
RIPA	radioimmunoprecipitation
RNA	ribonucleic acid
RNA-seq	RNA sequencing
sgRNA	Single guide RNA
TAM	Transient Abnormal Myelopoiesis
tAML	treatment-related AML
ubi	ubiquitin C
WISH	whole-mount in situ hybridization
WKM	whole kidney marrow
WT	wild type

Acknowledgements

My first thanks would be to my Mom and Dad, without their sacrifice and understanding, I would never even made to graduate studies. Apart from them, the other most important person is my supervisor Dr. Jason Berman. Jason, over the years, has been an excellent mentor and supported me during the good and bad patches of my Ph.D.; the trust and confidence he had in me helped me think independently and develop my current projects. I am not sure if someone else would have given a graduate student this freedom to work and implement their own ideas, for which I am really grateful. Working with Jason was a learning experience, both personally and professionally.

My lab members over the years have been an essential part of my development. I would particularly like to thank Dr. Sergey Prykhozhij, who took me under his tutelage and have taught me plenty of things over the past few years. I always cherish the interactions that I have with him daily that empowered me to gain knowledge. Our research associate, Nicole Melong, has been a fantastic friend inside the lab, without her helping hands this work would not have been possible. I also like to thank the master's and honours students (Corey Filiaggi, Melissa Richardson, Benjamin King, Rachel Woodside and Daniel Liwiski) that I have had the opportunity to mentor over the years, my science did significantly increase by teaching them and helping them troubleshoot experiments. Our fish technician, Gretchen Wagner, was a great source of help managing the fish, without whom making all the transgenic and mutants presented in this work would have been difficult.

Most importantly, I like to thank my graduate committee members, Dr. Roy Duncan, Dr. Graham Dellaire, Dr. Jan Rainey, Dr. Christopher McMaster and Dr. Craig McCormick (past), their

constructive criticism and thoughts have contributed immensely towards both my science and personality. I would also like to thank Dr. Trista North to have gleefully accepted to be my external examiner and thus contribute towards my scientific journey.

My Ph.D. would have never been a success, without my friends and family. My wife, who endured the hardships of stressful times during the course of my Ph.D. with smiling face provided all the support that helped me encounter the next day with cheer. My friends provided an incredible support system continuously providing motivation after failed experiments.

Chapter 1 - Introduction

1.1 Preamble

Blood cells are present in all vertebrates, and most of the higher invertebrates; these cells are produced throughout the lifetime of an organism. Mature blood cells are the functional entity of the blood system performing divergent duties from transporting oxygen to antibody production; but, these cells are short-lived and need to be systematically replenished by new cells. Blood stem cells are a rare population of the blood system and reside protected in a particular niche and with the power to reproduce themselves and also produce the entire blood hierarchy. The process through which a blood stem cell produces mature blood cells by passing through multiple intermediate stages is called "hematopoiesis."

Stem cells are broadly classified into three types: the totipotent stem cells that can create the entire organism, pluripotent stem cells that have the potential to produce the ectoderm, endoderm, and mesoderm and a more lineage-restricted multipotent stem cell. The blood stem cells (called hematopoietic stem cells or HSCs) are multipotent, as they can produce the entire range of blood cells. HSCs were the first defined stem cell through a series of elegant studies (Becker, McCulloch, & Till, 1963; Siminovitch, McCulloch, & Till, 1963; Till & McCulloch, 1961; A. M. Wu, Till, Siminovitch, & McCulloch, 1968), and ever since have been the most extensively studied stem cells in the human body. HSCs have been used in allogeneic stem cell transplantation in clinical settings to treat aggressive hematological malignancies including leukemia, some non-hematological malignancies, and immune disorders ever since 1968 (Gatti, Meuwissen, Allen, Hong, & Good, 1968).

One of the limitations of HSC based therapy is the ability to find an Human Leukocyte Antigen (HLA)-matched donor. Umbilical cord blood provides an alternate source of HSCs and with a lesser stringency in HLA-matching. However, the number of HSCs from an umbilical cord is not sufficient to reconstitute the hematopoietic system of a typical adult recipient (Brown & Boussiotis, 2008). For the last decade, researchers have tried to address this limitation by finding small molecules that are capable of expanding HSCs *ex vivo* before allogeneic stem cell transplantation (Chagraoui et al., 2013; Cutler et al., 2013; North et al., 2007)

Secondly, since the HSCs survive and keep producing mature cells for the entire life of the organism, the probability of them acquiring a genotoxic genetic lesion increases with age leading to leukemia. The effect of an aging hematopoietic system can also lead to bias in differentiation, reduced potency of HSCs to self-renew and clonal-dominance due to an HSC clone holding growth advantage as a result of mutation. This process is referred to as "clonal hematopoiesis." In some instances, individuals with clonal hematopoiesis progress to develop malignancies, and this progression is at present not completely understood. The evolution towards a malignancy dramatically hastens in cases of underlying genetic predisposition that offers a permissive environment for the establishment of various blood disorders. The mechanistic details underlying the rapid onset of malignancy in most cases is not well understood.

The current thesis predominantly revolves around the above points. For this thesis, a general overview of various concepts in hematopoiesis will be discussed. There are some controversies in the field that need to be resolved, and in those cases, based on the available experimental

evidence, certain assumptions are made. Since the model of interest in this thesis is the zebrafish, there will be periodical references to zebrafish hematopoiesis and niches, explaining how certain factors and behaviour evolutionarily differ from their mammalian cousins. Specifically, in this thesis I create novel models to study preleukemia to leukemia transition events.

1.2 Hematopoiesis and hematopoietic ontogeny

Mammalian blood development is a dynamic process and involves a transition from one anatomic site to another during embryogenesis until this role is assumed by the bone marrow, which continues to be the site of hematopoiesis for the life of the organism. In mammals, hematopoiesis begins in the blood island of the yolk sac and sequentially travels to aorta-gonad mesonephros (AGM), the fetal liver and ultimately to the bone marrow (Orkin & Zon, 2008). In zebrafish, a similar sequential transition occurs, starting from the intermediate cell mass (ICM) of the yolk sack and anterior lateral mesoderm (ALM), before proceeding to AGM and then subsequently to the caudal hematopoietic tissue (CHT) and the kidney marrow (KM) (Orkin & Zon, 2008)(Figure 1). Vertebrate hematopoiesis is divided into two phases: primitive hematopoiesis and definitive hematopoiesis.

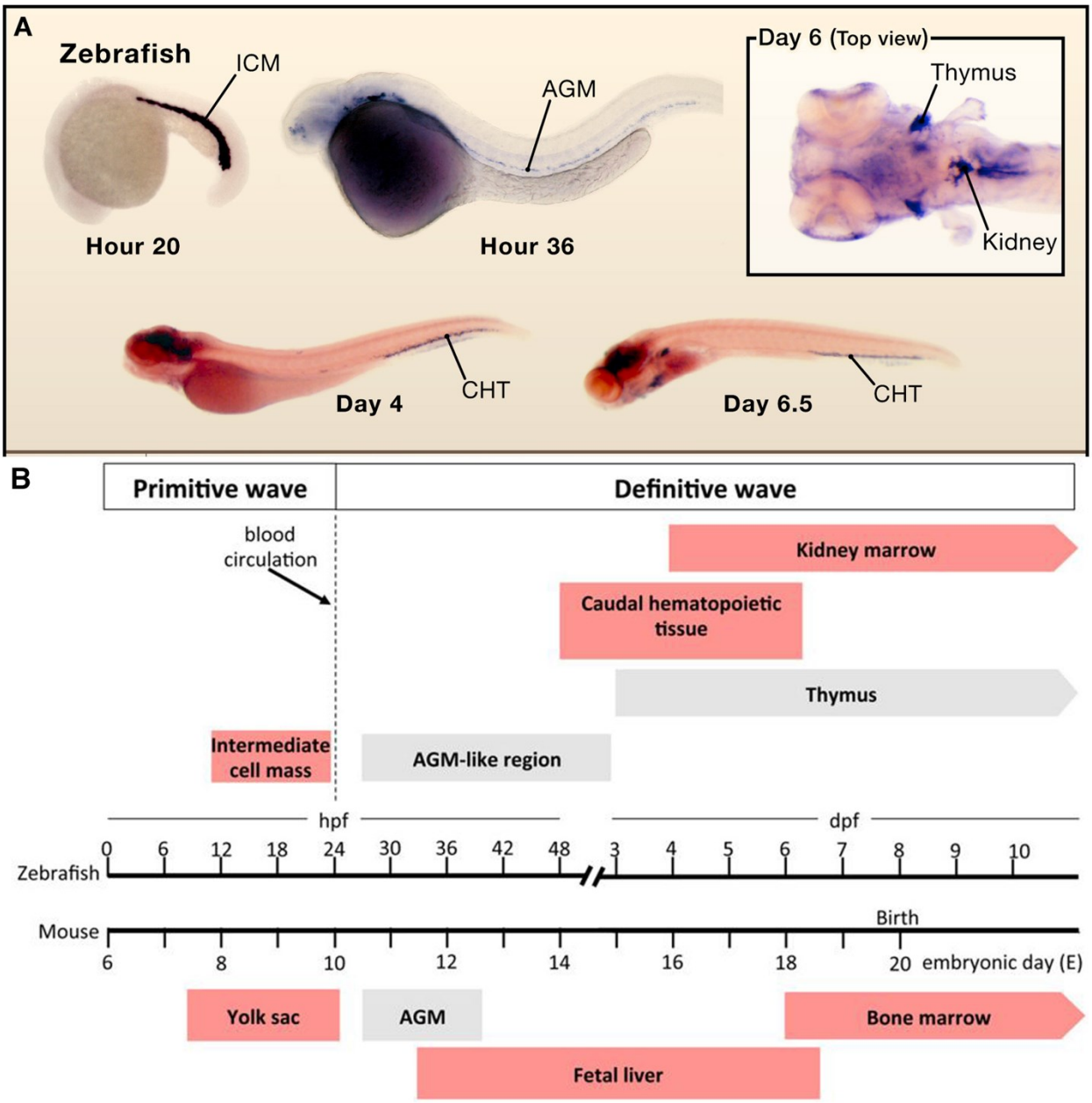

Figure 1: Sites of zebrafish hematopoiesis

A) Illustration of various sites of zebrafish hematopoiesis. Adapted: (Orkin & Zon, 2008)

B) Timeline of hematopoietic site transition in zebrafish and mice. Adapted: (Kulkeaw & Sugiyama, 2012). Reproduced under Creative Commons licence (CC 4.0).

Primitive Hematopoiesis

Primitive hematopoiesis is a term that corresponds to the blood development in the yolk sac (Golub & Cumano, 2013). During this wave of blood development, primitive blood precursors called erythro-myeloid precursors (EMPs) (Palis, Robertson, Kennedy, Wall, & Keller, 1999) originate from a common endothelial hematopoietic progenitor called the "hemangioblast." In zebrafish, hemangioblasts are cells localized in ICM that express the *stem cell leukemia* (*scl*) gene (Davidson & Zon, 2004).

The existence of hemangioblast as a cell that produces both hematopoietic and endothelial cells was confirmed using a variety of in vitro experiments (Choi, Kennedy, Kazarov, Papadimitriou, & Keller, 1998; Huber, Kouskoff, Joerg Fehling, Palis, & Keller, 2004). The ability of hemangioblasts to produce hematopoietic and blood cells was demonstrated in vivo in both zebrafish and Drosophila (Mandal, Banerjee, & Hartenstein, 2004; Vogeli, Jin, Martin, & Stainier, 2006), but in vivo experiments using both amphibian and mammalian models contradicted these findings. The murine lineage-tracing experiments have failed to provide any evidence of a hemangioblast producing both endothelial and hematopoietic cells in vivo (Lacaud & Kouskoff, 2017). The current argument is that the hemangioblast is a “state of competency” that might be restricted by growth factor signaling in vivo (Amaya, 2013). A series of experiments with amphibian models suggested hemangioblast cells that express both endothelial and hematopoietic markers only give rise to blood cells in vivo (C. T. Myers & Krieg, 2013). Furthermore, disrupting bone morphogenic and erythroid growth signals leads to the production of endothelial cells, suggesting

a clear role of microenvironmental factors in hemangioblast fate decisions (C. T. Myers & Krieg, 2013).

Despite all the controversies surrounding the bipotential fate of the hemangioblast, it is at least clear that it can produce EMPs, the hierarchically superior blood cell of primitive hematopoiesis. EMPs subsequently predominantly produces primitive erythrocytes, but also macrophages, megakaryocytes, and mast cells, albeit in small numbers (Perdiguero & Geissmann, 2015). The primitive erythrocytes help in oxygen transport for the rapidly growing embryo and at least in mammals can be easily distinguished from definitive erythrocytes by embryonic globin expression (Sankaran & Orkin, 2013). However, it is difficult to distinguish other lineages from their definitive hematopoiesis-derived counterparts. In zebrafish, the two sites of embryonic hematopoiesis are the intermediate cell mass (ICM) and the anterior lateral mesoderm (ALM), with each containing a bipotential hemangioblast population (Dooley, Davidson, & Zon, 2005) . The progenitors of ICM predominantly produce primitive erythrocytes and, less-frequently neutrophils. The ALM produces primitive macrophages that migrate to the rostral blood islands (RBI) and differentiate.

The two most controversial areas of primitive hematopoiesis are: (1) if there exists an HSC like cell upstream of the EMP that at least partially contribute to adult hematopoiesis in human and other model systems and (2) are the zebrafish ICM progenitors multipotent and if so, can they can give rise to primitive erythrocytes, neutrophils, thrombocytes, and lymphocytes? Some results support this notion (Warga, Kane, & Ho, 2009), while others contradict this idea (Le

Guyader et al., 2008). Unlike the murine system, the zebrafish field does not have an embryonic stem cell line that could help answer this enigma. However, with the advent of single-cell sequencing, the answer to this question might be near.

For this thesis, let us assume that in the zebrafish model during primitive hematopoiesis there is an scl+ hemangioblast population, that gives rise to a runx1+/gata1+ progenitor (EMP) that can subsequently give rise to primitive erythrocytes (gata1+/embryonic globin+), neutrophils (mpx+) and macrophages (mpeg+) (Figure 2).

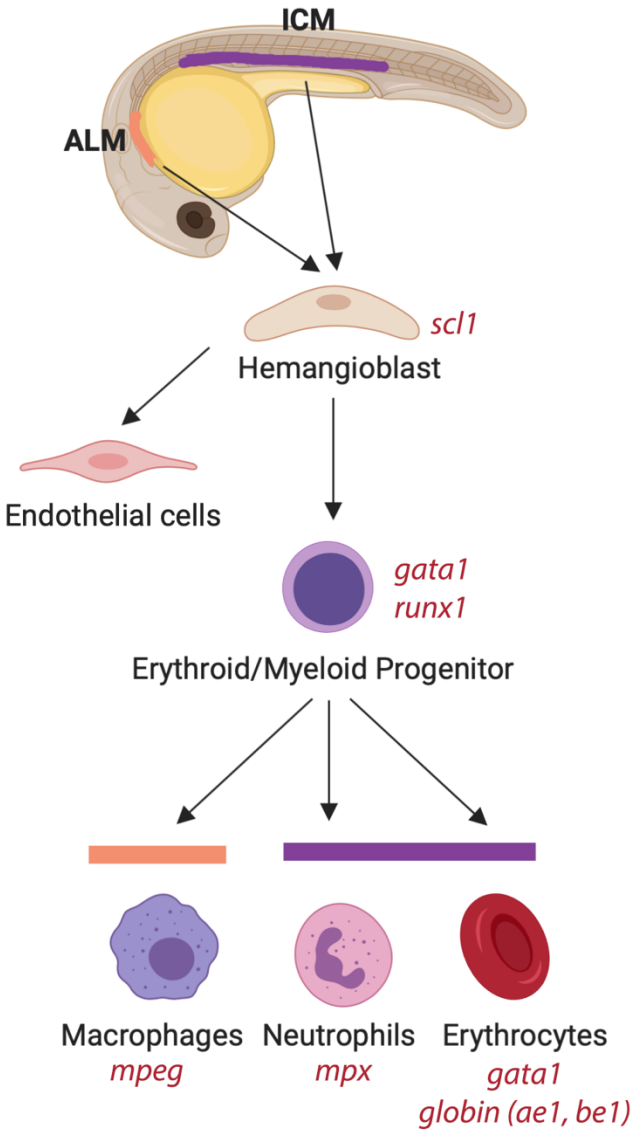

Figure 2: Primitive Hematopoiesis in Zebrafish

The blood cells contributing to primitive hematopoiesis originate from two sites: the ALM (Orange) and ICM (Purple). Both sites give rise to a biopotential cell called the hemangioblast that is capable of producing progenitors and mature cells. Experimentally, zebrafish hematopoiesis is studied using whole mount in situ hybridization (WISH); the probes used for this technique are labeled in red.

Definitive Hematopoiesis

Compared to primitive hematopoiesis, definitive hematopoiesis is well-studied. The so-called second wave of vertebrate hematopoiesis starts in the AGM region, following the rise of HSCs from the "hemogenic endothelium" present in the floor of the dorsal aorta. The hemogenic endothelium undergoes an endothelial-to-hematopoietic transition (EHT), producing HSCs (Eilken, Nishikawa, & Schroeder, 2009).

Even though both the hemangioblast and hemogenic endothelium are of endothelial origin, the cells of origin are distinct (M. J. Chen et al., 2011). The HSCs produced in the AGM move to the fetal liver in mammals. In zebrafish, HSCs move and repopulate the CHT, the zebrafish equivalent of the mammalian fetal liver (Murayama et al., 2006). Interestingly, primitive macrophages play an essential role in the mobilization of HSCs to the fetal liver/CHT by reconstructing the stroma through matrix metalloprotease-mediated extra cellular matric (ECM) degradation (Travnickova et al., 2015). HSCs start producing multipotent progenitors of all hematopoietic lineages and continue to seed organs like the thymus and the bone marrow (kidney marrow in zebrafish) near the end of prenatal life. During definitive hematopoiesis, HSCs that sit at the top of the hematopoietic hierarchy produce various progenitor cells with a limited degree of differentiation and self-renewal potential. These progenitors further create terminally differentiated and short-lived mature cells that perform different functions, including oxygen transport (erythrocytes), innate immunity (neutrophils), antibody production (B-cells). In humans and mouse models, the progenitors and mature cells are well-defined through cell surface markers and, with the help of multicolor flow cytometry, cell populations can be confidently identified and separated. The

absence of antibodies to isolate separate populations has been the biggest drawback of studying zebrafish hematopoiesis, even though flow cytometry can be performed from kidney marrow extractions using forward scatter as a measure of cell size and side scatter as a measure of granularity (Traver et al., 2003) or flow cytometry using reporter lines marking specific lineages. Various markers have been identified to represent lineage-commitment and are subsequently used to perform whole-mount in situ hybridization experiments.

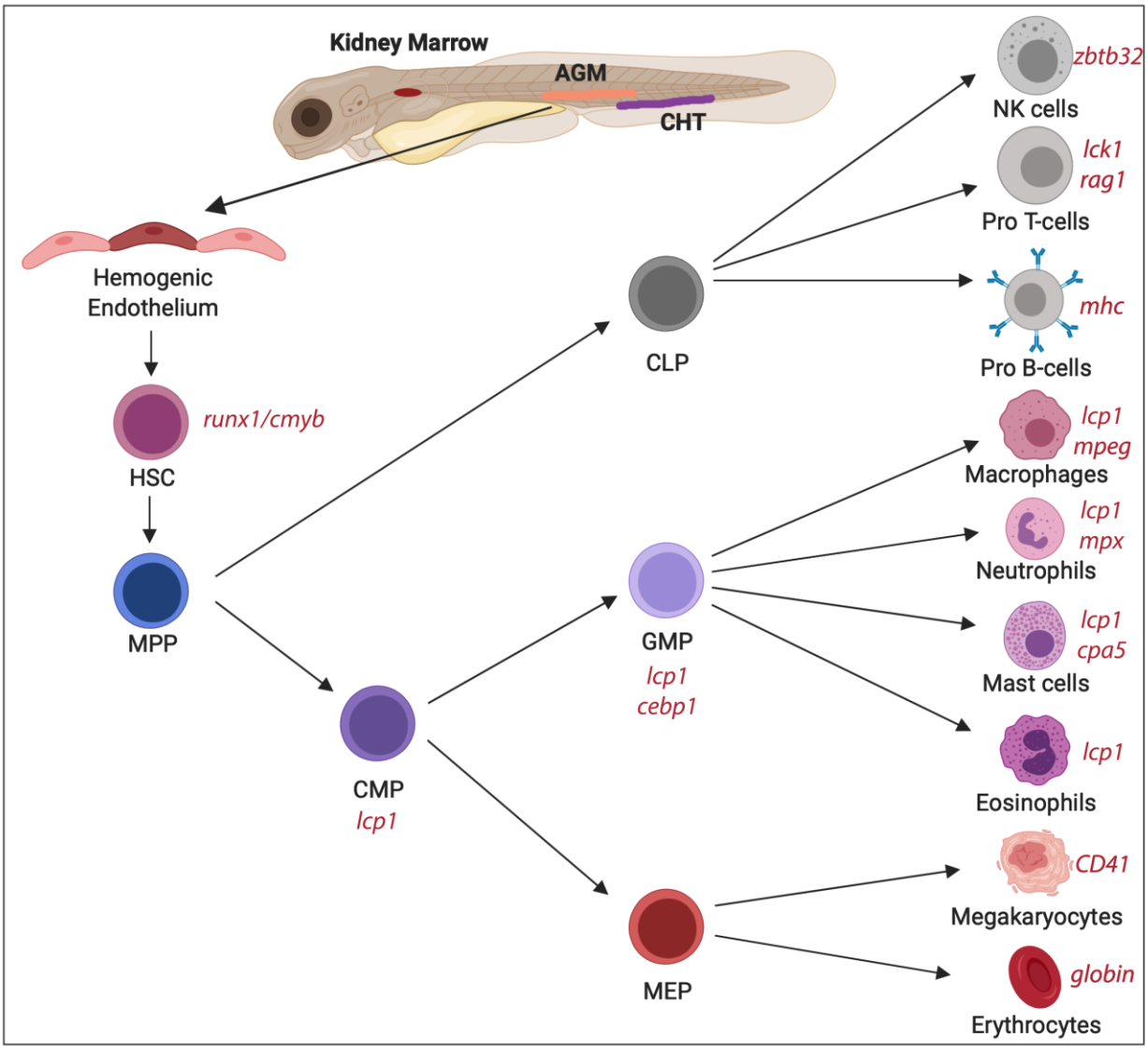

Figure 3: Definitive Hematopoiesis in Zebrafish

The hematopoietic niche is very dynamic in the early stages of definitive hematopoiesis. The HSCs originates from the ventral, dorsal aorta near aorta-gonad mesonephros (AGM; orange) and moves to the caudal hematopoietic tissue (CHT, Purple) and later to the Kidney marrow (Brown). The HSCs originate from a cell called hemogenic endothelium and can undergo self-renewal and multi-lineage differentiation. WISH probes are labeled in red.

1.3 Role of microenvironmental factors in hematopoiesis

Microenvironmental factors, including growth factors and adhesion molecules, meticulously control every aspect of hematopoiesis from niche dynamics to the process of HSCs differentiating into mature cells. Any aberrant expression of these factors might lead to a disruptive effect in either a single lineage or multiple lineages depending on the factor. For example, as seen above, ablation of primitive macrophage or suppression of matrix metalloproteinases (MMP) expression will lead to HSCs accumulating in the AGM, restricting their potential to migrate to the fetal liver (Travnickova et al., 2015). Distinct hematopoietic microenvironments also contribute to the pathogenesis of hematological disease; this will be discussed later in this chapter.

The knowledge of the environment surrounding the hematopoietic centre called "niche" in primitive hematopoiesis is nascent. Even though primitive hematopoietic cells are close to the endothelial niche in the blood island, they rarely interact (Al-Drees et al., 2015). A few studies have examined primitive erythrocytes. Transcriptome analysis of primitive erythroid cells expressing embryonic globin highlighted the presence of various receptors, including C-kit, TEK receptor tyrosine kinase (Tek), Transforming growth factor-beta receptor (Tgfbr) 1, Tgfbr3, Activin receptor (Acvr) 2b, and the Erythropoietin receptor (Epor) (Isern et al., 2011). Like in definitive erythropoiesis, the Kit receptor was only found on primitive erythroid progenitors (marked by their ability to form erythroid colonies) (Isern et al., 2011). However, in contrast to definitive erythropoiesis, an Epor knock-out experiment in mouse showed no impact on primitive erythropoiesis (Lin, Lim, D'Agati, & Costantini, 1996).

During definitive hematopoiesis, post emergence of the first HSCs, there is a short period when HSCs are maintained in AGM before they eventually move to the fetal liver. The AGM offers a permissive niche by providing secretory factors and anchorage. Analysis of cell clusters from the AGM showed that specific clusters have the potential to help HSC differentiation, and others provide self-renewal signals (Ohneda et al., 1998). A Boyden chamber assay involving AGM stroma and HSCs suggested that the importance of secretory factors outweighs the physical anchorage, at least in the AGM (Oostendorp et al., 2005). AGM stroma produces multiple cytokines that are known for their impact in HSC programming and maintenance, including stem cell factor (Scf), Flt3-ligand (Flt3l), interleukin-3 (IL-3), and bone morphogenic protein (Bmp) 4 (Al-Drees et al., 2015).

Post-migration from AGM, the fetal liver is the site of hematopoiesis, the HSCs continue to expand, as well as produce various mature cells (Sean J Morrison, Hemmati, Wandycz, & Weissman, 1995; Sánchez, Holmes, Miles, & Dzierzak, 1996). Megakaryocytes are, for the very first time, seen only in the fetal liver microenvironment (Brouard et al., 2017). The fetal liver contains a bipotential cell called the "hepatoblast"; hepatoblasts are capable of producing both hepatocytes and cholangiocytes (Payushina, 2012). The development stages of the fetal liver seem to offer the hematopoietic cells with a "Goldilocks zone" for short term survival and expansion before they ultimately move to the bone marrow (Fukumoto, 1992). Just as the HSCs arrive, the fetal liver undergoes extensive remodeling due to ECM degradation by MMPs (Travnickova et al., 2015). Some of the MMPs secreted are also known to downregulate collagen signaling (de Paula Ayres-Silva, de Abreu Manso, da Cunha Madeira, Pelajo-Machado, & Lenzi,

2011). The CHT, the zebrafish equivalent, has been well studied; where the first instance of endothelial cells forming a pocket around the HSCs, a process termed as "endothelial cuddling" were appreciated (Tamplin et al., 2015). Immediately after endothelial cuddling, rapid remodeling leads to the endothelial cells forming a pocket around the newly arrived HSCs in zebrafish CHT; this remodeling has also been consistently observed in mammalian fetal liver (Tamplin et al., 2015). Early publications have determined the expression of CD44 in the fetal liver endothelium in mice. At this time, the HSCs have been observed to express CD54 and could potentiate hyaluronic acid (HA) mediated interaction (Fukumoto, 1992). Endothelial cuddling could very well depend on these factors. The fetal liver also produces cytokines like Granulocyte Macrophage – Colony Stimulating Factor (GMCSF), Thrombopoietin (TPO), Granulocyte Clony Stimulating Factor (GCSF), and Insulin Growth Factor 2 (IGF2) (Miyauchi & Kawaguchi, 2014). However, when fetal hepatocytes start to mature into adult hepatocytes, HSCs move towards the bone marrow.

The driving force behind AGM to fetal liver migration is controversial. The fundamental dogma suggests that the CXCR4-CXCL12 axis drives this process (S. Chou & Lodish, 2010). At least in murine models, evidence has been generated using conditional CXCL12 knock-out models that CXCL12 is dispensable for fetal liver migration (Ara et al., 2003; Nagasawa et al., 1996). However, the CXCL12 knock-out mouse had reduced HSC colonization in both bone marrow and spleen, suggesting that this axis plays an essential role in bone marrow and spleen migration (Ara et al., 2003; Nagasawa et al., 1996). In zebrafish, administration of AMD3100, a CXCR4 inhibitor, impeded CHT colonization of HSCs (O. J. Tamplin et al., 2015). However, AMD3100 also leads to

the mobilization of mesenchymal stem cells (MSCs) and endothelial progenitor cells (Sun & Williams, 2016). At least in zebrafish, this hypothesis needs to be retested with a knock-out model of CXCR4 or CXCL12.

One clear concept that emerged from the above experiments was the fact that the CXCR4-CXCL12 axis plays a vital role in fetal liver to bone marrow homing (Ara et al., 2003; Nagasawa et al., 1996). The details we know about this transition are very primitive, given that this transition may have the compound effect of multiple factors and so very difficult to model. Modeling this might be important in terms of understanding the hematological disease that originates during neonatal hematopoiesis of fetal liver and continues to exist during adult hematopoiesis.

Once HSCs home to the bone marrow, they continue to be present in the bone marrow niche for their entire lifetime. The bone marrow niche is complex and harbours multiple cell types that contribute to HSC maintenance and self-renewal, including MSCs, adipocytes, osteoblasts, endothelial cells, megakaryocyte, nerve cells, monocytes, and macrophages (Boulais & Frenette, 2015; Crane, Jeffery, & Morrison, 2017; Sean J. Morrison & Scadden, 2014). The bone marrow is a rich source of anchorage-dependent and soluble factors that primarily function to maintain, retain, and expand HSCs. The perivascular stromal cells secrete CXCL12; SCF in soluble and membrane-bound forms in the niche by endothelial and lectin-expressing cells (Boulais & Frenette, 2015). The absence of membrane-bound SCF negatively impacts HSC levels in the organism (Barker, 1997). Endothelial cells also produce Notch ligands that help in expansion of HSCs in the bone marrow niche (Crane et al., 2017). Erythropoietin (EPO) and Thrombopoietin

(TPO) are produced in kidney and liver respectively and might contribute as soluble-factors towards HSC maintenance (Crane et al., 2017). Osteoblasts produces osteopontin, angiopoietin-1, and small amounts of TPO; these factors help maintain HSC quiescence (Boulais & Frenette, 2015).

The potential of HSCs to undergo multipotent differentiation, and self-renewal becomes impaired with age. HSCs usually tend to bias towards producing myeloid cells as aging progresses; a phenomenon described by an increase myeloid cytokines IL1β, IL6 and reduced endosteal membrane in the bone marrow niche (Ho et al., 2018). There is also a reduction in the levels of IGF1 in the bone marrow niche; the reduction in IGF1 contributes towards increased myelopoiesis and decreased HSC regeneration (K. Young, Loberg, Eudy, Bell, & Trowbridge, 2018). The findings related to an aging bone marrow niche directly correlate with the increase of myeloid malignancies with age.

1.4 Acute Leukemia

Blood-related malignancies that originate in the bone marrow and contributes to the aberrant increase of white blood cells with impaired function is called leukemia. Leukemias are either chronic or acute, depending on the time it takes to develop into a disorderly state.

An age-independent statistic suggests that leukemias are rare in nature, but in the pediatric subset, about 30% of all cancer are leukemia (Fiegl, 2016). Acute leukemia of the myeloid and lymphoid lineages are termed as acute myeloid leukemia (AML) and acute lymphoblastic leukemia (ALL), respectively. AML is a disease of old-age with a median age of diagnosis of 67 years; in contrast, ALL is common in pediatric patients, median age at diagnosis for ALL is 14 years (range 0-18 age) (Fiegl, 2016). Leukemia that does not arise as a result of any cytotoxic therapy or without previous history of hematopoietic malignancy is called *de novo* leukemia; if there was a history of chemotherapy or hematological malignancy, it is secondary leukemia. The difference between leukemia of old age and the pediatric population is the commonality of secondary AML (sAML) in adults with the presentation of an intermediary clonal disorder characterized by ineffective hematopoiesis called "myelodysplastic syndrome" (MDS). Most pediatric leukemias are de novo leukemia. MDS of childhood is very rare and commonly associated with inherited bone marrow failure syndromes (IBFS) (Glaubach, Robinson, & Corey, 2014).

Acute leukemias are somatically acquired genetic disorders with contributions from genetic lesions like translocations resulting in fusion genes or from point mutations. Models predict that somatic genetic lesions first occur in either an HSC or a progenitor cell, called a "leukemia-

initiating cell" (LIC). Multiple publications have shown that, upon transplantation, LICs can give rise to leukemia in murine models (Bonnet & Dick, 1997a; Chiu, Jiang, & Dick, 2010; Lapidot et al., 1994). LICs are rare cell populations in a leukemia and give rise to non-functional immature cells; these daughter cells cannot establish leukemia by themselves, but they contribute to the clinical manifestation of the disease (Bonnet & Dick, 1997a). Efforts focusing on identifying LICs based on surface markers did resolve a distinct combination of markers (Bonnet & Dick, 1997a; Passaro et al., 2015; Taussig et al., 2010), but the general suspicion is that the combination may vary based on individual cases depending on biological features.

Genetic predisposition in conditions like Down syndrome and chromosomal breakage disorders increase the chances of AML in childhood (discussed in detail in section 1.5). Point mutations in AML are common in myeloid transcription factors, tumor suppressor genes, spliceosome genes, DNA modification-related genes, nucleophosmin1 (NPM1), chromatin modifiers, cohesin complexes, and growth-factor receptors (Fiegl, 2016). Some point mutations including NPM1, IDH1, RAS gene mutations, RUNX1, CEBPA, WT1, PTPN11 and KIT and fusion genes including AML1-ETO, PML-RARA, CBFB-MYH11 are rarely seen in MDS but are commonly seen in de novo AML (Koeffler & Leong, 2017).

Clonal evolution of AML

AML is a clonal disease; a typical case of AML at diagnosis contains anywhere between a dozen and few hundred of mutations that have steadily accumulated with age. Normal hematopoietic stem and progenitor cells (HSPCs) also contain background mutations, and this mutational

background increases with aging; at times, a mutation can give rise to clonal supremacy under selective pressure leading to clonal hematopoiesis.

In a cancer genome, initiating mutations that contribute to genome instability occur very early in the evolutionary history of the clone. A critical condition for this clone is its ability to self-renew; the initiating genetic lesion should have happened in a multipotent hematopoietic cell that is capable of self-renewal, or the initiating mutation should confer upon the cell the capacity to self-renew (Corces, Chang, & Majeti, 2017). In the event this fails to happen, the mutation will be lost in due course as a result of terminal differentiation(Corces et al., 2017). Cells with a multipotent ability that carry a leukemia-initiating lesion are called pre-leukemic HSCs. The initial preleukemic lesion also contributes to the growth and survival advantage of the pre-leukemic HSCs.

In pediatric AML, the initiating event is frequently a genetic predisposition or a somatic fusion gene product that arise through a chromosomal translocation. In adult AML, initiating mutations are single nucleotide polymorphisms leading to a defective protein product. DNMT3A and TET2 loss-of-function mutation are the two most common initiating events along with IDH1/2 mutation and cohesin complex mutation (Papaemmanuil et al., 2016). NPM1 and CEBPA mutations occur both as an initiating event and a late event (Papaemmanuil et al., 2016). One of the reasons for the commonality of epigenetic factors TET2 and DNMT3A in pre-leukemia HSCs is their ability to provide clonal growth and survival advantage together with genomic instability.

1.5 Preleukemia and Preleukemic conditions

Preleukemia was a term first used to define MDS (Block, Jacobson, & Bethard, 1953). With the emergence of cytogenetics, next-generation sequencing data, and consortium-driven data collection efforts, the understanding of factors resulting in leukemia has increased, resulting in a multitude of disorders and genetic predisposition brought under the umbrella of preleukemia (Koeffler & Leong, 2017). For this thesis, any genetic perturbation that relatively increase the chance of having leukemia will be considered preleukemic, and this ranges from a Clonal Hematopoiesis of Indeterminate Potential (CHIP) mutation (see below) to MDS in adults to a germline mutation to any aberrant hematopoietic condition in the pediatric population. Discussed below are some preleukemic conditions that are relevant to this thesis.

Clonal Hematopoiesis of indeterminate potential (CHIP)

Increased prevalence of progeny from a single HSC clone is called clonal hematopoiesis. The increase of clonal contribution from a single cell is the basic definition of AML, as previously discussed, but, in many instances, individuals with clonal hematopoiesis stay healthy and do not develop any complications. Initially, sequencing studies showed that CHIP mutations only occur in about 10% of individuals older than 65 years but, using error-corrected sequencing (ECS) in a healthy cohort aged between 50-60 years, it was found that almost 95% had aging-related clonal hematopoietic mutations(Genovese et al., 2014; A. L. Young, Challen, Birmann, & Druley, 2016).

Individuals with acquired CHIP mutations in a cancer-related gene not only have an increased probability of developing leukemia and other hematological disorders but also have an increased

chance of developing cardiovascular diseases (Jaiswal & Libby, 2019). CHIP mutations in genes like *DNMT3A*, *TET2*, and *ASXL1* doubles the risk of developing atherosclerotic cardiovascular disease and poor-prognosis in heart failure (Jaiswal & Libby, 2019). Even though *TET2* mutations show a similar rate of leukemic progression to other CHIP mutations, it is also involved in polycythemia vera, systemic mastocytosis, essential thrombocythemia, and primary myelofibrosis, which represent preleukemic myeloproliferative neoplasm (MPNs) (Tefferi, Levine, et al., 2009; Tefferi, Pardanani, et al., 2009).

Trisomy 21

The presence of constitutional trisomy 21 in individuals results in the Down syndrome. Children with Down syndrome (DS) have 150 fold increase in the probability of developing acute myeloid leukemia (ML-DS) (Hasle, Clemmensen, & Mikkelsen, 2000; Lange et al., 1998). About 10-30% of DS children develop a preleukemic condition called Transient Abnormal Myeloipoiesis (TAM), the originates in the first few months of life (Kurahashi et al., 1991; Miyashita et al., 1991). TAM, in most instances, does not require any therapy and undergoes spontaneous remission (Lange et al., 1998; Massey et al., 2006). TAM gives rise to a blast population of immature megakaryocyte cells that harbour a truncated GATA1 transcription factor gene (GATA1s). The GATA1s mutation is considered a pathognomonic feature of ML-DS and, there has been evidence that this mutation occurs *in utero* (Taub et al., 2004; Wechsler et al., 2002).

ML-DS arises during the first four years of life, with approximately 20-30% of individuals with TAM progressing into ML-DS (Gamis et al., 2011; Klusmann et al., 2008; Lange et al., 1998; Massey et al., 2006). The initial TAM clone acquires further mutations in order to progress into ML-DS;

common mutations include cohesin complex mutations and colony stimulating factor 2 Receptor B (CSF2RB) mutation.

Bone marrow failure syndromes

Bone marrow failure is a collective term given to a group of acquired or inherited hematological disorders characterized by single or multi-lineage cytopenia. Bone marrow failure includes but is not limited to Fanconi anemia, Diamond-Blackfan anemia, dyskeratosis congenita, and Shwachman-Diamond syndrome. For this thesis, some relevant bone marrow failure syndromes will be introduced.

Fanconi anemia is an autosomal recessive disorder characterized by progressive cytopenia, eventually leading to bone marrow failure (Joenje & Patel, 2001; Rosenberg, Greene, & Alter, 2003). Patients with FA are at risk for developing both leukemia and solid tumours (Joenje & Patel, 2001). FA patients have a germline mutation in one of the 23 FA related genes playing an active role in DNA repair, loss of which leads to genomic instability resulting in accumulation of further mutations (Koeffler & Leong, 2017). FA is a preleukemic condition that increases the risk of AML by 15,000 fold, and diagnosis is usually made before 20 years of age (Auerbach & Allen, 1991; Rosenberg et al., 2003). The secondary genetic lesions are mostly chromosomal losses or gains with monosomy 7 and 1q duplication being the most common genetic aberrations (Auerbach & Allen, 1991).

Diamond-Blackfan anemia related mutations are found in structural protein components of the 40s and 60s ribosomal units; the mutations are mainly heterozygous (Narla & Ebert, 2010; Shimamura & Alter, 2010). Clinically, patients with Diamond-Blackfan anemia shows signs of anemia with macrocytosis (larger red blood cell), cytopenia of reticulocytes (early red blood cell precursors) but with normal marrow cellularity (Lipton & Ellis, 2009). A dosage imbalance in ribosomal proteins that is usually stoichiometrically-balanced leads to upregulation of p53, that leads to cell cycle arrest and apoptosis, further resulting in cytopenia (Narla & Ebert, 2010). Almost 98% of Diamond-Blackfan anemia is diagnosed within the first year of life (Narla & Ebert, 2010). DBA diagnosis is preleukemic, and a cancer predisposition, approximately 20% of Diamond-Blackfan anemia patients develop either leukemia or solid tumours by the age of 46 (Vlachos, Rosenberg, Atsidaftos, Alter, & Lipton, 2012).

Shwachman-Diamond syndrome (SDS) is an autosomal recessive disorder (Boocock et al., 2003). About 90% of SDS patients have a biallelic mutation in Shwachman-Bodian-Diamond Syndrome (*SBDS*) gene (Boocock et al., 2003). The SBDS gene plays a vital role in ribosome biogenesis, and RNA processing. A mutation in SBDS leads to downregulation of multiple ribosomal proteins involved in rRNA and mRNA processing (Narla & Ebert, 2010). As seen in DBA, aberrant functions of translational machinery upregulate p53 that also plays the role of monitoring protein translation (Constantinou, Elia, & Clemens, 2008). Other than p53 upregulation, SBDS loss can also lead to chromosomal instability through p53 independent mechanisms (Austin et al., 2008). Together, both these factors contribute to a bone marrow failure hematological phenotype characterized by anemia and/or neutropenia, often leading to

pancytopenia and bone marrow hypocellularity (Shimamura & Alter, 2010). SDS is not only limited to ineffective hematopoiesis but can also lead to exocrine pancreatic insufficiency, short stature, and skeletal abnormalities (Shimamura & Alter, 2010). SDS is characterized by a predisposition to developing MDS and leukemia with transformation of 18% and 36% at 20 and 30 years, respectively (Donadieu et al., 2005). SDS patients who develop AML/MDS have a poor prognosis (K. C. Myers et al., 2017).

Mastocytosis

Mastocytosis is a myeloproliferative neoplasm (MPN). Approximately 90 % of mastocytosis patients harbour a *KIT* gain-of-function mutation, most prominently an aspartate to valine substitution in 816th codon (D816V) (Chatterjee, Ghosh, & Kapur, 2015; Jawhar et al., 2017). Independently of mastocytosis, this mutation is also seen in 10-15% of core binding factor leukemias (CBF-AML) (Nick et al., 2012; S. A. Wang et al., 2013; L. Zhao et al., 2012). The World Health Organization (WHO) classifies mastocytosis into seven different categories that include cutaneous mastocytosis (CM), indolent systemic mastocytosis (ISM), smoldering systemic mastocytosis (SSM), systemic mastocytosis with non-associated hematologic non-mast cell disease (SM-AHNMD), aggressive systemic mastocytosis (ASM), mast cell leukemia (MCL), mast cell sarcoma (MCS) and extracutaneous mastocytoma (Horny et al., 2008).

Mastocytosis is both seen in pediatrics and adults. Pediatric mastocytosis generally has an excellent prognosis (Chatterjee et al., 2015), whereas adult onset systemic mastocytosis is associated with a poor outcome and a median survival of 41 months post-diagnosis. Adult

systemic mastocytosis has a progression rate of 6% into leukemia (MCL and AML) (Lim et al., 2009), and the prognosis is worse in individuals that progress to leukemia (Chatterjee et al., 2015).

Co-operating mutations in *KIT*-mutated mastocytosis are mostly mutations of epigenetic factors including *TET2* (23%), *DNMT3A (12%)*, *ASXL1(12%)* and *CBL (4%)*(Traina et al., 2012). Another study estimates the co-occurrence of *KIT D816V* and *TET2* mutation at 50% (Tefferi, Levine, et al., 2009)

1.6 Preleukemia to leukemia transformation

Preleukemia to leukemia progression follows a clonal evolution model in which the cell that possesses the initiating mutation acquires additional mutations in order to survive and outcompete other clones. In the case of AML, the clonal population that is responsible for the disease usually contains from a dozen to few hundred mutations. Understanding of the preleukemia to leukemia transformation has improved in recent times due to the increase in depth of next-generation sequencing technologies. Another phenomena that is currently not very well understood is the contribution of the microenvironment in leukemic progression.

As suggested above, subsequent mutation that occurs in a clone after the occurrence of initiating mutation is vital towards progression, sometimes this might not be sufficient, and the permissive microenvironment could contribute towards the survival of the cells harbouring the initiating mutation and aid in clonal evolution. The first assertion of the importance of the microenvironment in cancer was as early as 1889 through Paget's soil and seed hypothesis (Paget, 1889). Paget observed that the metastatic cells from breast cancer metastasized in a non-random way and preferentially migrated to selected organs (Paget, 1889). Paget concluded that the microenvironment might play a key role in preferential migration of these cells (Paget, 1889).

The role of the microenvironment

The microenvironment is a decisive factor both in childhood and adult leukemia. Preleukemic clones containing leukemia-specific chromosomal translocations originate very early in development during fetal hematopoiesis. Current wisdom from disease modeling in preclinical

models suggests a requirement for the accumulation of other mutations in order for this clone to expand to cause blast crisis, characterized by increased blast cells in blood and bone marrow (Jan et al., 2012). This clone needs to survive until this scenario occurs, and microenvironment is vital for this to occur.

MLL/KMT2A translocations are known to occur *in utero* like other translocations. Clinically individuals with an MLL translocation give rise to B-ALL and AML; even though this was not replicable in murine models until recently. Murine models only presented with AML upon transplantation of *MLL-AF9* transduced HSCs (Krivtsov et al., 2006), but transplantation of MLL-AF9 HSCs during fetal liver hematopoiesis led to a B-ALL presentation (Rowe et al., 2019). This study provides a key example as to how the microenvironment can determine the lineage fate of leukemia.

Another example of the microenvironmental influence on leukemia is the pathogenesis of ML-DS. A Down syndrome fetus carries a full or partial trisomy for chromosome 21 and a subset of early myeloid precursors acquire a GATA1 mutation as early as the first trimester in utero (Bhatnagar, Nizery, Tunstall, Vyas, & Roberts, 2016). Neonates with DS often present with TAM, which harbours the signature GATA1s mutation of ML-DS (Roy et al., 2012). TAM presents with an increase in megakaryocyte-erythroid progenitors (MEP) (Roy et al., 2012). The fetal liver microenvironment and the fetal liver to bone marrow transition might play a crucial role in the pathogenesis of ML-DS in two different ways: (1) the fetal liver is a permissive environment for megakaryocyte differentiation (Brouard et al., 2017); (2) the preleukemic clones are dependent

on granulocyte macrophage colony secreting factor (GM-CSF) secreted in fetal liver. GM-CSF produced in the bone marrow is limited in comparison to the fetal liver, thus, the clones are pushed to acquire an activating mutation in growth factor receptor CSF2RB (Labuhn et al., 2018). An additional study that highlights the microenvironmental effect is a report involving *Dicer1* and osteoblast progenitors in the murine bone marrow (Raaijmakers et al., 2010). An experimental mouse knock-out of *Dicer1* in osteoblast progenitor cells developed an MDS like phenotype (Raaijmakers et al., 2010). Further experiments did show downregulation of the *Sbds* gene, involved in SDS (discussed previously in section 1.5) in Dicer1 deficient osteoblast progenitors (Raaijmakers et al., 2010). Knock-out of the *Sbds* gene in osteoblasts yielded a similar result. Transplantation of hematopoietic cells from this mouse into wild-type recipients restored the phenotype of these cells, indicating the role of microenvironment independent of intrinsic disorders in hematopoietic cells (Raaijmakers et al., 2010). A retrospective study showed that mesenchymal stromal cells from MDS patients expressed low levels of *DICER1* and *SDBS* (Santamaría et al., 2012). A mechanism for this was later proposed. In a murine model mesenchymal stem and progenitor cells (MSPCs) lacking *Sbds* induced genotoxic stress in the HSPCs Toll Like Receptor 4 (TLR4) dependent hyperpolarization of mitochondria (Zambetti et al., 2016).

Similarly, an inflammatory cytokine milieu is also known to propel MDS towards leukemia. Studies have shown upregulation of proinflammatory cytokines like interleukin (IL)-1β, IL-6, interferon(IFN)-γ, and tumor necrosis factor (TNF)-α in MDS to leukemic progression (Flores-

Figueroa, Gutiérrez-Espíndola, Montesinos, Arana-Trejo, & Mayani, 2002; Marcondes et al., 2008; Tamura, Ogata, Dong, & Chen, 2003; Tennant et al., 2000).

1.7 Preclinical models of leukemia

Genetic lesions characteristic of leukemia have been well-defined due to advances in cytogenetics and sequencing technologies; this has given rise to numerous experimental models. Multiple model organisms have influenced our understanding of hematology, including non-human primates, mouse, zebrafish, frog, snake, and Drosophila. Some of these models, while not commonly used, possess inherent advantages that have been vital in answering key questions. For example, a frog model was used to answer critical question about the bipotential competence state of the hemangioblast during primitive hematopoiesis (C. T. Myers & Krieg, 2013).

Our understanding of leukemia has greatly advanced due to genetic models and patient-derived xenografts. To define and discuss every preclinical model is outside the scope of this thesis; therefore, this section will be limited to an overview of xenograft models that lead to the development of the model system used in Chapter 3 and *TET2* mutant murine and zebrafish models that influence the discussion of Chapter 4.

Patient-derived xenograft models

A key rationale for developing the patient-derived xenograft (PDX) model is because of the fact that ex vivo culture of patient-derived leukemia cells does not entirely represent the heterogeneity of leukemia even using the most sophisticated culture conditions. Intrinsic properties of the organism like sheer stress and other chemical moieties present in the milieu provided by the PDX models make them more clinically relevant than cell culture dishes. Modeling preleukemic conditions like MDS has been even more complicated, mainly due to the

limited availability of cell lines and evidence that these cell lines do not accurately recapitulate the condition (Drexler, Dirks, & MacLeod, 2009).

Murine xenograft models

Murine xenograft models have evolved from the use of nude mice to NSG (NOD/LtSz-SCID IL2Rγ null) mice that lack the murine immune system completely. The use of an immunodeficient murine xenograft model to evaluate leukemic potential using limited dilution and serial transplantation is the gold-standard of PDX studies (Bonnet & Dick, 1997a; Lapidot et al., 1994). Despite being completely immunodeficient, some leukemic clones survive poorly in mice. Leukemic samples harbouring AML1-ETO and CBFB-Myl11 fusions result in low to modest engraftment in NSG mice (Goyama, Wunderlich, & Mulloy, 2015). Murine xenograft models also show very low engraftment with patient-derived preleukemic cells from MDS and myeloproliferative neoplasms (Rongvaux et al., 2013). The low levels of engraftment have been attributed to lack of conservation of cytokines in the microenvironment (Rongvaux et al., 2013).

A good example is a lack of conservation of GM-CSF, IL-3, macrophage-colony stimulating factor (M-CSF) between human and mice at the amino acid level; and as a result, no-cross-reactivity to the human receptors (Song et al., 2019; Spits, 2014). A fact that is not surprising considering that the most recent common ancestor of mouse and human lived ~90 million years ago (Mya) (Kumar & Hedges, 1998), resulting in an evolutionary difference of approximately 180 million years (Murphy et al., 2007). Thus, in order to compensate for these limitations, efforts to

"humanize" these model systems have led to the introduction of human factors in conjunction with human cell populations.

Various studies have shown that humanizing mice to express human cytokines improves engraftment in PDX models. For example, AML1-ETO samples had impressive engraftment rates in the presence of human thrombopoietin (TPO) (Rongvaux, Willinger, Takizawa, Rathinam, Auerbach, Murphy, Valenzuela, Yancopoulos, Eynon, Stevens, et al., 2011). A handful of humanized mouse model exists, including the NSG-SGM3 mouse and MISTRG mouse (Rongvaux et al., 2013). The concept of humanized mice expressing human cytokines was first presented through the making of the transgenic NSG-SGM3 (NSGS) mice that ubiquitously express SCF, GMCSF, and IL3 **(**M Wunderlich et al., 2010**)**. Experiments with this mouse did show superior engraftment of leukemic cells compared to normal mice (M Wunderlich et al., 2010). The leukemic cells proliferated much more rapidly under the influence of the human cytokines and did not show any signs of exhaustion, surviving several serial transplantation experiments (M Wunderlich et al., 2010). When transplanted with human HSPCs, the chimerism was observed much earlier compared to NSG mice, and chimeras were both seen in peripheral blood as well as in the bone marrow (Wunderlich et al., 2018). However, long term HSC potential dramatically decreased, as the clones did not survive in secondary serial transplants (Nicolini, Cashman, Hogge, Humphries, & Eaves, 2004). Xenotransplanted HSPCs showed multi-lineage differentiating capacity with an increased tendency to form T-cells compared to NSG mice (Nicolini et al., 2004); NSG mice also provided the first documentation of mast cell differentiation from HSPCs in a murine xenograft system (Bryce et al., 2016b).

MISTRG (**M**-CSF, **I**L-3, GM-CSF, **S**IRPa, **T**PO, **R**AG2$^{-/-}$ IL2R**g**$^{-/-}$) mice are the latest addition to the humanized murine model (Rongvaux et al., 2014). The MISTRG mouse was made in a RAG2-/- IL2Rg-/- background and has homozygous knock-in of 5 human cytokines: M-CSF, IL-3, GM-CSF, SIRPa, and TPO to replace their genes in the mouse loci (Rongvaux et al., 2014). MISTRG mice showed improved HSC retention abilities and protected capacity for long-term self-renewal, evident by serial transplant experiments where the HSPCs showed multi-lineage engraftment through at least four serial transplants; this was potentially due to the localized expression of human cytokines (Rongvaux et al., 2014). The lack of mouse cytokines leads to defective production of host cells, leading to niche clearance, positively impacting the xenograft (Spits, 2014). With the expression of M-CSF, there was an increase in human macrophages, and since macrophages secrete IL-15, human NK cells were detected both in the marrow and peripheral blood (Rongvaux et al., 2014). MISTRG mice also showed superior engraftment potential with leukemia samples compared to the NSG mouse. Both NSG mice and MISTRG mice exhibited improved engraftment capacity of MDS samples; creating the first possible xenograft model to study a preleukemic condition (Medyouf et al., 2014; Song et al., 2019).

Zebrafish xenograft model

In comparison to the murine xenograft model, the zebrafish xenograft model is a rudimentary model in terms of technology development. The nascent status of this model is partly due to the late inception of xenograft studies in zebrafish; the first zebrafish xenograft study was published only in 2005 (Lee, Seftor, Bonde, Cornell, & Hendrix, 2005), more than three decades after the

first published mouse xenograft (Giovanella, Yim, Stehlin, & Williams Jr, 1972; Rygaard & Poulsen, 1969).

Despite its late inception, the zebrafish model offers several prominent features not seen in rodent models, like low-cost maintenance, the requirement for fewer cells to perform xenograft experiments, and large experimental animal numbers that provide improved statistical power and enhanced imaging capacity. Zebrafish xenografts also benefit from an immuno-permissive larval stage without adaptive immune system for the first 4 weeks of life that eliminates the need of immunosuppressive compounds. These advantages have led to this model gaining popularity, resulting in its rapid evolution post its first description.

Before this thesis, successful xenograft human leukemia cells and primary samples were performed (Bentley et al., 2015; Corkery, Dellaire, & Berman, 2011; Pruvot et al., 2011b), and several variables were standardized, including the optimal housing temperature of the larvae post xenograft as 35°C (Haldi, Ton, Seng, & McGrath, 2006). Various sites of injections into the larvae, including the yolk sac, common cardinal vein (duct of Cuvier), caudal vein, and hindbrain ventricle have been described. Each of these sites has their advantages and disadvantages, and the conventional wisdom is that the sites need to be chosen based on individual experiments (Veinotte, Dellaire, & Berman, 2014).

Mouse xenografts are typically performed in an immunocompromised setting to avoid immune rejection of human cells; the zebrafish does not develop a functional adaptive immune system

until 30 days post-fertilization (dpf), providing a window to perform xenograft experiments without the need to immunocompromise fish (Lam, Chua, Gong, Lam, & Sin, 2004). Previously, performing adult xenograft experiments in fish have been remarkably tricky due to the need for immunosuppressive compounds (Stoletov, Montel, Lester, Gonias, & Klemke, 2007). Recently, immunocompromised zebrafish that lack B-cells and T-cells have been used to successfully perform adult xenograft experiments (Moore et al., 2016; Tang et al., 2014; Yan et al., 2019).

Limitations of zebrafish xenograft model

Zebrafish are more distant to human than mice (Murphy, Pringle, Crider, Springer, & Miller, 2007), so the microenvironment is much more diversified due to evolutionary distance. Even though the zebrafish offers a live incubator for human cells; some of the cells might not survive or proliferate in an alien microenvironment as in the case of human HSPCs (Pruvot et al., 2011b). Like in mice, the lack of cross-reacting cytokines in zebrafish might also impact therapeutic efficacy in the context of a PDX (Theodora Voskoglou-Nomikos, Joseph L Pater, & Lesley Seymour, 2003). The biggest drawback of the zebrafish xenograft compared to mouse systems is the failure to reproducibly isolate human cells post-xenograft to perform serial transplant experiments.

TET2 loss-of-function models in murine and zebrafish

Ten-Eleven Translocation (TET) family members include three paralogues named TET1, TET2 and TET3 that are α-ketoglutarate dependent methylcytosine dioxygenase that catalyzes the conversion of methylcytosine to 5-hydroxymethylcytosine. As outlined earlier in this chapter, loss-of-function of DNA methyltransferase TET2 is common in various hematological disorders,

including AML and MDS. Mutations in *TET2* are also present in healthy individuals that do not develop any clinical consequences. Overrepresentation of *TET2* loss-of-function mutations in myeloid disease has attracted efforts to model TET2 mediated hematopoietic disorders.

In humans, TET2 loss-of-function is usually a somatic mutation initially seen in low frequencies during clonal hematopoiesis. Most of the models that will be discussed here are germline mutant models and conditional knock-out models that could lead to an exaggerated disease phenotype. The first murine Tet2 knock-out model was described in 2011 (Z. Li et al., 2011). The germline mutant model showed a chronic myelomonocytic leukemia (CMML) like phenotype, with elevated neutrophils and monocytes and reduced erythrocytes (Z. Li et al., 2011). Leukemia development was rapid and led to the death of one-third of the Tet2 deficient mice, with evidence of splenomegaly and hepatomegaly (Z. Li et al., 2011). The hematopoiesis-specific conditional knock-out mouse led to myeloproliferation that subsequently progressed to develop a CMML like-phenotype (Moran-Crusio et al., 2011). Other observations using this mouse model include increased self-renewal of HSCs and increased myeloid bias (Moran-Crusio et al., 2011); both these observations are characteristics of TET2- mutant cells in clonal hematopoiesis.

A comparative study of both the germline and conditional knock-out lines suggested that only the germline knockouts developed fatal leukemia during the 15 months follow up study (Quivoron et al., 2011) albeit; this study showed disordered myeloid and lymphoid development in conditional mice (Quivoron et al., 2011). Last year, two independent groups published that Tet2 deficient mice developed a permissive environment for developing a bacterial infection

(Meisel et al., 2018; Shen et al., 2018). One significant finding was that bacterial infections in Tet2 deficient model contributed to the development of a myeloproliferative phenotype (Meisel et al., 2018).

Prior to this thesis, three prominent models have been described in zebrafish. The first description employed an anti-sense RNA called a "morpholino" to block *tet2* expression transiently (Ge et al., 2014). The findings report pan-cytopenia across primitive and definitive hematopoiesis and a reduced global 5hmC level (Ge et al., 2014).

A *tet2* zebrafish knock-out model was generated by creating a frameshift leading to a premature stop codon before the catalytic site (Gjini et al., 2015b). There was no observed change in primitive or definitive hematopoiesis in this model (Gjini et al., 2015b). The first sign of a hematological defect was at 8-months, where *tet2* mutant zebrafish exhibited a decrease in erythrocytes and increased myeloid progenitors (Gjini et al., 2015b). Eleven-month old *tet2* mutants showed multi-lineage dysplasia restricted to myeloid and erythroid lineages (Gjini et al., 2015b). Myeloproliferation, a significant effect of *tet2* deficiency was not defined (Gjini et al., 2015b).

The third model is a *tet2/3* double mutant (Li et al., 2015). The double mutants showed no significant defect in primitive hematopoiesis. However, these mutants showed a defective definitive hematopoiesis presentation, which was mainly due to a defect in the vasculature of

the dorsal aorta where the HSCs originate (Li et al., 2015). Consequently, there was a reduction in HSCs leading to a multi-lineage reduction of cells (Li et al., 2015).

1.8 Hypothesis and Objectives

Clonal evolution of leukemia is studied by performing in-depth sequencing analysis of patient samples. The results from this methodology suggest an increase in the mutational burden of the leukemic clone under selective pressure that ultimately leads to clinical presentation. The lack of suitable model systems has impeded progress in modeling this phenomenon and further strengthening our understanding of preleukemic-to-leukemic transition.

Despite a five-decade history and the availability of severely immunocompromised hosts, the mouse xenograft system has been only recently been successful with preleukemic transplants due to human cytokine expressing mice (Medyouf et al., 2014; Song et al., 2019). Zebrafish xenograft models are not as far developed and standardized as their murine counterparts and are still undergoing evolution to improve precision and reproducibility.

Preleukemic cells are primitive, even though they have clonal growth advantage, their proliferative capacity is less than that seen in leukemic samples. In a process to establish a zebrafish xenograft platform as a tool for performing preleukemic xenografts, specific experiments testing multiclonal survival have to be performed initially. Specifically, a xenograft experiment involving the most primitive human blood cells, the HSPCs, needs to be undertaken, and multilineage engraftment needs to be elucidated. Performing this proof-of-principle study will highlight the capacity of the zebrafish as an in vivo model for supporting the survival of the most primitive cells, without perturbing the ability of HSPCs to produce multi-lineage human blood cells. However, previous publications have highlighted that HSPCs do not survive in

zebrafish (Pruvot et al., 2011b), giving rise to a need to develop zebrafish that express human cytokines to support HSPC survival.

Secondly, despite the use of highly immunocompromised mice, in-depth clonal analysis elucidates that the mouse, at most, retains one to three clones from a highly heterogeneous AML xenograft (Klco et al., 2014). In a preleukemic sample are less heterogeneous compared AML, and thus avoiding sample dropout is the key to successful engraftment. So, validation of AML xenograft for survival and multiclonal retention in the fish expressing human cytokines would be an important improvement. With this in mind, ***the objective of chapter 3 is to develop a zebrafish model that expresses human cytokines followed by xenotransplants with human HSPCs and AML samples to determine multi-lineage differentiation and clonal retention, respectively***.

In the genetic modeling spectra, there is an avalanche of work focused on modeling diseases after the availability of CRISPR-Cas9 technology (Ceasar, Rajan, Prykhozhij, Berman, & Ignacimuthu, 2016). Similar efforts have been made in modeling preleukemic conditions. *TET2* mutations found in humans are overrepresented in leukemia and other hematological disorders of different lineages. The overrepresentation of TET2 mutations is also common in CHIP; but most individuals with CHIP do not progress to leukemia or other clinical presentations. ***My objective in chapter 4, therefore, is to model tet2 loss-of-function in zebrafish using CRISPR-Cas9 technology and thereby understand how a transition from preleukemia to a myeloproliferative phase occurs with the influence of microenvironmental changes.***

Some preleukemia to leukemia transition is independent of the contribution from microenvironmental factors. Some of the initiating driver mutations are responsible for survival and proliferative mechanisms without depending on the microenvironment in a cell-intrinsic manner. The increased survival, rapid proliferative capacity, and downregulation of genotoxic stress response mechanisms by increased growth-factor signaling in a ligand-independent manner increases the probability of acquiring additional mutations. ***In chapter 5 of this thesis, a cell-based model of the KIT D816V mutation, commonly found in human systemic mastocytosis and other myeloid disorders, is used to investigate how cell-intrinsic pathways are regulated through constitutively active growth factor signaling leading to the survival of the clone and accumulation of progressive mutations.***

Overall, this thesis will use three different model systems in order to determine the event permissive of preleukemia to leukemia transformation. The specific experimental objectives involving the three models are as follows

1) To develop a novel zebrafish transgenic line expressing human hematopoietic specific cytokines and determining if the fish provides a permissive environment to the survival of Human AML and HSPCs.
2) To develop a tet2 loss-of-mutant zebrafish model and determine the cause of leukemic transformation.
3) To determine the dimerization and downstream signalling pattern of KIT D816V mutant.

Chapter 2: Materials and Methods.

2.1 Study approval

All zebrafish studies reported were approved by the Dalhousie University Committee on Laboratory Animals (UCLA), under protocol #17-132 and #17-007 (formerly14-116). The collection and use of human samples in the study were approved by the IWK Health Centre Research Ethics Board (REB# 1007549).

2.2 Creation of transgenic fish expressing human cytokines

The constructs for the making the transgenic fish were made using traditional and Gateway™ cloning. Briefly, tagBFP2 was amplified from pME-tagBFP2, and human SDF1a was amplified from pBabe-SDF1α-Puro (Addgene, #12270). Overlap extension cloning was performed to make BFP-P2A-hSDF1α with AgeI and NotI-XhoI flanking on 5' and 3' ends, respectively, and was sub-cloned into pCR2.1 by TOPO cloning. The plasmid containing 4.3kb zebrafish *cxcl12* promoter (pminitol2-zsdf1α-DsRed) was obtained (Glass et al., 2011). The construct downstream of DsRed that includes the SV40 polyA (pA) site and 3' minitol2 site was amplified with NotI on the 5' end and SacI-XhoI on the 3' end. The created NotI-SV40pA-SacI-XhoI amplicon was inserted into the pCR2.1-BFP-P2A-hSDF1α plasmid creating a pCR2.1-BFP-P2A-hSDF1α -SV40pA-3'minitol2 plasmid. Restriction digestion was performed using AgeI and SacI to excise the DsRed-polyA and 3' minitol2 site from pminitol2-zsdf1α -DsRed and was replaced by BFP-P2A-hSDF1α – polyA-3'minitol2 site that was excised using AgeI and SacI from the pCR2.1 plasmid resulting in pminitol2-zsdf1α -tagBFP2-P2A-hSDF1α plasmid. This plasmid has been deposited in Addgene (#127550).

Human stem cell factor (SCF)/KITLG and human granulocyte-macrophage stimulating factor (GM-CSF)/CSF2 were cloned downstream of the bidirectional tetracycline response element. The transactivation sequence was cloned under a ubiquitin-c promoter using a Gateway™ cloning approach. Two separate transgenic fish were produced by co-injecting CXCL12 together with *tol2* mRNA and the construct coding for rtTA with the construct coding for SCF/KITLG and GM-CSF/CSF2 together with tol2 mRNA into embryos from *casper* (*nacre*$^{-/-}$; *roy*$^{-/-}$) mutants (White et al., 2008). These fish were further crossed in the F2 generation to produce an F3 multi-transgene expressing GM-CSF/CSF2, SCF/KITLG, and SDF1α /CXCL12 zebrafish (referred to as the GSS fish). For all the experiments, we used *casper* larvae as the background control, and for brevity, I refer to it as control throughout Chapter 3.

2.3 Cell lines and cell culture.

The human Jurkat T-ALL cell line (ATCC#PTS-TIB-152) was cultured in RPMI1640 (Gibco) supplemented with 10% fetal bovine serum (FBS, Gibco). Jurkat cells express high levels of CXCR4, a receptor of CXCL12 (Cancer cell line encyclopedia (CCLE), Broad Institute) and hence was the preferred cell line to carry out migration experiments with the hCXCL12 expressing transgenic fish. The human CMK Down syndrome AML cell line was a kind gift from Dr. Jeffery Taub (Wayne State University, Detroit, MI, USA). The cells were cultured in RPMI1640 (Gibco) with 10% FBS (Wisent). Human embryonic kidney cells (HEK 293 cells) were cultured in DMEM (Gibco, 21063029) supplemented with 10% FBS (Gibco) at 37°C in 5% CO2. SC macrophage/monocyte cell line was cultured in IMDM containing HEPES and supplemented with 10% FBS, 0.05 mM 2-mercaptoethanol, 0.1 mM hypoxanthine, and 0.016 mM thymidine.

2.4 Yolk sac xenograft experiment for evaluation of migration and proliferation.

For migration experiments, CXCL12 expressing larvae and WT larvae were gamma-irradiated with at a dosage of 15Gy in a 137Cs γ-irradiator at 72 hours post-fertilization (hpf). Human Jurkat cells in culture were labeled with a cytoplasmic fluorescent dye (CMTMR Orange, Invitrogen) and resuspended in flow buffer (1X PBS, 1mM EDTA, 2% FBS). Approximately 50-100 Jurkat cells were injected into the yolk sac of larvae two hours post-irradiation and observed for migration for three days post-injection. The samples were blinded and scored for no migration, local dissemination (cells dispersed throughout the yolk sac) and migration (cells present outside of the yolk sac), and the identity was revealed after scoring.

Cell proliferation was assessed using *casper* larvae and fish expressing SCF/KITLG and GM-CSF/CSF2 (referred to as GS fish). Embryos were maintained in E3 embryo medium (5mM sodium chloride, 0.17mM potassium chloride, 0.4mM calcium chloride and 0.16mM magnesium sulphate, pH 7.5 supplemented with 0.05% methylene blue [v/v]) and were treated with 10μg /mL of doxycycline hydrochloride daily from 24 hpf to induce hKITLG and hCSF2 expression. CMK cells were labeled with a cytoplasmic fluorescent dye (CellTracker™ Blue CMAC dye, Gibco) and resuspended in flow buffer. We injected the cells into the yolk sac of 3 dpf larvae and cell proliferation quantified at 1 (baseline), 2 and 3 dpi using a dissociation protocol previously described by our group (Bentley et al., 2014; Corkery et al., 2011; Melong et al., 2017; Rajan, Dellaire, & Berman, 2016).

2.5 Human umbilical cord and bone marrow samples.

Fresh human umbilical cord blood (UCB) and human leukemia bone marrow (BM) samples were collected from patients at IWK Health Centre (Halifax, NS, Canada) after formal patient consent. The UCB and BM samples were subjected to density gradient centrifugation using Lymphoprep (StemCell Technologies) and followed by RBC lysis. Further, lineage-depleted (lin-) human hematopoietic stem cell and progenitor cells (HSPCs) were enriched using immunomagnetic separation (Easysep^{TM} human progenitor cell enrichment kit, Stemcell Technologies). Both, the HSPCs isolated from UCB and mononuclear cells isolated from BM samples were stored in liquid nitrogen until required for experimental use. A fraction of these cells was used for purity verification by flow cytometry using human CD34 and CD38 antibody.

2.6 Orthotropic xenograft experiments with primary samples.

Zebrafish larvae (from control and GSS transgenic fish) were collected and grown in E3 embryo medium. Both the transgenic larvae and control larvae were treated with 10 μg/mL doxycycline hydrochloride (Sigma Aldrich) from 24 hpf to induce the expression of SCF/KITLG and GM-CSF/CSF2 and as a control, respectively. All larvae were irradiated at 72 hpf using a 137Cs γ-irradiator (GammaCell 3000, Theratronics) with a 15Gy central radiation dosage to induce *cxcl12* promoter activity and niche clearance of the organism for transplant. Human patient-derived samples were thawed 2 hours before injection and were revived in MarrowMax (Gibco). Cells were then labeled according to the manufacturer's protocol with a cytoplasmic green fluorescent dye (CellTracker™ Green CMFDA Dye, Invitrogen) to facilitate in vivo cell tracking according to manufacturer instructions. The cells were then resuspended in flow buffer (PBS + 2% FBS + 1mM

EDTA), and loaded into a pulled-glass capillary tube, and approximately 150-250 cells were injected into the common cardinal vein. Embryos were screened immediately following injection to confirm that cells were present in circulation.

2.7 Antibody neutralization.

Mononuclear cells were obtained from primary T-ALL bone marrow biopsies using density-gradient centrifugation using lymphoprep; the samples were frozen in liquid nitrogen until further usage. The samples were thawed and seeded in MarrowMax and treated with either anti-CXCR4 (MAB171, R&D Systems) or IgG2A isotype control (MAB003, R&D Systems). The cells were incubated overnight with 4μg/ml isotype control or CXCR4 targeting antibody before injection. Flow cytometry was used to evaluate successful antibody neutralization. The cells were then orthotropically injected into the circulation of fish as described above.

2.8 RNA isolation and targeted transcriptome analysis.

RNA extraction was performed using the guanidium thiocyanate-phenol-chloroform (TRIzol) protocol using phasemaker tubes (Thermofisher, A33248) according to manufacturer instructions. RNA was stored at -80ºC until transcriptome sequencing. Targeted transcriptome sequencing was performed using HemeV2 kit (ArcherDx) for the AML samples and using the Human Stem Cell & Differentiation Markers (333002, QIAseq Targeted RNA Panels, Qiagen) for UCB samples.

2.9 Immunoblotting.

Zebrafish embryos at 24 hpf or 48 hpf were deyolked using an ice-cold Ringer's solution (116 mM NaCl, 2.9mM KCl, 5mM HEPES pH 7.2) with 1mM EDTA and 0.3mM Phenylmethyl Sulfonyl Fluoride (PMSF). The deyolked samples were then homogenized using 22G syringes in RIPA with an additional 1% SDS, cOmpleteMini Protease Inhibitor, 2mM sodium orthovanadate, 10mM sodium fluoride, 20mM sodium beta-glycerophosphate, and 1mM PMSF. The samples were left to lyse in ice for 30 minutes, and the lysate was cleared by centrifugation at 16000 xg at 4°C for 20 minutes. The protein was quantified by a micro BCA assay (Thermofisher, 23225). About 5ug of protein was loaded into each well of a Bio-Rad stain-free Any KD gel (Biorad, 4568123). The separated proteins were transferred to a 0.2-µm nitrocellulose membrane, blocked with 5% whole milk, and probed using anti-p53 (1:200, ab77813, Abcam), anti-SCF (C19H6, Cell Signaling; 1:500) and anti-GMCSF (ab9818, Abcam; 1:500) antibodies. The same blot was stripped (Restore plus, Thermofisher, 46428), blocked using 5% BSA and probed using β-actin HRP conjugated antibody (1:1000, 13E5, Cell Signaling). The β-actin served as a loading control. In both cases, antibody signal was amplified using SuperSignal™ Western Dura Extended duration substrate (Thermofisher, 34076), and intensity calculations were performed using Image Lab (Biorad).

2.10 Immunofluorescence and imaging.

Zebrafish larvae were fixed with 4% PFA overnight and dehydrated in methanol and stored at -20C until further processing. Samples were rehydrated before processing. For cryosections, the larvae were stored in 30% (w/v) sucrose solution overnight. Larvae were arranged, and molded-in OCT embedding medium (Fisher HealthCare) and 15-micron sagittal sections were made.

Samples were blocked with blocking buffer containing BSA and donkey serum and incubated in primary rabbit anti-human CD33 antibody (ab221558, 1:50) overnight at 4°C. The secondary antibody incubation with anti-rabbit Alexa Fluor 488 (ab150073, Abcam;1:400) was performed room temperature for an hour for the sections. Nuclear counterstain was performed using DAPI at the concentration of 1μg/ml. Samples were mounted in DAKO fluorescent mounting media and imaged in Zeiss LSM710 (63x, Zoom = 1.5 and NA=1.4; 10x, NA=0.45). All imaging of live zebrafish was performed upon immobilizing the zebrafish in 1% low melting agarose using a Zeiss Axio Observer (5x, NA= 0.16; 10x, NA=0.3)

2.11 Data Analysis of Error-corrected RNAseq results

Following preparation and sequencing with the QIAseq RNA Panel (Qiagen), reads were demultiplexed via their i7 adapter sequences. Reads sharing the same unique molecular index were aligned to form read families. Error-correction of read families and generation of consensus sequences were performed as described previously (Wong, Tong, Young, & Druley, 2018). Consensus sequences were locally aligned to the human reference genome hg19 using Bowtie2 and processed with Mpileup using parameters -BQ0 -d 10,000,000,000,000 to remove coverage thresholds. Targeted transcriptome analysis from the Heme V2 kit was performed via a custom cloud environment with ArcherDx software (Version 5.1.8). Results from the ArcherDx software was further analyzed using R; briefly, data cleaning was performed in order to generate high confidence hits by sub-setting the values to Allele Fraction (AF)>=0.002 and Alternate Output (AO, the number of transcripts containing the SNP variant)>4 and data was further subset to only those SNPs that had an existing COSMIC ID or known clinical significance.

2.12 Design and synthesis of sgRNA and Cas9 mRNA

The sgRNA targeting exon2 of the zebrafish *tet2* gene was identified using SSC and was ranked based on efficiency scores (H. Xu et al., 2015). Oligonucleotides were ordered flanking the T7 promoter sequence and an overlap sequence on the 5' and 3' end of the spacer sequence, respectively (Table 1). The sgRNA templates were created using an overlap-extension PCR as previously defined (Prykhozhij et al., 2018). The synthesized template was in vitro transcribed to create uncapped sgRNAs using MEGAshortscipt T7 kit according to the manufacturer's instructions (Thermo Fisher Scientific, AM1354). Zebrafish codon-optimized capped Cas9 mRNA was made from a linearized pT3TS-nCas9n plasmid (Addgene, 46757) using mMessage mMachine T3 kit (Thermo Fisher Scientific, AM1348) and purified with LiCl precipitation according to the manufacturer's instructions.

2.13 Generation of *tet2* mutant zebrafish.

The zebrafish *tet2* gene was manipulated using CRISPR/Cas9 technology. Briefly, Cas9 mRNA was injected into single cell-stage zebrafish embryos along with a cocktail of 6 sgRNA (Table 1). The injected embryos were grown to adulthood and genotyped by PCR amplifying a 2.7 kb region using LongAmp® Taq DNA Polymerase (M0323, New England Biolabs). The WT allele yielded a 2.7kb product, while the deletion allele yielded a 600 bp product.

Table 1: List of single guide RNA sequences used to produce zebrafish tet2 mutant.

sgRNA	Position	gRNA Sequence	Theoretical Efficacy Score	Direction
gRNA #1	41	GAAAAGACCAGCAATGAGA	0.688	+
gRNA #2	166	GGTCCCTGCTAACTTGCAG	0.5026	+
gRNA #3	302	AGGATTTGGGATAAAAGTG	0.6925	+
gRNA #4	353	CCCAAACATAACAAGGCAG	0.8395	+
gRNA #5	1760	CTAAAAAAGCTTAAAACAG	0.9675	+
gRNA #6	2209	GCGAATGCACCTTCTGCAG	0.9995	+

2.14 Whole mount *in situ* hybridization.

Digoxigenin-labeled probes were created by performing in vitro transcription from linearized plasmids or PCR products containing T7 promoter. Whole-mount in situ hybridization was performed on stage-matched larvae fixed with 4% paraformaldehyde using *cmyb/runx1, gata1, mpx, lcp1, cpa5,* and *cebp1* probe as previously defined (Bennett et al., 2001; Lauter, Söll, & Hauptmann, 2011).

2.15 Gene expression analysis using qRT-PCR.

RNA extraction was performed using the guanidium thiocyanate-phenol-chloroform (TRIzol) protocol using phase-lock tubes according to manufacturer instructions. The total-RNA obtained was treated with DNAse I to eliminate any remaining DNA. Subsequently, RNA was reverse transcribed into cDNA using a Luna cDNA synthesis kit according to the manufacturer's

instructions. qRT-PCR was performed using SYBR green with ROX as a passive reference (BrightGreen - Low ROX, ABM) and Quantstudio 3 (Thermofisher). The primers used for qRT-PCR are tabulated (Table 2). Primer efficiencies was determined by performing a standard curve using five different dilutions.

Table 2: List of quantitative RT-PCR primers used in this study

Target	**Forward Primer**	**Reverse Primer**	**Description**
eef1a1	CCTTCGTCCCAATTTCAGG	CCTTGAACCAGCCCATGT	housekeeping gene
hprt1	ATCCGCCTCAAGAGTTACCA	TGTCCTCCACAATCAAGACG	housekeeping gene
hsp90ab	TCAAAAATCAACGAAACTAACCAA	GGAAGGCAAAGGTCTCAGC	housekeeping gene
tet1	GATCTGTAGGCTCAGGAGGTGT	CTGAGTTTGCCTCTGACTCAAC	target gene
tet2	TGCTTATGAGAACCCAACAGTG	ATGGCCAGCATGAGCTTG	target gene
tet3	CGCTGTGGACTCAATGAAGA	AAAGAGAATGAAGCTCCACAGG	target gene
hbae1	AAAGTCATCCTTCCACAATGAGT	GGGGTAGACAATCAACATCCTG	target gene
hbae3	GATCGGCCGTGAGACTCTT	GGAGAGTTGGGGCTTAGGTC	target gene
hbbe1	ACGACGTCATTGGTCCTCA	GCAGCAACCATTGGGTTT	target gene
hbbe3	TTGTGTGGACAGCTGAGGAG	CGGATAGACGACCAAGCATC	target gene
gata1	GAGCATGTAGGAGCGTATTC	AGTGGTAGAGGAGTGTAAGG	target gene
p21	AGCTGCATTCGTCTCGTAGC	TGAGAACTTACTGGCAGCTTCA	target gene

2.16 Gene expression and methylation analysis

Hematopoietic cells from kidney marrow were extracted from adult zebrafish between 3-6 months of age by dissection. Samples were age-matched within experiments. Subsequently, the dissected tissue was suspended in a buffer containing PBS and 2% rainbow trout serum. The single-cell suspension was obtained by vigorous pipetting and passing through a 70-micron filter. The obtained single-cell suspension was snap-frozen and stored in -80°C for further experiment. The MeDIP (Methylation immunoprecipitation) was performed at the Michael Smith Laboratories, Vancouver, B.C. The sequencing files were processed using Model-based Analysis of ChIP-Seq (MACS, version 2.1.2) (Yong Zhang et al., 2008), a ChIP-Seq peak-finding algorithm that performs peak calling, fold change and FDR determination using Benjamini-Hochberg procedure. For analysis in MACS, the FDR cut-off was set at 0.01, and both positive (mutant vs. WT) and negative peaks (WT vs. mutant) were obtained. The statistics and fold changes were then processed using the ChIPpeakAnno library (Zhu et al., 2010). Briefly, the peak data from three replicates were overlapped and annotated into different genomic features by mapping to zebrafish GRCz10 as the reference genome. The frequency plot was plotted using the ggplot2 library. The genomic features that did not involve a coding sequence were subset and mapped to the nearest coding genes to obtain the list of promoter and distal-promoter regions that were methylated. The sequences obtained from the above analysis were then used to find motifs and binding sites using Regulatory Sequence Analysis Tools (RSAT) web-server (Thomas-Chollier et al., 2012). For RNAseq analysis from blood cells in kidney marrow, samples were prepared as suggested above, and a poly-A enriched RNAseq was performed through Genewiz (Genewiz, New Jersey, USA). Briefly, the cDNA library was made and sequenced on an Illumina HiSeq. The

adapter sequences from the output were removed using Trimmomatic (v0.36), and the trimmed reads were mapped to *Danio rerio* GRCz10.89 using STAR aligner (v2.5.2b) to generate the BAM file. The BAM files were subsequently processed using featureCounts function from the Subread package (v.1.5.2). The raw counts were normalized, and statistics were performed using the edgeR package. Codes used for RNAseq analysis has been uploaded to GitHub to enable reproduction. (https://github.com/vinothkr11/zebrafishtet2)

2.17 O-dianisidine Staining.

For O-dianisidine solution, larvae were treated with O-dianisidine solution (O-dianisidine (0.6 mg/mL)), sodium acetate (0.01 M, pH 4.5), H_2O_2 (0.65%), and 40% ethanol) for 15-20 minutes in the dark and subsequently washed with PBST followed by bleaching with potassium hydroxide (KOH) and hydrogen peroxide solution (H_2O_2). O-dianisidine staining were visualized under a Zeiss V20 stereo microscope. Images from O-dianisidine was quantified as previously defined (Metelo et al., 2015).

2.18 Hit and Run CRISPR method

Single guide RNA (sgRNA) was designed, synthesized, and *in vitro* transcribed as suggested above. Fresh human umbilical cord blood (UCB) were collected from patients at IWK Health Centre (Halifax, NS, Canada). HSPCs was isolated as described above and were stored in cryovial in liquid nitrogen until use. HSPCs were thawed and cultured for less than 48 hours in serum-free media StemSpan™ SFEM II (Stemcell Technologies, 09605) along with StemSpan™ CC110 (Stemcell Technologies, 02697), an HSC cocktail containing recombinant cytokines. Hi-Fi Cas9 protein

(10µg/µl) (IDT, 1081060) and diluted to 1µg/µl using nuclease-free water. A ribonucleoprotein (RNP) complex was made by incubating 1.5µg of Cas9 protein with 1µg of sgRNA for 20 mins at room temperature. The cultured HSCs were washed twice with PBS and resuspended in Buffer T at 200,000 cells in 10µl per replicate, RNP was added, and the mixture was electroporated using the Neon electroporation system with the following settings: 1600 V, 10ms, three pulses. The electroporated cells were transferred to fresh SFEMII media with CC110 and cultured for four days. Following this, the cells were changed to a differentiation media containing SFEMII and StemSpan™ Erythroid Expansion Supplement (Stemcell technology, 02692) and cultured for 14 days with regular media exchange every 2-3 days.

2.19 Vectors and cloning

pCDNA3.1-KIT WT and KIT D816V plasmids were a kind gift from Lars Rönnstrand (Lund University, Sweden). For cloning purposes, intermediate vector pCR2.1-KIT ICD del816-822 was created by performing overlapping extension PCR from pCDNA3.1-KIT WT and inserting into pCR2.1 by performing TOPO cloning (TOPO-TA cloning, ThermoFisher Scientific, 451641). Mammalian two-hybrid vectors - pACT, pBind, pG5*luc*, pBind-ID, and pACT-MyoD were from CheckMate Mammalian Two-hybrid kit (Promega, E2440). KIT ICD WT, KIT ICD D816V, and KIT ICD del816-822 were PCR amplified and inserted into pACT and pBind vectors using BamHI and NotI restriction digestion. The iSplit BiFC plasmids, pC4EN-F1-GAFm (Addgene plasmid # 39870) and pC4-RHE-PAS (Addgene plasmid # 39869) were a gift from Vladislav Verkhusha (Albert Einstein College of Medicine, New York). The iSplit BiFC plasmids for wild-type (WT) and D816V mutant versions of *KIT* were constructed in two steps. In the first step, the FLAG-tagged WT and

D816V *KIT* PCR products were amplified from the original KIT plasmids using BamHI-KIT-for and BamHI-FLAG-KIT-rev primers. In parallel, the HA-tagged WT and D816V *KIT* PCR products were amplified using BamHI-KIT-for and BamHI-HA-KIT-rev from the same initial templates. The linker (GGGGSGGGGS), containing versions of GAFm and PAS inserts, were amplified with NcoI-GAFm_for and XhoI-GAFm_rev and with NcoI-linker-PAS_for and XbaI-PAS_rev from pC4EN-F1-GAFm and pC4-RHE-PAS respectively.

2.20 Transfection of mammalian cells

For experiments involving transfection, HEK 293 cells were seeded overnight, and transfection was done in 12-20-hour window post-seeding using Fugene 6 transfection reagent (Promega, E2691) according to the manufacturer's recommendation. Recombinant human SCF (Thermo Fisher, PHC2111) was used for KIT stimulation at 500ng/ml.

2.21 Lentiviral transduction of mammalian cells

The 293T cells co-transfected was plated in a 10cm petri dish and transfected with 3.5µg - pMDG.2, 3.2µg - pCMVΔ8.2, 3.2µg - pCMVΔ8.2 and 10µg of the gene expression vector between 12-20 hours after seeding using 60µl of Fugene 6 transfection reagent (Promega, E2691). The viral media was collected at 48 hours post-transfection and infected in the presence of polybrene (8µg/mL) by spinoculation at 1200xg for 1 hour. The cells were allowed to replicate for 48 hours and were subsequently selected with the respective antibiotic.

2.22 Mammalian Two-hybrid assay

About 10^4 293T cells were seeded per well of the 96 well plate. After incubating the cells post-seeding for 12-20 hours, each well was transfected with 100 ng of DNA. The pBind, pACT, pG5*luc* vectors were transfected in equimolar ratios, and in order to maintain a constant mass of DNA in transfection mix across various samples, the DNA mass was compensated using p5E-MCS vector. About 48-hour post-transfection, cells were washed with PBS, lysed, and luminescence was measured using a dual-luminescence reporter assay system (Promega, E1910) using a Luminoskan Ascent Microplate Luminometer (ThermoFisher Scientific, 5300173).

2.23 Bimolecular Fluorescence Complementation

About 10^5 cells were seeded into each well of a 24-well plate, and cells were transfected between 12-24 hours post-seeding with about 500ng of DNA consisting of PAS, GAFm and pEGFP-N1 vectors in equal molar ratios. piRFP (iRFP713) was a gift from Vladislav Verkhusha (Addgene plasmid #31857) and was used as a positive control for flow-cytometry analysis. Cells were trypsinized 48 hours post-transfection, and flow-cytometry analysis was performed using a FACS Aria III (BD Biosciences). The data were analyzed using FlowJo based on iRFP713 expression.

2.24 Circular Dichroism (CD) Spectropolarimetry

Peptides comprising 30 amino acids surrounding the region 816th amino acid were purchased (ChemPeptide Limited, Shanghai, China). 100 µM of lyophilized peptides were then solubilized using 50mM sodium phosphate buffer, pH 7.4. Far-ultraviolet CD spectra for the peptides were recorded at 37°C using J-810 spectropolarimeter (Jasco, Easton, MD) at 20nm/min with a data

pitch of 0.1 nm from 260 nm to 185 nm. For the experiment involving hydrogen bond induction, 100 micromolar peptides were then lyophilized and resuspended in 100% - 1,1,3,3,3-Hexafluoro-2-Propanal (HFIP). The far-UV CD spectra were determined at a temperature of 37°C at 50nm/min with a data pitch of 0.1 nm from 260 nm to 185 nm. All data were collected in triplicate, averaged, blank measurements were subtracted and presented as mean residue ellipticity (θ).

2.25 Total and phospho-proteomics

In order to provide an easy understanding of the methodology, a schematic is provided as an overview (Figure 4).

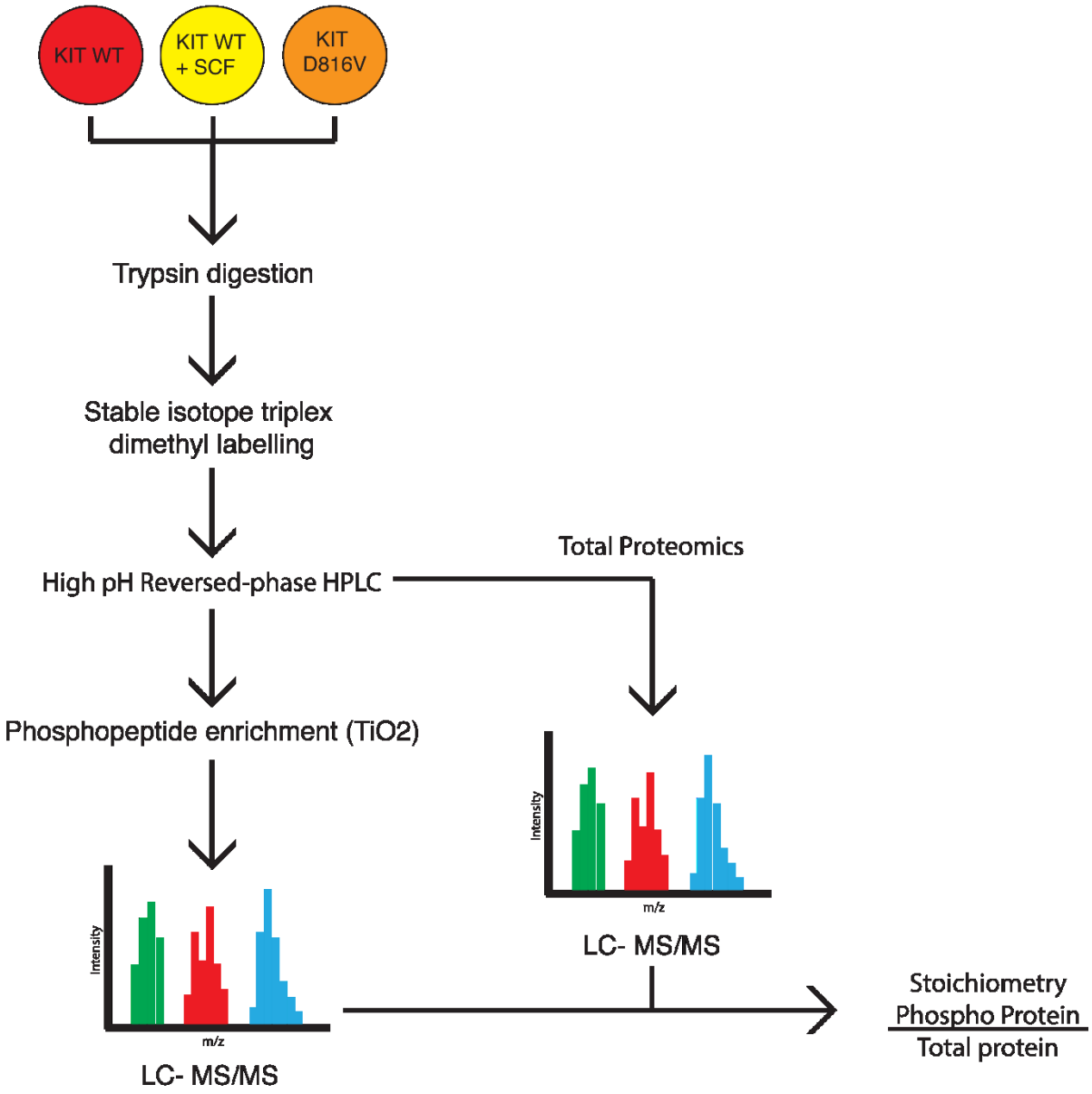

Figure 4: Overview of Total and Phosphoproteome analysis

Briefly, protein samples were digested into peptides, dimethyl labeled, and fractionated using HPRP-HPLC. A fraction was isolated to perform total proteome, and the remaining sample was enriched for phosphopeptides using TiO2 beads. The fractions were analyzed separately, and the results were analyzed.

Sample preparation and lysis

SC cells transduced with *KIT* WT or D816V and cultured as previously described. Once cells reached 70% confluency, cells were washed with PBS and cultured overnight in IMDM containing 2% charcoal-stripped FBS, 0.05 mM 2-mercaptoethanol, 0.1 mM hypoxanthine, and 0.016 mM thymidine. Cells were washed in PBS and 200ng/mL SCF was added to one subset of the KIT WT expressing cells - this sample was labeled *KIT* WT+SCF. After 10 minutes incubation at 37C, the cells were centrifuged at 1000x*g* for 2 minutes at 4C; the supernatant was removed and then it was flash-frozen in liquid nitrogen and stored at -80C for further use. Quadruplicates of samples each belonged to a different passage number were collected. The frozen cells were resuspended in lysis buffer (50mM Tris, 150mM NaCl, 1% IGEPAL pH-7.4 add protease and phosphatase inhibitor cocktail (Complete Mini, Roche, and PhosphoSTOP, Roche) and nine volumes of 100mM TEAB was added to the lysate. The lysate was homogenized in a homogenizer (~2000rpm by three strokes setting). Protein concentration was measured using micro BCA.

Reduction, alkylation, and trypsin digestion

Approximately 3.3 mg of protein sample was aliquoted and precipitated in 100% acetone at -20°C overnight followed by centrifugation at 16,000X*g* for 30 minutes at 4°C. Upon air drying, samples were resuspended in 50mM TEAB, pH 8.0, and reduced with 50mM DTT at 60°C for an hour at 1000 rpm. Alkylation was done using 100mM IAA at room temperature in the dark for 30 min at 750 rpm. Proteins were digested by addition 1:100 (w/w) of trypsin to the sample at 37°C overnight at 750 rpm. The reaction was stopped by acidifying the samples to pH below 3 by the

addition of formic acid. Upon addition of 0.1% TFA (final volume), samples were desalted on a C18 column.

Stable isotope dimethyl triplex labeling

Desalted samples were air-dried and resuspended in 50mM TEAB by sonication. Peptides were quantified with UV visible spectrometry at absorbance 205nm, and 2 mg of peptides were labeled by dimethyl triplex labeling. Briefly, samples were resuspended in 2ml 50mM TEAB and labeled by adding 170µL of either 6M $NaCNBH_3$ (light and medium labeling) or 6M $NaCNBD_3$ (heavy labeling) (Sigma Aldrich). Samples were then incubated for 1 hour at room temperature following the addition of either 80µL of formaldehyde (light labeling) (Sigma Aldrich), 150 µL of deuterated (D2) formaldehyde (intermediate labeling) (20% w/w in D_2O) (Cambridge Isotope Laboratories) or 150 µL of ^{13}C and deuterium (D2-C13) labeled formaldehyde (heavy labeling) (20% w/w in D_2O) (Sigma Aldrich). The reaction was combined in equal proportion, brought up to 1mL and 0.1% final volume of TFA was added. The reaction was immediately desalted in a C18 reversed-phase column and air-dried. The air-dried samples were stored frozen at -80°C until further use.

High-Performance Liquid Chromatography

For High pH Reverse Phase (HPRP)- High Performance Liquid Chromatography (HPLC), dried sample pellets were resuspended in 500 µL solvent A (10 mM NH_4HCO_2, 30% ACN (v/v), pH=2.7) and loaded onto an ONYX C18 monolithic column (100 mm x 4.6mm) (Phenomenex) at a flow rate of 1ml/min. Elution was performed with a gradient of 0–100% solvent B (10mM NH_4CO_2H;

95% ACN v/v; pH 8.0. The first 56 fractions (0.5ml) were collected and amalgamated into 14 samples (e.g., fractions 1, 15, and 29 and 43 were combined to make fraction 1). The collected samples were air-dried in a vacuum concentrator and stored frozen at -80°C until further use.

Phosphopeptide enrichment

Peptides were resuspended in 62.5% ACN/H20, 10% v/v of the resuspended peptides were removed for total protein analysis. One part of lactic acid (LA) was added to 3 parts of the remaining peptides (50% ACN/2M LA). TiO_2 beads (400ug/100ug of peptides, GL Sciences) was equilibrated with 100% ACN, washed twice with 50%ACN/2M LA. The bead slurry and the peptide sample were added to an equilibrated C8 spin-tip that was washed once with 50%ACN/0.1%TFA and thrice with 70% ACN/ 0.1% TFA to remove unbound peptides. Then, phosphopeptides were released from the TiO2 beads by addition of 50 ul of 0.3 N NH_4OH, pH 10.5 and by 1-minute incubation and subsequently eluted from the C8 reversed-phase column by 70% ACN/ 0.1% TFA. The mix was immediately acidified by addition of formic acid to prevent degradation of phospho-moieties and air-dried in a vacuum concentrator.

Mass spectrometry

Enriched phosphopeptides and total peptides were analyzed VelosPro Orbitrap mass spectrometer coupled with Nano-LC pump (UltiMate 3000, Thermofisher). The peptides were preconcentrated with 4 µm PicoFRIT C18 column (New Objective). Peptides were injected with solvent A (0.1% FA in water) at a flow rate 300nl/min and eluted by 0–37% solvent B (0.1% FA in ACN) with an overall run-time of 180 min.

Data Analysis

The reads were mapped to the human proteome (UP000005640), quantified, and normalized using Proteome Discoverer (Thermofisher). The normalized data were processed using R (v3.5.1). Briefly, the normalized data were cleaned (tidyr library), plotted (ggplot2 library), KSEA enrichment (KSEA app library) was performed, and heatmap was generated using the data from KSEA enrichment. Pathway analysis of total proteome was performed using cluster profiler library.

2.26 Cell cycle analysis

SC cells were serum-starved using the IMDM containing 2% charcoal FBS overnight. KIT WT, KIT D816V, and KITWT+SCF (200ng/ml SCF treated) cells were either treated with 100nM Rapamycin or with DMSO (control) for 4-5 hours. The cells were washed with ice-cold PBS and fixed and permeabilized using 70% ice-cold ethanol overnight. The cells were washed twice with PBS+0.1% Triton X-100 and 0.2 µM SYTOX Green was added to the cells. The cells were kept in the dark until analysis in FACS ARIA III, the cells were excited using 488nm laser, and the emitted light was allowed to pass through 515-545 nm bandpass filter before reaching the PMT. The results were analyzed using FlowJo (v10.6.1).

2.27 Statistical Analysis

All statistical analysis was carried out using the R programming language (R Version 3.5.1). For experiments involving categorical variables, Chi-square test of independence was performed to

obtain the p-value, and for proliferation experiments, a student t-test was performed. For all experiment involving quantitative statistics, a student t-test was performed.

Chapter 3: Transgenic zebrafish expressing human hematopoietic cytokines result in improved engraftment and survival of human hematopoietic stem cells and patient derived leukemia.

3.1 Introduction

The availability of xenograft models has greatly influenced our current understanding of leukemogenesis and stem cell biology over the last decade. Patient-derived xenografts provide a better microenvironmental and stromal context than any *in vitro* system for maintaining the clonal heterogeneity inherent in human cancers, and this is of translational importance in the performance of assays that involve pharmacological intervention and response (Hidalgo et al., 2014; Siolas & Hannon, 2013). Current gold standard xenograft assays use small mammals, like the mouse, with a depleted immune system, which have been refined over many years from their original derivation (Bonnet & Dick, 1997b; Lapidot et al., 1992; Larochelle et al., 1996; Shlush et al., 2014). However, findings from these murine xenografts may not be congruent with similar experimental results observed in human studies (Theodora Voskoglou-Nomikos, Joseph L. Pater, & Lesley Seymour, 2003). Given the fact that human tumours arise in the context of human stroma, including immune cells, these discrepancies in murine xenografts may be accounted for, at least in part, by a lack of evolutionary conservation of microenvironmental signaling pathways between humans and rodents. Some human samples do not engraft in a foreign host; while in other cases, following successful initial engraftment, the chimera disappears over time. Cytokines present in the microenvironment, which are essential for the differentiation and maintenance of individual cells are not entirely conserved across species (Brocker, Thompson, Matsumoto,

Nebert, & Vasiliou, 2010). For example, there is a lack of conservation of interleukin 3 (IL-3) and granulocyte-macrophage stimulating factor (GM-CSF/CSF2) between humans and mice at the amino acid level, evidenced by the fact that mouse IL-3 and GM-CSF do not react with their respective human receptors (Manz, 2007; Willinger et al., 2011). Thus, to compensate for these limitations, efforts to "humanize" rodent model systems have led to the introduction of human factors in conjunction with human cell populations (Morton et al., 2015; M. Wunderlich et al., 2010).

Various efforts have been made to introduce human factors into model organisms, including the injection of recombinant proteins like PIXY321 (GM-CSF/IL-3 fusion protein) (Lapidot et al., 1992), a cost-efficient method to enable human cytokine expression using knock-in (Rongvaux, Willinger, Takizawa, Rathinam, Auerbach, Murphy, Valenzuela, Yancopoulos, Eynon, & Stevens, 2011; Willinger et al., 2011) and transgenic technologies (Traggiai et al., 2004; M. Wunderlich et al., 2010), where researchers have introduced various factors including erythropoietin (EPO) and IL-3. The approach of humanizing mice has been successful to the extent that it permits enhanced engraftment and, depending on the cytokine introduced, differentiation and maintenance of specific cell lineages. For example, humanized transgenic SGM3 mice expressing human stem cell factor/KIT ligand (SCF/KITLG), GM-CSF and IL-3 showed a significant increase in the myeloid (Coughlan et al., 2016) and mast cell compartments (Bryce et al., 2016a) and improved engraftment efficiency of human acute myeloid leukemia (AML) cells (M. Wunderlich et al., 2010). This modified murine xenograft model provides a unique advantage to enhance clonal heterogeneity and thereby enrich for more robust and meaningful responses to pharmacological

interventions. However, the mouse model remains laborious in terms of handling and techniques; is limited to small numbers of animals; and human cells take months to fully engraft. As such, they are not amenable to high or medium throughput drug screening efforts. Moreover, these mouse models are not practical to inform therapeutic decisions in patients in a clinically actionable time frame.

We previously pioneered a zebrafish larval xenograft assay to study human leukemia progression and demonstrated the feasibility of employing this platform for primary patient bone marrow-derived T-cell acute lymphoblastic leukemia (T-ALL) samples (Bentley et al., 2014; Corkery et al., 2011; Rajan et al., 2016). The zebrafish xenograft platform offers several advantages, including a high level of genetic conservation with humans at the protein level (Howe et al., 2013) with the added benefit of visual tractability of human cells in an organism amenable to medium throughput chemical screening (Liu et al., 2014; North et al., 2007). However, similar to mice, zebrafish express evolutionarily divergent cytokines or altogether lack cytokines that are critical to the maintenance of human cell clonal heterogeneity. Previous publications have suggested that the receptors and ligands of the IL-3 subfamily that include IL-5, GM-CSF, and IL-3 are absent in zebrafish (Stachura et al., 2013), and *in silico* analysis reveals that the critical cell migration chemokine, CXCL12/SDF1α, is conserved less than 50% at the amino acid level between humans and zebrafish.

In early mammalian hematopoiesis *in utero*, the site of hematopoiesis moves from the aorta-gonad-mesonephros (AGM) to the fetal liver and finally to the bone marrow (Orkin & Zon, 2008).

Zebrafish hematopoiesis mirrors these mammalian "niche dynamics", but fertilization is *ex-utero* in the zebrafish, and these stages occur over the first few days of life, resulting in a unique opportunity for experimental manipulation. In zebrafish, the transition of hematopoietic precursor cells occurs from the AGM to the stroma of a tail region called the caudal hematopoietic tissue (CHT), which has been characterized as the fetal liver equivalent in teleost fish (Murayama et al., 2006; Owen J. Tamplin et al., 2015). Upon colonization of the CHT, hematopoietic cells expand, differentiate and mature and are poised for the subsequent transition to the kidney marrow (KM) of the fish (Murayama et al., 2006), which is the primary site of adult hematopoiesis. While zebrafish leukemia xenograft platforms have been successful (Bentley et al., 2014; Corkery et al., 2011), previous studies have documented that human hematopoietic stem and progenitor cells (HSPCs) do not survive in zebrafish for more than 12 hours (Pruvot et al., 2011a), raising concerns whether the zebrafish host enables HSPC survival and clonal expansion post-transplantation. As such, zebrafish xenograft approaches to date share a critical flaw in lacking an optimal microenvironment to support the clonal evolution of human HSPC and leukemia cells, questioning the clinical transferability of findings from this model. To address this critical gap, I generated a humanized zebrafish that expresses multiple human hematopoietic-specific cytokines. I subsequently transplanted primary human-derived HSPCs and leukemia cells followed by clonal heterogeneity evaluation using error-corrected sequencing (ECS). Using these humanized zebrafish models, I show that transgenic fish expressing human cytokines prolong survival and differentiation of human HSPCs. Furthermore, in the presence of these key cytokines, transplanted leukemia cells exhibit hematopoietic niche homing that more accurately models the behavior of human leukemia. These results lay the foundation for a new

paradigm in zebrafish xenograft-based drug discovery platforms for molecular targeting of human leukemia and expansion of HSPCs.

3.2 Generating "humanized" transgenic zebrafish

To improve the current zebrafish platform for human leukemia and HSPC xenografts, I generated transgenic zebrafish expressing human hematopoietic cytokines. Cytokines that are poorly conserved between human and zebrafish but demonstrated to be critical for normal hematopoiesis were chosen for this study. In this regard, the CXCR4 ligand, CXCL12/SDF1α was my first priority, given its functions, which include stem cell fate decisions such as expansion, homing, self-renewal, differentiation, control of stem cell exhaustion and protection against genotoxic stress (Greenbaum et al., 2013; Sugiyama, Kohara, Noda, & Nagasawa, 2006; Yanyan Zhang et al., 2016). Both GM-CSF/CSF2 and SCF/KITLG were determined to be essential candidates based on prior mouse experiments (M. Wunderlich et al., 2010). Due to its redundant function with CXCL12 and GM-CSF/CSF2, I did not incorporate IL-3, which was previously employed in mouse models. We developed two independent transgenic zebrafish models. The first expressing human CXCL12 under the zebrafish *cxcl12* promoter (Figure 5A-B). The second expressing human KITLG and CSF2 under a tetracycline-inducible promoter (Figure 5C-D).

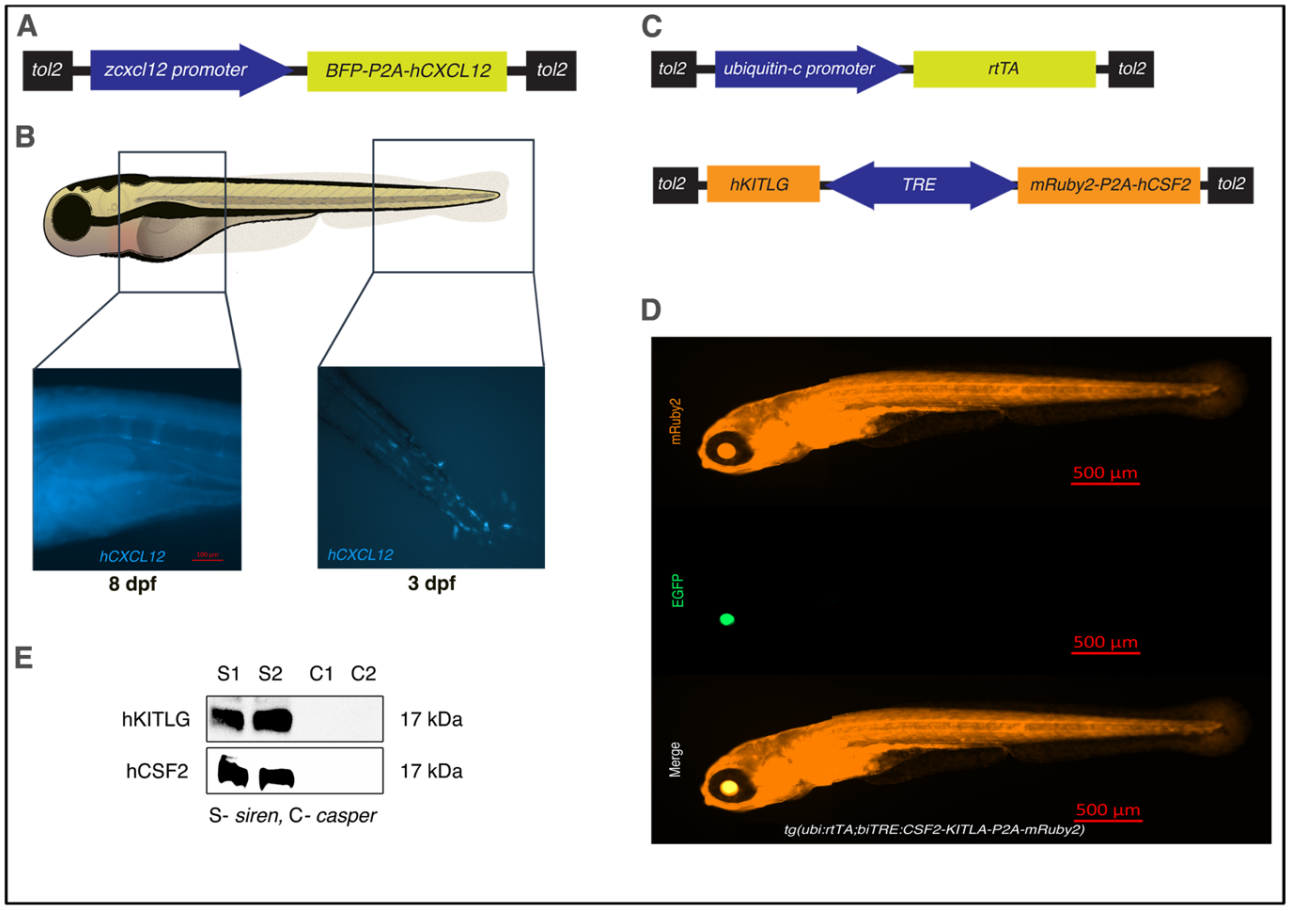

Figure 5: Humanized transgenic zebrafish expresses human CXCL12, KITLG, and CSF2.

A. A cartoon of the construct used to make the transgenic zebrafish expressing human CXCL12 (hCXCL12) along with *tagBFP2* under the zebrafish *cxcl12* promoter.

B. Representative image of a transgenic zebrafish expressing human CXCL12 in the posterior hemal arc near the tip of the tail at 3 days post-fertilization (dpf). CXCL12 expression continues to progress anteriorly through the hemal arc (representative image shows 8 dpf larvae).

C. A cartoon of the constructs used to make the *tet*-inducible human SCF/KITLG and GM-CSF/CSF2 expressing zebrafish.

D. Representative image of the human SCF/KITLG (hKITLG) and GM-CSF/CSF2 (hCSF2) expressing zebrafish. Image specification: Magnification =5x, NA= 0.16

E. Representative Western blot showing expression of human GM-CSF/CSF2 (hCSF2) and SCF/KITLG (hKITLG) in transgenic zebrafish. S1 and S2 denote samples from the transgenic larvae, and C1 and C2 are samples from control *casper* larvae. (SCF/KITLG= stem cell factor/KIT ligand, GM-CSF/CSF2=granulocyte-monocyte colony stimulating factor/colony stimulating factor 2).

3.3 Humanized zebrafish demonstrate enhanced human leukemia cell migration and proliferation

I initially performed validation experiments using the CXCL12 and GM-CSF/CSF2-SCF/KITLG compound transgenic models separately. The CXCR4-CXCL12 axis is critical for cell migration and homing (Peled et al., 2000). Therefore, I selected migration as a mode of validation for the human CXCL12-expressing transgenic zebrafish. Jurkat cells are a human T-ALL cell line that expresses high levels of CXCR4, the cognate CXCL12 receptor (Barretina et al., 2012). Zebrafish *cxcl12* promoter expression begins only at 72 hpf, so we injected Jurkat cells into the yolk sac of CXCL12 and *casper* control larvae at 72 hpf and screened for migration at 3 days post-injection (dpi). There was no migratory difference between the cells injected into control versus CXCL12 fish (Figure 6A). However, expression of CXCL12 may be low at this time point and is restricted to the posterior hemal arc near the tail. Previous publications have shown that DNA double-stranded breaks caused by either gamma irradiation or chemical agents like 5-fluorouracil or etoposide can cause an increase in CXCL12 expression (Glass et al., 2011; Ponomaryov et al., 2000). Thus, I gamma irradiated zebrafish larvae with a sub-lethal dose of radiation two hours before transplantation and repeated the assay. Then, I observed a drastic increase in the number of CXCL12 larvae that exhibited human T-ALL cell migration compared to the controls (Figure 6B). From the cells that migrated out of the yolk sac, I also saw hematopoietic niche-specific homing to the CHT at 144 hpf and later to the kidney marrow at 216 hpf (Figure 7 A&B).

For the transgenic fish expressing GM-CSF/CSF2 and SCF/KITLG (GS fish), I used CMK, a human Down syndrome acute myeloid leukemia (ML-DS) cell line for validation. While CMK cells survive in culture without additional cytokines, previous experiments in our hands demonstrated drastic

cell death in zebrafish xenograft assays, suggesting that they are susceptible to their microenvironment (Figure 6D). Recent findings demonstrate that GM-CSF/CSF2 enhances the survival in Down syndrome transient abnormal myelopoiesis (TAM), suggesting a growth advantage for ML-DS under GM-CSF/CSF2 rich conditions (Labuhn et al., 2018). When CMK cells were injected into the GS larvae, xenografts demonstrated increased cell proliferation at 3 dpi compared to *casper* controls. Strikingly, this was preceded by a sudden decrease in the number of CMK cells in both control and transgenic larvae at 2 dpi. These cells were injected into the yolk sac, an acellular environment, which may have resulted in delayed proliferation due to the restricted access of injected cells to circulating human cytokines. Thus, moving forward, all xenografts were performed by injection directly into the bloodstream of larval zebrafish, which is likely more anatomically relevant to adult human hematopoiesis. Recently, it had been emphasized that the hematopoietic process is not only regulated by soluble factors and adhesion molecules but also through mechanochemical mechanisms like blood flow contributing to blood stem cell regulation through the stimulation of YAP-TAZ (Theodore et al., 2017); therefore, xenografting of human primary hematopoietic cells into the blood stream could likely improve the performance of the current zebrafish xenograft model.

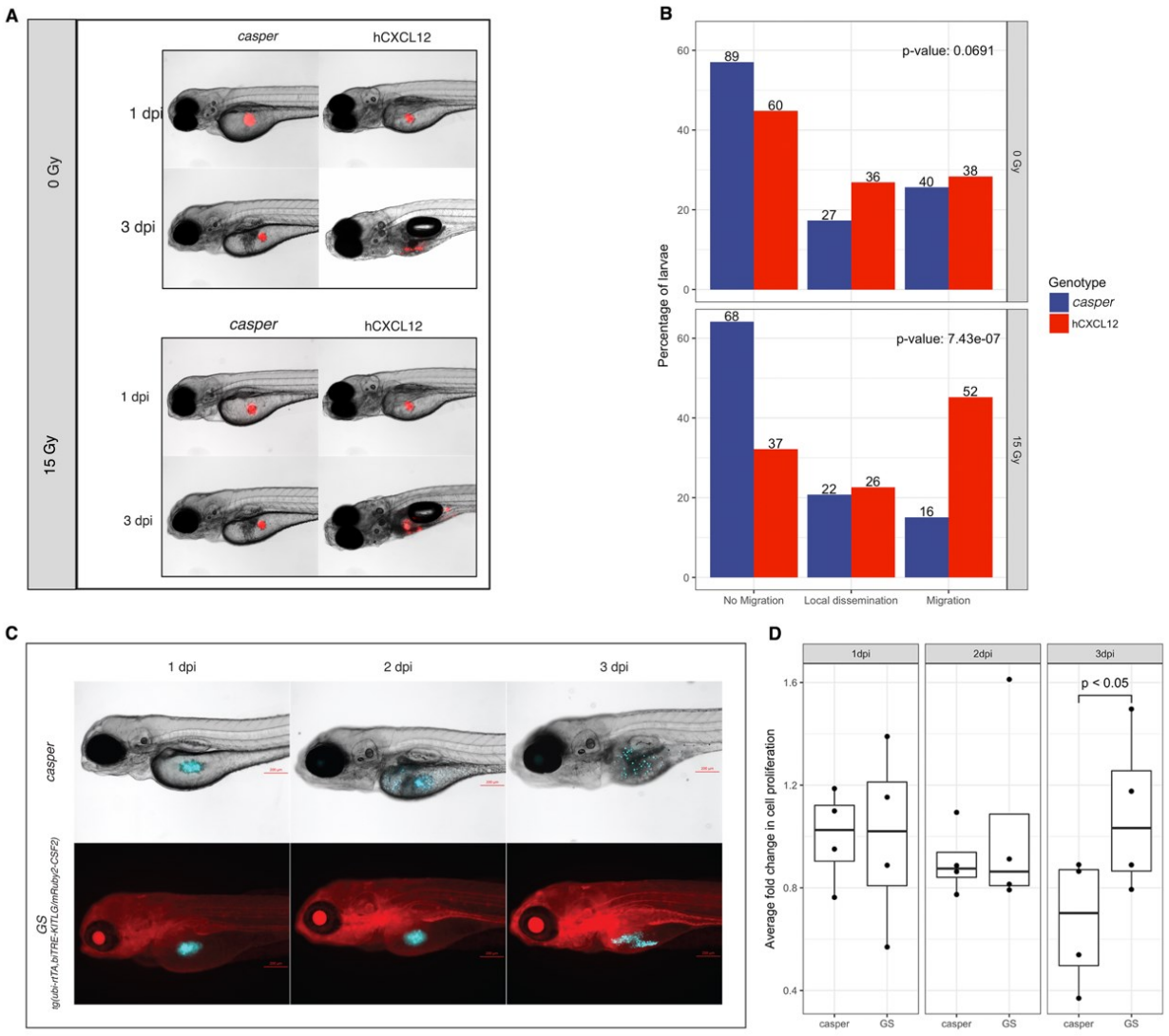

Figure 6:Irradiation of human CXCL12-expressing transgenic zebrafish dramatically increases cell migration, while ML-DS cells exhibit enhanced proliferation in the presence of CSF2/GM-CSF and KITLG/SCF

A. Human Jurkat cells (highly express CXCR4, the receptor for CXCL12) were xenografted into control *casper* and CXCL12-expressing larvae, which were further divided into two groups: one which received 15Gy irradiation and the other no irradiation at 72 hours post-fertilization (hpf). Larvae were screened for cell migration at 144 hpf. Representative images of control and CXCL12-expressing larvae that were not irradiated. Representative images of control and CXCL12-expressing larvae following 15Gy gamma irradiation (Right panel).

B. Quantification of cell migration was classified into “no migration,” “local dissemination” (dissemination within the yolk sac) and “migration” (distant migration beyond the yolk

sac). Results represent 3 independent experiments. Numbers on the bar denote the total number of larvae per classification.

C. Representative images of zebrafish injected with CMK cells (myeloid leukemia of Down syndrome (ML-DS) cell line).

D. Cell proliferation was quantified in transgenic larvae expressing GM-CSF/CSF2 and SCF/KITLG (GS fish) and *casper* controls following enzymatic digestion and dissociation at one-day post-injection (dpi) (baseline), 2 dpi and 3 dpi. The analysis included fluorescence microscopy and cell counting. At 2 dpi there was a slight decrease in cell numbers in both transgenic and control larvae. By 3 dpi there was an increase in the number of cells in GS larvae, whereas cell numbers in control larvae decreased. Data presented represents four replicates.

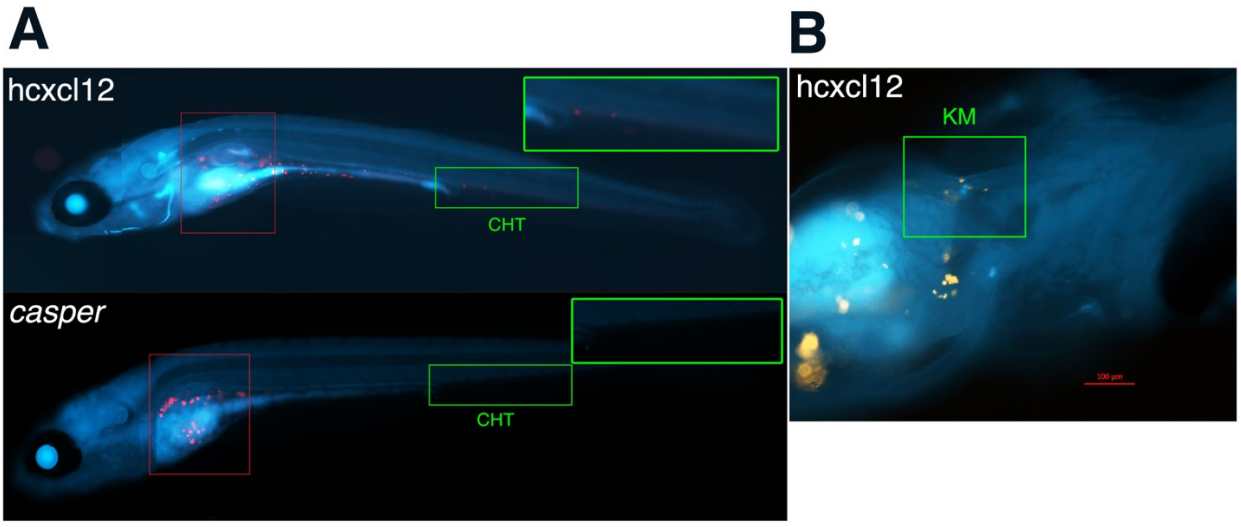

Figure 7: Jurkat cells home to the CHT and KM following transplantation into the CXCL12 transgenic fish.

A. Fluorescence microscopy shows Jurkat cell migration towards the zebrafish caudal hematopoietic tissue (CHT), the zebrafish equivalent of the human fetal liver at 6 days post-fertilization (dpf).

B. Ventral view of zebrafish with cell migration towards the kidney marrow (zebrafish equivalent of bone marrow) at 9 dpf.

3.4 GSS transgenic larvae show improved response to drug administration compared to controls

Following these validation experiments, both transgenic zebrafish lines were crossed to create a GSS (GM-CSF/CSF2, SCF/KITLG & SDF1α/CXCL12) triple transgenic fish. Taking into account the previous observation from Section 3.3, I wanted to evaluate in the xenotransplantation of human cells into the circulation of GSS fish improved proliferation compared to yolk-sac injection. We injected CMK cells both into the yolk and circulation of the larvae and found that there was a trend of increased proliferation in cells injected into circulation compared to that injected into yolk-sac (Figure 8A). I was then curious about the fitness of our model in a preclinical drug testing scenario. The ML-DS CMK cells were established from a ten-year-old patient who responded to cytarabine; so, I wanted to see if this response remains true in the context of GSS larvae. We injected CMK cells into the circulation of both GSS and *casper* larvae. The larvae were divided into two groups, and one group was administered with 1 mM cytarabine one day-post injection. While there was no significant difference between the cytarabine administered and untreated *casper* groups ($p=0.94$), the GSS larvae administered with cytarabine did show a significant decrease in the number of cells compared to the untreated control ($p=0.005$) (Figure 8B).

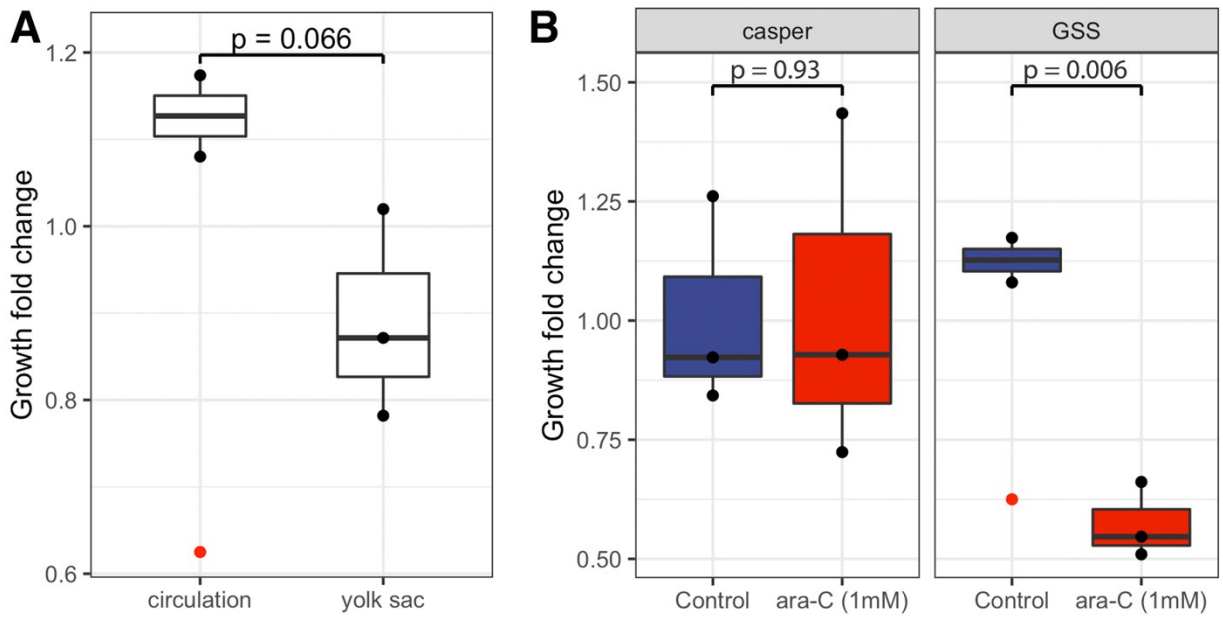

Figure 8: AML cells xenografted into GSS larvae show greater sensitivity to chemotherapy compared to control

A. Human CMK cells were xenografted into the yolk-sac and orthotopically into the circulation of the GSS larvae. A proliferation assay was performed at 3 dpi and number of cells at 1 dpi was measured as a baseline. Bar plot shows the number of cells normalized to the number of cells at the baseline. A p-value was calculated with a Student-t-test.

B. Human CMK cells that are responsive to cytarabine (ara-C) were xenografted into control *casper* and GSS larvae. The larvae were further divided into two groups, one of them were administered with 1 mM cytarabine, and the other was left untreated. Baseline number of cells in each group was calculated before drug administration (1 dpi) and the proliferation readout was measured 2-days-post-treatment (3 dpi). Bar plot shows the number of cells normalized to the number of cells at the baseline. The p-value was calculated with a Student-t-test on *casper* and GSS larvae separately.

3.5 GSS transgenic larvae show increased mortality compared to controls when transplanted with primary AML cells

I wanted to compare engraftment and expansion of primary patient-derived leukemias in the GSS larvae to controls. These xenografts were performed orthotopically by injecting primary AML cells into the circulation (common cardinal vein) at 72 hpf. We xenografted four distinct pediatric patient-derived AML samples: a CBL exon 8 deletion with *KMT2A-MLLT3* (*MLL-AF9*) fusion by karyotype (A23352); *KRAS* G12C point mutation (A23280), *KMT2A-MLLT3* fusion (AS12029811) and a ML-DS sample. Immediately post-injection, larvae were screened to select for similar number of cells in both GSS and control groups of fish. I tracked the larvae until one of the groups reached 50% mortality and used the remaining larvae for targeted error-corrected RNA sequencing (RNA-ECS; done in collaboration with the Druley Lab) (Figure 9A). While the number of days required to reach 50% mortality varied across AML samples, the GSS fish consistently suffered greater mortality compared to control larvae, indicating increased cellular proliferation and leukemic burden (Figure 9A). When transplanted with human HSPCs, both control and GSS larvae showed almost negligible death, indicating that the increased mortality was a result of leukemia proliferation and not injection artifact. Since most leukemias are heterogeneous, they provide us with genetic polymorphism or mutation-specific biomarkers that enable screening for conservation of heterogeneous clones present in the initial leukemia sample. I prepared RNA from human AML xenografted control and GSS zebrafish and performed RNA-ECS to quantify clonal variability and conservation via the relative abundance of human leukemia-specific gene transcripts in the background of zebrafish transcripts. While some SNP variants were detected alternatively in the GSS or the control fish, the GSS fish overall retained a higher number of SNP

variants, representing more leukemic clones than the control fish. Mutations like NOTCH (5094 C>T) and ALK (3375 C>A), which are silent and hence not pathogenic were only present with a high allelic frequency (AF>0.5) in GSS xenografts, suggesting elimination of some clones in the controls (Figure 9B). Altogether, the data from both the control and GSS xenografts yielded 46 high confidence nucleotide variants, only 23 (50%) were represented in controls compared to 42 (or 93.4% of) variants represented in the GSS zebrafish. This finding demonstrates that the GSS zebrafish provides a superior microenvironment for survival and expansion of human AML clonal diversity (Figure 9B).

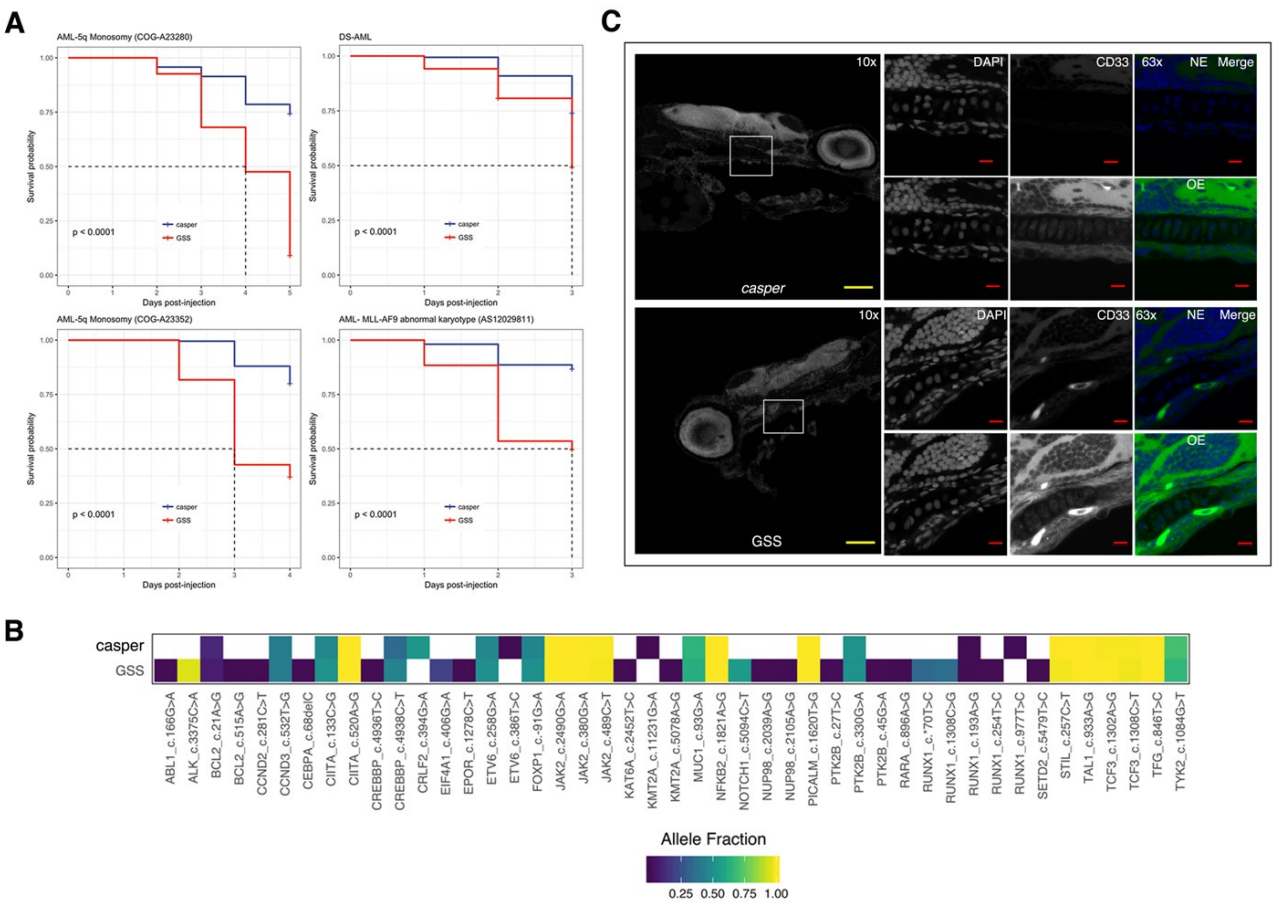

Figure 9: Patient-derived AML transplantation into GSS transgenic larvae increased AML-related disease mortality and showed increased clonal representation in comparison to control larvae.

A. Kaplan-Meyer curve showing increased AML related mortality in GSS larvae transplanted with each of four different patient-derived AML samples compared with *casper* control larvae transplanted with the same samples ($p<0.0001$).
B. Heat map showing increased clonal representation in the GSS larvae compared to control larvae transplanted with the same sample as measured by RNA-ECS. Different colors represent allele frequency from 0.002 (dark blue) to 1 (yellow). The white box represents an absence or allele frequency of less than 0.002.
C. Representative immunofluorescence images from sagittal zebrafish sections showing human CD33+ AML cells localized in the kidney marrow of the GSS transgenic. The left panel shows an overview of the fish section at 10x, and the white box highlights the region of interest. The top three right panels show images taken under normal exposure based on controls and the overexposed image shown in the middle of the lower three panels illustrates the kidney morphology. The parameters were kept constant between GSS and control sections during imaging (N=5). Yellow scale bar is equivalent to 100 µm, and the

red scale bar is equivalent to 10 μm. (GSS=GM-CSF/CSF, SCF/KITLG, CXCL12/SDF1α expressing transgenic zebrafish; RNA ECS=RNA error-corrected sequencing). The top panel shows images from KM of control larvae injected with human AML samples, where leukemia cells are not present, and the bottom shows GSS larvae with human CD33+ AML cells. Image specifications: 10x images: NA=0.45; 63x images: NA=1.4, Zoom = 1.5.

3.6 The CXCR4-CXCL12 locus is dispensable for the migration of human leukemia cells to the caudal hematopoietic tissue (CHT) but necessary for homing to the kidney marrow

During validation of the *CXCL12* transgenic zebrafish, I injected Jurkat cells into the yolk sac of 3 dpf larvae, and a proportion of the cells transplanted into the transgenic larvae showed migration to the CHT, a region equivalent to the fetal liver in humans. When we performed primary AML xenografts and injected these cells into circulation, cells migrated to CHT uniformly in both control and transgenic larvae. Importantly, however, we observed a profound difference in kidney marrow homing, with primary AML samples injected into the GSS larvae showing a propensity to migrate to the KM, which was not seen in controls (Figure 9C). In *CXCL12* KO mouse models, HSCs migrated from the AGM to the fetal liver, but fetal liver to bone marrow homing was impaired (Nagasawa et al., 1996; Zou, Kottmann, Kuroda, Taniuchi, & Littman, 1998). However, previous *in vitro* studies showed that both fetal liver and bone marrow-derived HSCs can respond to CXCL12 stimuli in a Boyden chamber assay (Christensen, Wright, Wagers, & Weissman, 2004). Together, these findings highlight that while the CXCR4-CXCL12 axis is critical in bone marrow homing, it may be dispensable for fetal liver homing. I wanted to see if the homing of human leukemia cells to the zebrafish CHT was CXCL12-CXCR4 dependent. To address this question, we returned to T-ALL where we had initially seen differential homing using Jurkat cells, and this time employed a primary patient-derived T-ALL sample expressing very high levels of CXCR4. This sample was injected into the circulation of GSS and control larvae. The majority of the T-ALL cells in both control and GSS transgenic larvae migrated and stationed in the CHT, consistent with publications from other groups (Sacco et al., 2016; Tulotta et al., 2016). However, in contrast to other zebrafish reports (Sacco et al., 2016; Tulotta et al., 2016), following the

addition of either a CXCR4-targeting antibody or isotype control, transplanted human T-ALL cells continued to migrate to the CHT (Figure 10 A & B). The above data is consistent with murine data and suggests that the CXCR4-CXCL12 axis does not significantly contribute to the migration of cells to the fetal liver.

A

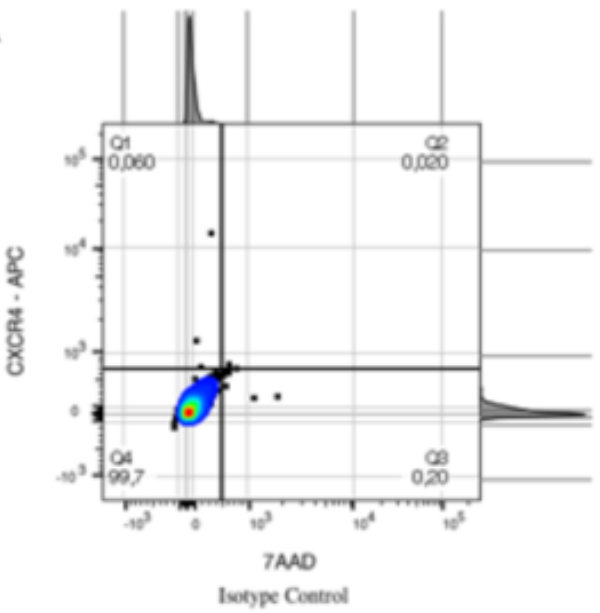

Isotype Control

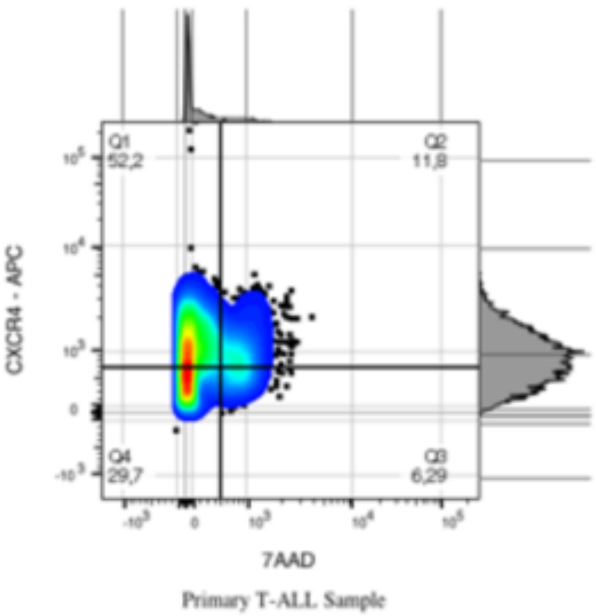

Primary T-ALL Sample

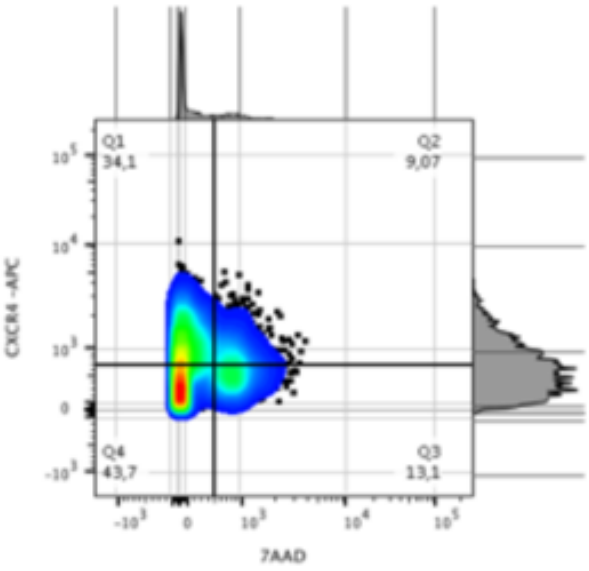

Neutralization Iso Ctrl

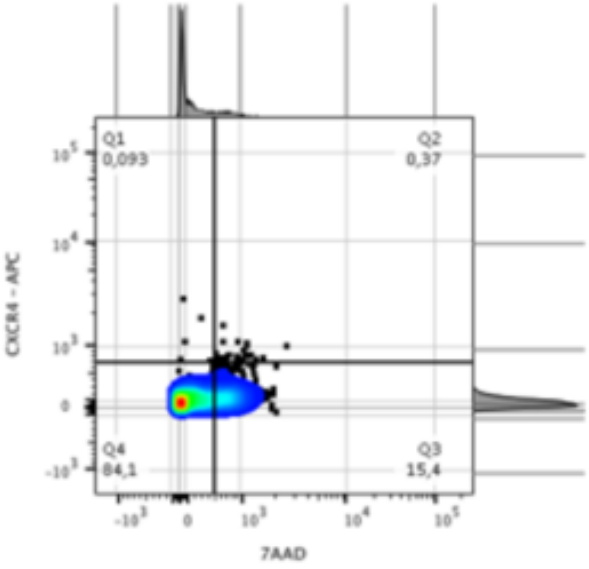

Neutralization with Fusin

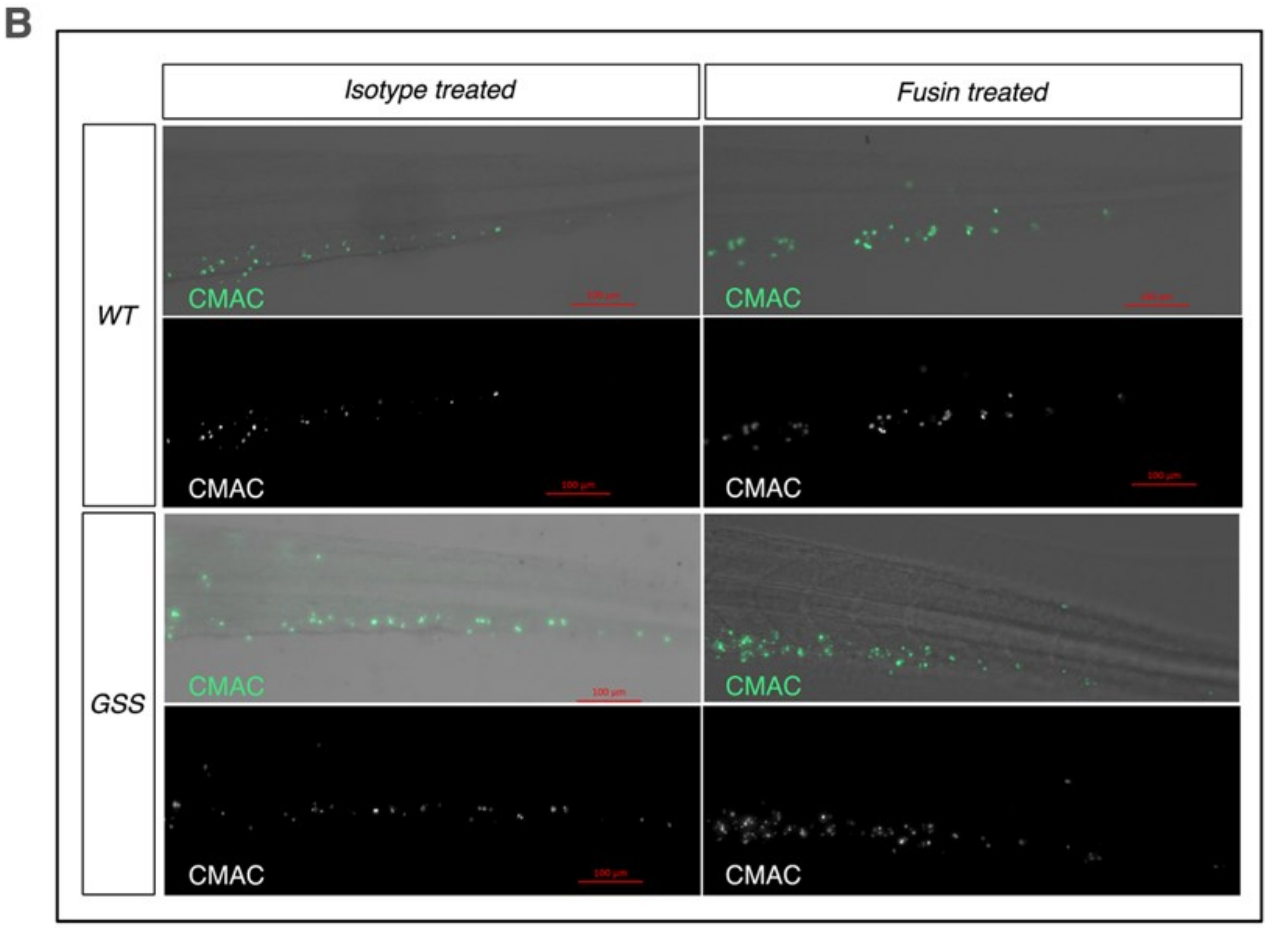

Figure 10: CHT migration of human leukemia cells are not dependent on CXCR4-CXCL12 axis.

A. Flow cytometry images demonstrate inhibition of the CXCR4 receptor using the anti-CXCR4 antibody (fusin).
B. Representative images from *casper* control and GSS larvae transplanted with isotype or fusin treated patient-derived T-ALL sample shows no difference in migration upon neutralization with CXCR4 antibody. (GSS=GM-CSF/CSF, SCF/KITLG, CXCL12/SDF1α) expressing transgenic zebrafish)

3.7 Xenotransplantation of human hematopoietic stem cells and progenitor cells into GSS fish exhibits both enhanced self-renewal capacity and multi-lineage differentiation

Despite the widespread success of human tumour cell engraftment in zebrafish, normal tissue xenografts, including hematopoietic cells, have not been reported to successfully engraft (Pruvot et al., 2011a). Given the enhanced proliferation observed for human leukemia samples transplanted into the GSS zebrafish, I wanted to determine if the presence of human cytokines could enhance human HSPC survival and differentiation in a zebrafish host. In collaboration with Dr. David Rittenberg (Department of Obstetrics and Gynecology, IWK Health Centre/Dalhousie University), the gynaecologist collected umbilical cord blood from newly delivered infants, and I isolated lineage depleted (lin^-) cells, which are highly enriched for human HSPCs. These cells were fluorescently labeled with a cytoplasmic dye and transplanted into the circulation of both *casper* control and GSS larvae at 72 hpf. Consistent with previous reports, human HSPCs did not survive past 24 hours in control larvae (Pruvot et al., 2011a), but HSPCs transplanted into GSS larvae continued to survive past 48 hours after which time, the cells began losing the cytoplasmic dye (Figure 11A). I extracted RNA for targeted exon sequencing from both control and GSS-injected larvae between 20-24 hpi. Of the three samples sequenced, only one injected control larva had a detectable level of human transcript, in contrast to the GSS larvae, for which all 3 HSPC xenografted samples were found to have detectable human transcripts present. To further determine if human transcripts are truly absent in the control fish, the Druley lab performed another round of ECS-RNA library preparation and increased the starting total RNA from 100 ng to 300-500 ng (depending on RNA availability). The absence of detectable level of human transcript was confirmed. Upon targeted transcriptome sequencing, I found that multilineage

differentiation occurred in both GSS and control larvae, but with a myeloid bias. In the lymphoid lineage, only B-cells were sufficiently tractable and transcripts of early T-cell markers, *CD3E* and *PTCRA*, were entirely absent, suggesting an absence of T-cell differentiation (Figure 9B). In terms of self-renewal capacity, HSPCs transplanted into GSS larvae showed increased expression of both *CD34* and *GATA2* (Figure 11B). Specifically, there were 194 and 4682 error-corrected transcripts of the human CD34 gene in 100 ng total RNA input for control and GSS samples respectively. While CD34 is a *bona fide* HSPC marker in hematopoietic cells, GATA2 is required for the maintenance, generation, and survival of HSPCs (de Pater et al., 2013). The increased expression of CD34 and GATA2 suggest that HSPCs undergo self-renewal only in the cytokine-rich context found in GSS larvae, but not in controls. Interestingly, there was an increase in human *caspase-3* expression, a pro-apoptotic marker, in HSPCs injected into control fish compared to the GSS larvae, suggesting an increased tendency to undergo apoptosis, providing a mechanism underlying the reduced survival of these human cells in the absence of human cytokines.

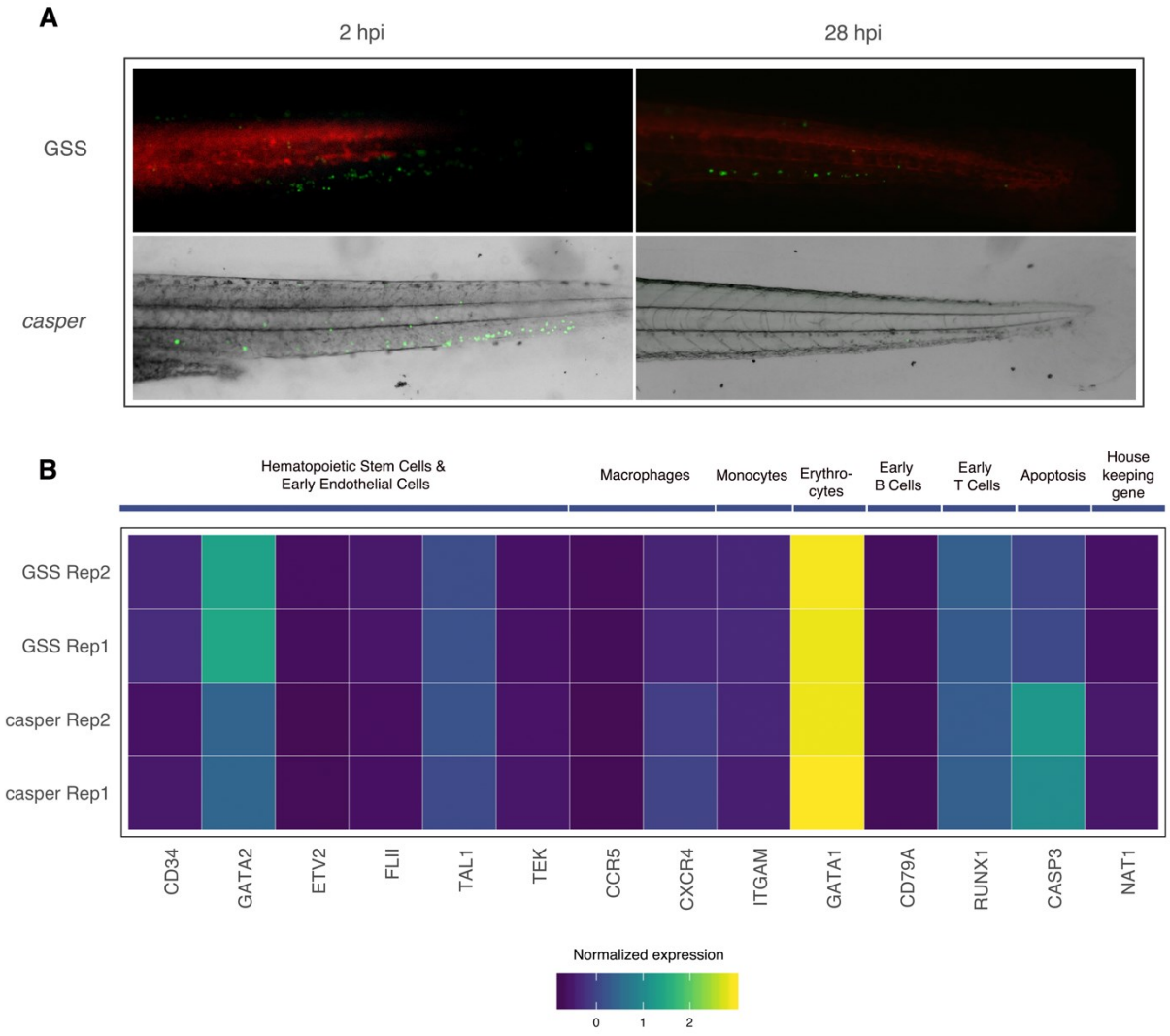

Figure 11: UCB-derived HSPCs show engraftment, self-renewal and multilineage differentiation in GSS larvae.

A. Representative image of GSS larvae and *casper* control larvae transplanted with UCB derived HSPCs. Image shows near complete absence of HSPCs in control larvae at 28 hours post-injection (hpi), whereas the HSPCs continue to survive in the GSS larvae at 28 hpi. Image specification: Magnification =10x, NA= 0.3
B. Heatmap from RNAseq analysis of transplanted HSPCs shows the increased expression level of self-renewal specific genes in HSPCs transplanted into GSS larvae. Control and GSS larvae showed an identical expression of different lineage-specific genes (UCB=umbilical cord blood; HSPCs=hematopoietic stem and progenitor cells; GSS=GM-CSF/CSF, SCF/KITLG, CXCL12/SDF1α expressing transgenic zebrafish).

3.8 Discussion

While murine xenografts have provided essential insights into human leukemia pathogenesis (Bonnet & Dick, 1997b; Lapidot et al., 1992; M. Wunderlich et al., 2010), and despite even greater opportunities provided by even more immunocompromised hosts, this model system continues to have limitations. Primary leukemia xenografts remain challenging in mice for many reasons, including intrinsic leukemic properties, absence or lack of bioactivity of some of the human factors found in the host microenvironment, and the presence of innate immune cells in the organism that eliminate transplanted cells. Moreover, the complexity of these murine xenograft experiments, including the time to engraftment (typically 3-6 weeks) renders studies difficult to conduct in a high throughput setting, and thus not easily amenable to clinically actionable drug screening experiments. The Berman lab in collaboration with the Dellaire lab, has pioneered human leukemia xenografts in zebrafish larvae and shown that this approach is amenable to medium-throughput drug screening in an actionable timeframe of 1-2 weeks (Bentley et al., 2014; Corkery et al., 2011). However, the issue of conserved elements within the tumour microenvironment is also applicable, as illustrated by previous unsuccessful efforts to develop sustainable human HSPC zebrafish xenografts (Pruvot et al., 2011a).

To address the inherent limitations of the zebrafish microenvironment for sustaining human tumour xenografts, we created a humanized zebrafish model, the GSS fish that expresses human CXCL12/SDF1α, SCF/KITLG, and GM-CSF/CSF2, to enhance human HSPC and patient-derived leukemia engraftment to enable real-time preclinical therapeutic studies. As prior humanized mouse models informed our choice of cytokines, the GSS fish resembles the NSG-SGM3 mouse model (Nicolini, Cashman, Hogge, Humphries, & Eaves, 2003; M. Wunderlich et al., 2010), which

expresses three cytokines with poor conservation between mouse and humans: GM-CSF, SCF, and IL-3. Zebrafish, being more evolutionarily distant, have only 20% conservation with the human CXCL12 ligand (Figure 12 A-B) and considerable alteration in the CXCR4 binding region in humans (Figure 12C). IL-3 is a critical factor in expansion and chemotaxis of hematopoietic cells, but hematopoietic cytokines often perform redundant functions. For its expansion and homing function, IL-3 activates Raf/MEK/ERK signaling and small GTPases such as Rac and Ras. CXCL12 follows a very similar mechanism of action and additionally controls the fate of HSCs by restricting differentiation and enhancing stemness (Arai et al., 2005). Also, GM-CSF, IL-3, and IL-5 share a common beta chain that acts as a signaling subunit (Rossjohn et al., 2000). GM-CSF also redundantly activates STAT and JAK2 pathways like IL-3 (Ihle, 1995). So, I hypothesized that together SCF, GM-CSF, and CXCL12 would compensate for the absence of human IL-3. Previous observations revealed that even though there is minor to low cross-reactivity of human GM-CSF and SCF between mouse and humans, overexpression in the NSGS mice increased the number of mouse myeloid cells at the expense of erythropoiesis (Nicolini et al., 2003). Since cytokine genes are expressed transiently, and at low levels, we considered that the quantity of cytokines secreted would be high in transgenic organisms, due to the use of powerful promoters and multiple integrations of the transgene, which might lead to increased stress in the animals.

A


hu_CXCL12/1-93
zf_CXCL12a/1-99

B


huCXCL12/1-93
zfCXCL12b/1-97

C

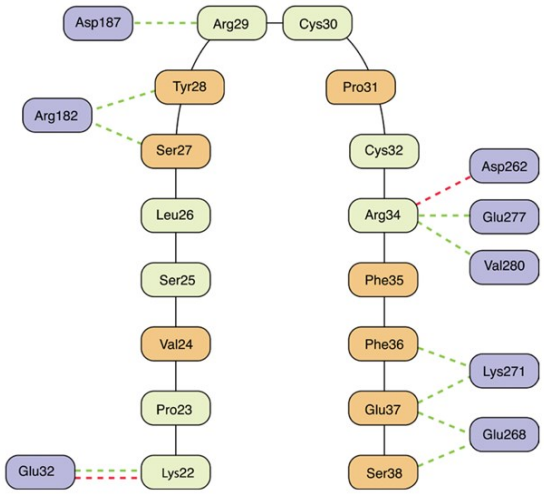
Asp187
Arg29
Cys30
Tyr28
Pro31
Arg182
Ser27
Cys32
Asp262
Leu26
Arg34
Glu277
Ser25
Val280
Phe35
Val24
Phe36
Lys271
Pro23
Glu37
Glu268
Glu32
Lys22
Ser38

Figure 12: Protein sequence alignment shows low conservation of the CXCR4 locus of CXCL12 between zebrafish and humans.

A&B. Protein sequence alignment between human CXCL12 and zebrafish CXCL12a and CXCL12b respectively. The red line indicates the known CXCR4 binding region, as observed in human.
C. Graphical overview of CXCL12-CXCR4 binding in humans. Amino acids conserved between human and zebrafish are enclosed in green boxes, those lacking conservation are in orange boxes and those from amino acids from CXCR4 are in violet boxes. The green dotted lines represent hydrogen bonds and the red dotted line represents salt bridges. Modified from Xu et al.(L. Xu, Li, Sun, Li, & Hou, 2013)

Also, the effect of prolonged exposure of human GM-CSF and SCF had not previously been studied in zebrafish, hence our choice of an inducible promoter.

I first showed that patient-derived AML cells show decreased disease latency and increased mortality of the GSS larvae, results that are consistent with findings from the NSG mouse model (M. Wunderlich et al., 2010) and can be applied in drug testing with survival as a readout. Using ECS, we demonstrated that human AMLs transplanted into GSS larvae maintain better clonal representation than transplants into zebrafish lacking human cytokines. These experiments highlight that clones that fail to survive in control larvae continue to survive in GSS larvae. The cells in the GSS larvae also specifically homed to the KM of the fish, while this was not observed in controls. These findings are indicative of the GSS fish providing a more clinically representative microenvironment to that found in humans.

Given the results observed with patient-derived AML transplantation into GSS zebrafish, I hypothesized that these humanized zebrafish might provide an improved host environment for engrafting human blood stem cells, which to date has been a challenge in the zebrafish field (Pruvot et al., 2011a). As previously demonstrated, UCB-derived HSPCs did not survive in control larvae but survived greater than 48 hours in the GSS larvae. ECS performed from these two different transplant populations revealed upregulation of human genes specific to self-renewal only in the GSS larvae. The maintenance of this key stem cell characteristic exclusively in the GSS larvae affirms the utility of the "GSS human HSPC model" as a platform for studying drugs that enhance stem cell expansion *in vivo*. By contrast, I saw significant levels of all transcripts

associated with multi-lineage differentiation in both control and GSS larvae, with the common exception of T-cell differentiation. While the myeloid bias in GSS fish might be expected due to expression of GM-CSF and SCF (Nicolini et al., 2003; M. Wunderlich et al., 2010), an absence of lymphoid cell differentiation in control larvae may be accounted for by the natural timeline of zebrafish lymphocyte development (the thymus does not appear until 5 dpf) and the lack of endogenous lymphoid-specific cytokines at this experimental time point. With the growing interest and efficacy in T-cell mediated cancer immunotherapy and the absence of a fully functional adaptive immune system in zebrafish larvae until a month of age, this model is poised for further manipulation with respect to T-cell differentiation as a future platform for the preclinical testing of novel immunotherapy approaches using human cancer and HSPC co-transplantation.

In summary, through the generation of novel humanized zebrafish that express key hematopoietic cytokines, the model in this chapter exploits the previously recognized imaging and higher throughput screening advantages of the zebrafish model system to create a powerful new preclinical tool. The GSS fish in conjunction with ECS bar-coding, can be used to screen for and also validate anti-leukemic and stem cell expanding therapeutics and contribute to the goal of providing biologically rational personalized treatment to patients.

Chapter 4: TET2-Loss-Of-Function Mutation Initiates a Proliferative Phenotype Upon Induction of Emergency Hematopoiesis.

4.1 Introduction

TET (ten-eleven-translocation) proteins are enzymes capable of catalyzing the reaction from 5-methylcytosine (5mC) to 5-hydroxymethylcytosine (5hmC) using ferrous iron and α-ketoglutarate as co-factors (H. Wu & Zhang, 2011). There are three TET orthologues seen in vertebrates: TET1, TET2, and TET3. Loss-of-function mutations in *TET2* are seen extensively in various human hematological disorders, including myelodysplastic syndrome (MDS)(Haferlach et al., 2013) and acute myeloid leukemia (AML), and in particular, in acute erythroblastic leukemia (AEL, AML-M6). While the impact of *TET2* mutations in the context of normal leukemia cytogenetics is still debated, *TET2* mutations are strongly correlated with poor prognosis in AML with intermediate-risk cytogenetics (W.-C. Chou et al., 2011).

Mutations in *DNMT3A*, *ASXL1* and *TET2* are the three most common mutations found in Clonal Hematopoiesis of Indeterminate Potential (CHIP) (Genovese et al., 2014). AML-related mutations in *TET2* and *DNMT3A* are ubiquitous in CHIP (A. L. Young et al., 2016). Individuals with a CHIP mutation have a modestly elevated chance of progressing to AML (Genovese et al., 2014), but many remain free of any hematopoietic malignancy throughout their lifetime (A. L. Young et al., 2016). The key question is what differentiates individuals harboring a *TET2* mutation who progress to leukemia from *TET2* mutant individuals who remain healthy.

TET2 differs biochemically from TET1 and TET3; the two latter TET proteins contain a ZF-CXXC (Zinc Finger-Cysteine-X-X-Cysteine) domain that helps in DNA binding. TET2 lacks the ZF-CXXC domain and the MBD (methyl-CpG binding domain). However, the TET2 N-terminal domain can bind SNIP1 (SMAD nuclear interacting protein 1), acting as a bridge between TET2 and various transcription factors to promote DNA binding (L.-L. Chen et al., 2018). This behaviour suggests that while TET1 and TET3 may be ubiquitous only depending on specific DNA binding motif in their catalytic activity, TET2 may be specific to transcription factor binding regions like distal promoter elements and enhancers (Rasmussen et al., 2019).

I generated a *tet2* mutant zebrafish that does not show any compensation from other *tet* genes. When I examined steady-state hematopoiesis of these mutants, they showed no change in the hematopoietic stem cell compartment but exhibited reduced numbers of lineage-committed cells. However, this reduction in lineage-restricted cells did not impact functional processes like hemoglobin synthesis. Transcriptomic and epigenetic analysis revealed an epigenetic-mediated restriction in hematopoietic differentiation of the mutant. Epigenetic analysis suggested deregulated ribosomal homeostasis and an upregulation of p53 observed in several inherited bone marrow failure syndromes (Elghetany & Alter, 2002). Further, the induction of stress hematopoiesis in the context of tet2 loss, led to a proliferative preleukemic phenotype.

4.2 Zebrafish *tet2* mutant shows no compensation from *tet* paralogs

I used CRISPR-Cas9 technology to create a 2.1 kb deletion within the exon 2 of the zebrafish *tet2* gene (Figure 13A & 13B). This *tet2* mutation resulted in a frameshift leading to a premature stop

codon that resulted in a small peptide of 19 amino acids (aa). I then utilized a previously developed algorithm (Nishikawa, Ota, & Isogai, 2000), to predict if there was a chance of an alternate start codon. The algorithm returned a 999aa truncated product, but with low reliability of 27%. This truncated Tet2 protein, if indeed translated, would contain an intact catalytic domain as determined from cDNA sequencing (Figure 13C). Other possible alternate codons and their possible products had even lower reliability than the 999aa product. The heterozygous mutant was outcrossed and subsequently incrossed it at least twice to generate a maternal zygotic mutant. Even in the case that a mutant allele might produce a truncated tet2 mutant protein (999aa compared to 1715aa), it would lack the binding site responsible for bridging partner proteins and thus poor recruitment to transcription factor binding sites (TFBS). The mutant also lacks Ser70 (Ser99 in human), a previously defined 'phospho-switch' that upon phosphorylation stabilizes the TET2 protein (D. Wu et al., 2018). The advantage of having stable mutant mRNA is the absence of a compensatory mechanism triggered by nonsense-mediated mRNA decay (El-Brolosy et al., 2019). The stability of *tet2* mRNA was consistently confirmed using quantitative reverse transcription (qRT)-PCR (Figure 14A). Even though this mutation did not have any effects on the viability of the zebrafish, the *tet2* mutant exhibited consistent and significant reduction in body size compared to *tet2* wild-type fish as seen during hatching and larval stages (Figure 14B).

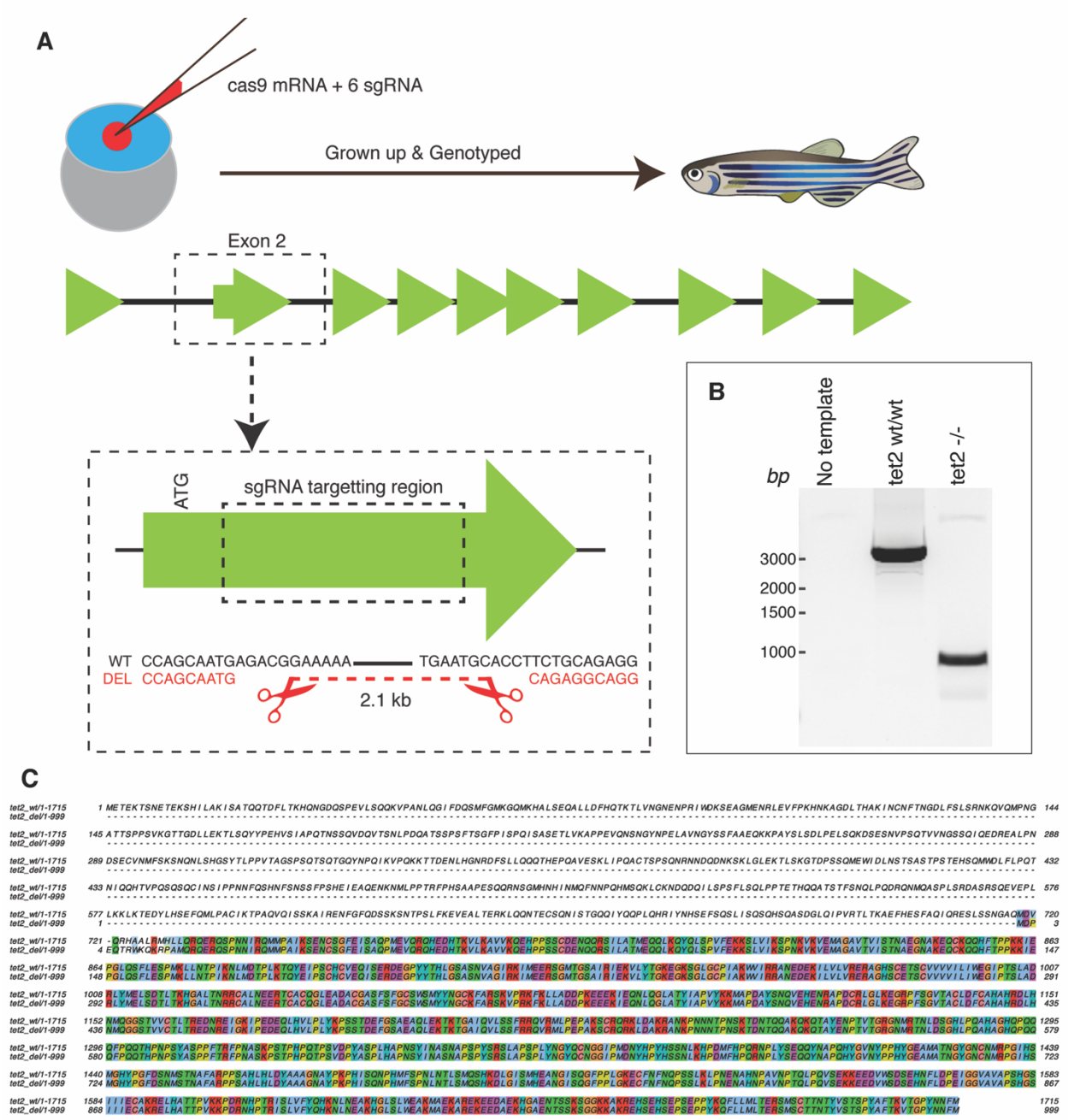

Figure 13: Generation of tet2 deficient zebrafish.

- **A.** A cocktail of Cas9 mRNA and six sgRNAs targeting exon2 was injected into single-cell stage zebrafish embryos resulting in a *tet2* mutant with 2.1kbp base pair (bp) deletion in exon 2.
- **B.** A PCR-assay spanning exon2 was developed that gives rise to a 2.7kbp amplicon in wild-type embryos. Agarose gel electrophoresis image shows a 3 kb band in the wild-type sample and <1 kb band in the *tet2-/-* sample. The mutant amplicon was further sequenced

using Sanger sequencing to find the absolute coordinates of the deletion and determined to be ~600bp in length.

C. PCR product from the tet2 mutant (Figure 13B) was Sanger sequenced. The resulting product was fed into a transcription start site predicting algorithm. The product with the maximum reliability was translated and aligned using Muscle algorithm.

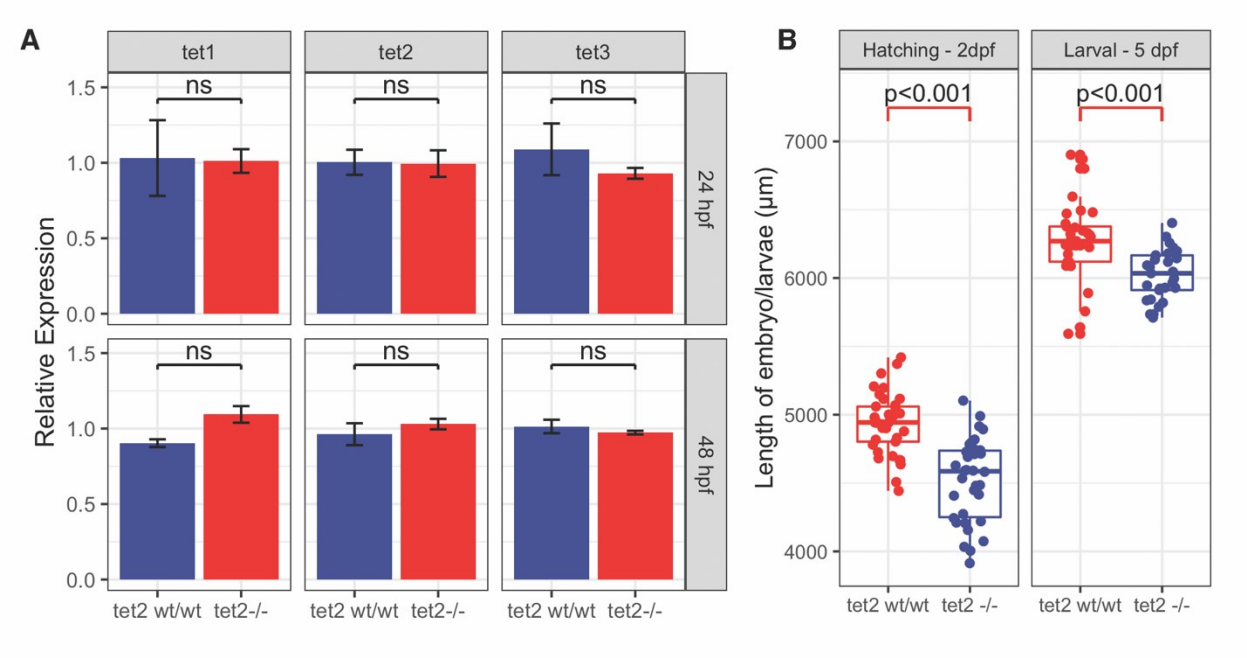

Figure 14: The zebrafish tet2 mutant shows no compensation from tet-paralogues.

(A) Quantitative RT-PCR of *tet* genes during the time periods of both primitive and definitive hematopoiesis showed no significant change in expression between wild-type and *tet2* deficient larvae.

(B) *tet2* deficient zebrafish are significantly smaller in size in comparison to wild-type zebrafish at both 2 and 5 dpf.

4.3 Zebrafish *tet2* mutants show no difference in HSCs but a decrease in myelopoiesis

I subjected the zebrafish *tet2* mutant and wild-type embryos to whole-mount *in situ* hybridization to examine the effect of *tet2* loss on zebrafish blood development during both primitive (24 hours post-fertilization; hpf) and definitive hematopoiesis (>48 hpf). First, I looked for any perturbations in the hematopoietic stem cell and progenitor cells (HSPCs) using a combination *cmyb/runx1* probe but did not observe any significant change in the HSPC pool (Figure 15A). I then examined the myeloid lineage and specifically early myeloid progenitors using the *pu.1 (spi1)* probe. I found that at two different time points, *tet2* mutant larvae showed a decrease in myeloid progenitors compared to WT larvae ($p<0.01$) (Figure 15B). Further, using probes specific to neutrophils and their progenitors (*mpx*), pan-leukocyte (*lcp1*) and mast cells (*cpa5*), I found a consistent and significant decrease in expression in *tet2* mutant larvae compared to wild-type larvae (Figure 15C-15E).

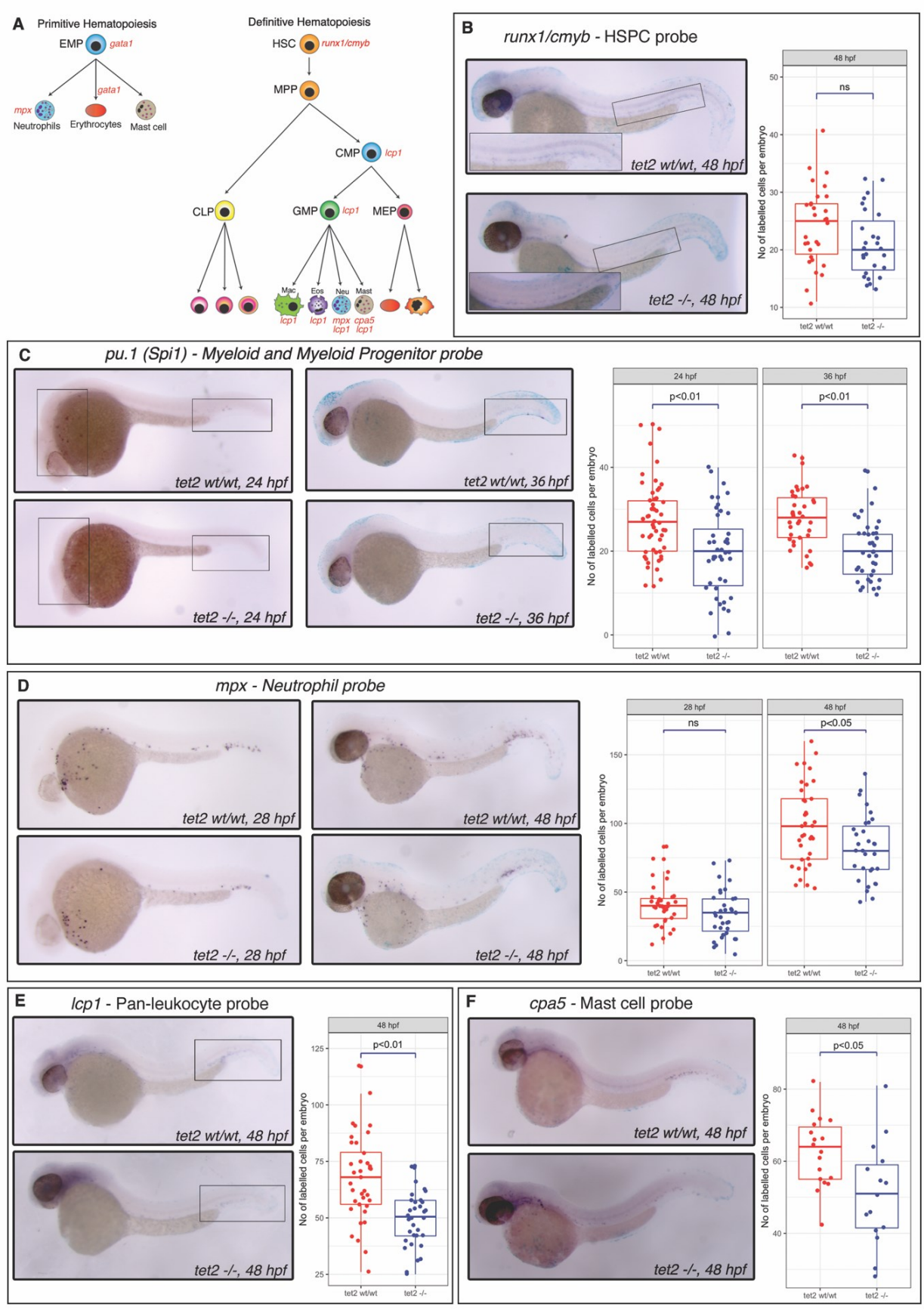
A
Primitive Hematopoiesis
EMP
gata1
gata1
mpx
Neutrophils
Erythrocytes
Mast cell
Definitive Hematopoiesis
HSC
runx1/cmyb
MPP
CMP
lcp1
CLP
GMP
lcp1
MEP
Mac
Eos
Neu
Mast
lcp1
lcp1
mpx
lcp1
cpa5
lcp1
B
runx1/cmyb - HSPC probe
tet2 wt/wt, 48 hpf
tet2 -/-, 48 hpf
48 hpf
ns
No of labelled cells per embryo
tet2 wt/wt
tet2 -/-
C
pu.1 (Spi1) - Myeloid and Myeloid Progenitor probe
tet2 wt/wt, 24 hpf
tet2 wt/wt, 36 hpf
tet2 -/-, 24 hpf
tet2 -/-, 36 hpf
24 hpf
p<0.01
36 hpf
p<0.01
No of labelled cells per embryo
tet2 wt/wt
tet2 -/-
D
mpx - Neutrophil probe
tet2 wt/wt, 28 hpf
tet2 wt/wt, 48 hpf
tet2 -/-, 28 hpf
tet2 -/-, 48 hpf
28 hpf
ns
48 hpf
p<0.05
No of labelled cells per embryo
tet2 wt/wt
tet2 -/-
E
lcp1 - Pan-leukocyte probe
tet2 wt/wt, 48 hpf
tet2 -/-, 48 hpf
48 hpf
p<0.01
No of labelled cells per embryo
tet2 wt/wt
tet2 -/-
F
cpa5 - Mast cell probe
tet2 wt/wt, 48 hpf
tet2 -/-, 48 hpf
48 hpf
p<0.05
No of labelled cells per embryo
tet2 wt/wt
tet2 -/-

Figure 15: tet2 deficient zebrafish demonstrate reduced myelopoiesis.

(A) Markers used for whole mount *in situ* hybridization that mark various blood cell lineages during primitive (24- and 28-hours post-fertilization; hpf) and definitive hematopoiesis (48 hpf) based on time of origin. EMP – Erythroid Myeloid Progenitor, HSC – Hematopoietic Stem Cell, MPP- Multipotent Progenitor, CLP – Common Lymphoid Progenitor, CMP – Common Myeloid Progenitor, GMP – Granulocyte/Macrophage Progenitor, MEP – Megakaryocyte/Erythroid Progenitor.

(B) Hematopoietic stem and progenitor cells marked by *runx1/cmyb* probe show no significant change ($p=0.14$) between wild-type and *tet2* deficient zebrafish larvae.

(C) Zebrafish *tet2* deficient larvae show reduced myeloid and myeloid progenitor cells compared to wild type both during primitive ($p<0.001$) and definitive hematopoiesis ($p<0.001$).

(D) Neutrophils in *tet2* deficient zebrafish demonstrate no reduction during primitive hematopoiesis ($p=0.09$), but significantly reduced during the definitive phase compared to wild-type larvae ($p=0.0107$).

(E) Monocytes are reduced in *tet2* deficient larvae during definitive hematopoiesis compared to wild-type larvae ($p<0.001$).

(F) Mast cells are reduced in *tet2* deficient larvae during definitive hematopoiesis compared to wild-type larvae ($p=0.0117$).

4.4 Zebrafish *tet2* mutants show a decrease in erythropoiesis with no difference in hemoglobin production

I then used a *gata1* antisense RNA probe to look at erythroid progenitors and found that there was a decrease in erythropoiesis (Figure 16A). Since erythroid cells are abundant and I cannot accurately count the exact number of these cells, I performed qRT-PCR and found that there was decreased *gata1* expression in *tet2* mutant larvae compared to wild-type larvae (Figure 16B). Even though there was a decrease in erythroid progenitors, *tet2* mutants survived to adulthood. We then looked at gene expression levels of embryonic globin genes. All of the four prominent embryonic globin exhibited trends of downregulation in *tet2* mutants compared to wild-type, which was maintained at 48 hpf where three out of four embryonic globin genes were down-regulated significantly ($p<0.05$) and the remaining one showed a trend to downregulation (Figure 16C). To assess function, I performed o-dianisidine staining and quantified the hemoglobin level based on automated intensity quantification. We found that there was no significant change in hemoglobin levels in *tet2* mutant versus wild-type larvae (Figure 16D), despite downregulated globin mRNA levels. This finding may be due to the robustness of embryonic globin mRNA to produce enough hemoglobin.

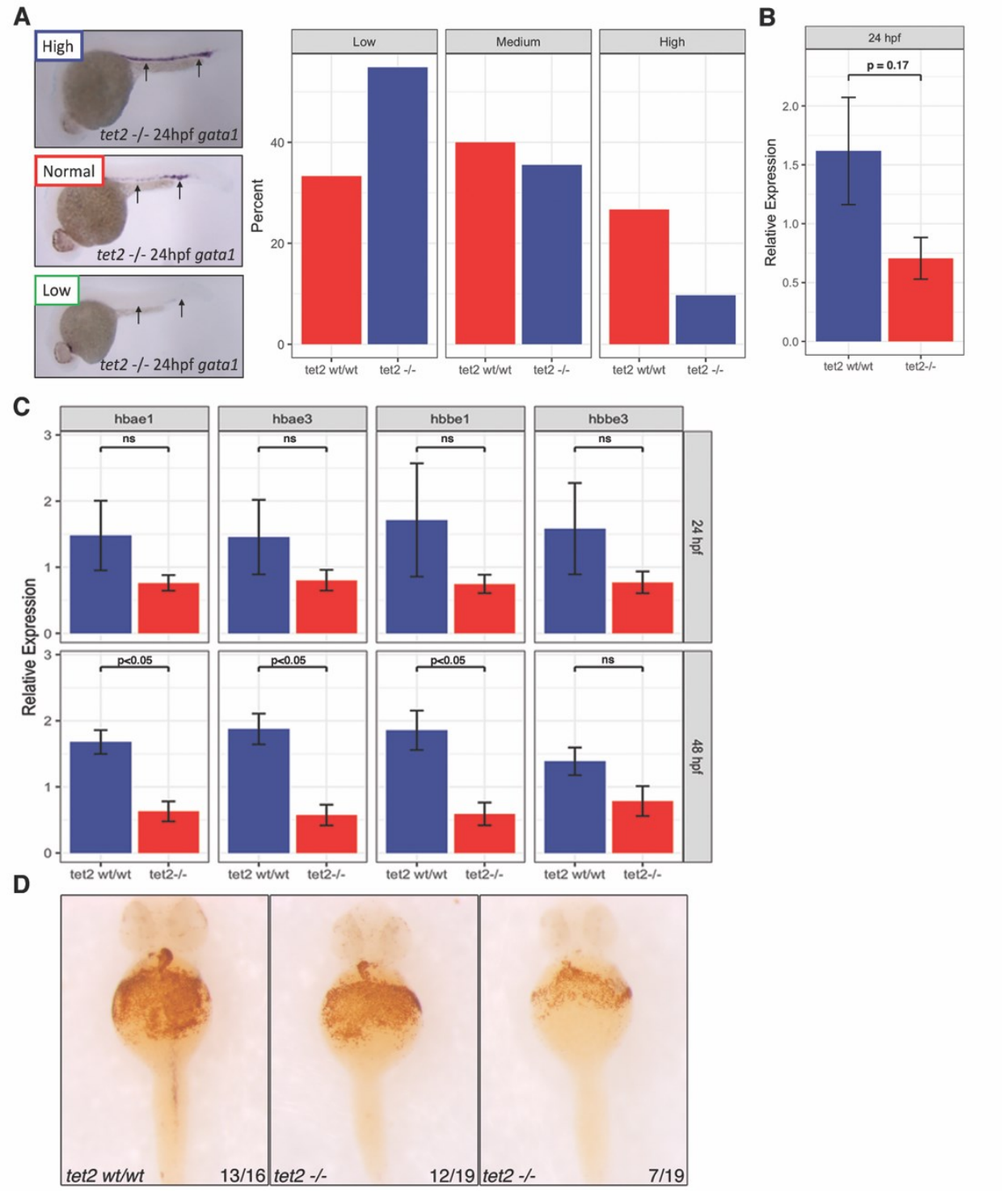

Figure 16: tet2 deficient zebrafish display reduced erythropoiesis.

(A) Erythroid progenitors were labeled using the *gata1* RNA probe. Embryos were classified into three groups, as highlighted. Bar graphs show that more than 50% of *tet2* deficient embryos had a lower number of gata1+ cells.

(B) Quantitative RT-PCR shows a trend of decreased *gata1* expression in *tet2* deficient larvae compared to the wild-type control.

(C) Quantitative RT-PCR of embryonic hemoglobin genes shows a trend of reduced expression across all hemoglobin genes during primitive hematopoiesis; while during definitive hematopoiesis, there was a significant ($p<0.05$) reduction in alpha embryonic globin 1 (*hbae1*), alpha embryonic globin 3 (*hbae3*) and beta embryonic globin 1 (*hbbe1*).

(D) O-dianisidine staining for hemoglobin showed no change in hemoglobin levels between wild-type and *tet2* deficient larvae.

4.5 Zebrafish *tet2* mutants show increased methylation specific to key hematopoietic promoters

Since tet2 is a DNA methylcytosine dioxygenase that catalyzes the reaction from 5mC to 5hmC, I carried out methylated and hydroxymethylated DNA immunoprecipitation followed by sequencing (MeDIP-Seq and hMeDIP-Seq) from the hematopoietic cells extracted from the kidney marrow of adult zebrafish (3-6 months) in collaboration with Hirst lab (University of British Columbia, Vancouver). This experiment aimed to verify the DNA methylation effects of my *tet2* mutant and implications on the methylation status caused by possible tet2 DNA binding. I analyzed the peaks from both the enriched and negatively enriched data and mapped them to genomic features. My analysis showed that there was reduced hydroxymethylation in the regions of the proximal promoters and intragenic regions compared to the negative peaks. The methylation pattern was comparable for proximal promoter intragenic regions when compared between positive and negative peaks (Figure 17A). TET2 specifically binds to promoter and intragenic regions to perform catalysis (Rasmussen et al., 2019). The above findings strongly corroborate that my *tet2* mutant shows reduced 5mC to 5hmC conversion. I then carried out RNA sequencing and found downregulation of key hematopoiesis-related genes, including adult beta globin (*hbba1*), major histocompatibility complex and solute carrier family genes (Figure 17B). Among the upregulated genes were tripartite motif (TRIM) family proteins (Figure 18). This protein family plays key role in activation of innate immunity and interferon signalling (Hatakeyama, 2017).

Further, I subjected the peak sequences from methylation data to transcription factor (TF) peak-motif analysis and found that the transcription factors corresponding to TFBS are critical factors

related to HSC differentiation (Figure 17C). These included Homeobox A10 (HOXA10), a master regulator of postnatal hematopoiesis that controls erythrocyte/megakaryocyte differentiation through the transcription of *GATA1* downstream (Magnusson et al., 2007). One of the two homologues of hoxa10 present in the zebrafish (hoxa10b) was downregulated in the RNAseq results (Figure 17B). Forkhead box (FOX) gene families, which are *bona fide* hematopoietic differentiation factors, were similarly downregulated. Regulatory Factor X2 (RFX2), known to bind to a critical cis-enhancer downstream of the IL5 receptor α (*IL-5Rα*) gene contributing to eosinophilic and basophilic differentiation, was also downregulated (*12*), as was Zinc Finger Protein 384 (ZNF384), a gene with a high propensity to be a partner in fusion in B-cell leukemia. We also looked for corresponding genes whose promoters were highly methylated, and this list (Table 3) included 5S rRNAs, an essential component of the 60s ribosomal complex (Ciganda & Williams, 2011) and jumonji domain-containing protein 6 gene (*jmjd6*), encoding an enzyme known for its function of hydroxylation and demethylation of histones and nucleic acids, as well as RNA splicing. Similar to TET2, this enzyme is also dependent on ferrous iron (Fe^{2+})- and 2-oxoglutarate (2OG) to perform catalysis (Kwok, O'Shea, Hume, & Lengeling, 2017). A low dosage of both of these genes would adversely affect protein translation through aberrant ribosome assembly and defective mRNA splicing, respectively.

Table 3: List of methylated promoters in tet2 mutant vs wild type meDIP.

Ensembl Gene ID	Symbol
ENSARG00000001859	dbx1b
ENSDARG00000055558	pimr63
ENSDARG00000055558	pimr63
ENSDARG00000074639	CABZ01090749.1
ENSDARG00000075584	itfg1
ENSDARG00000075584	itfg1
ENSDARG00000075584	itfg1
ENSDARG00000088349	U5
ENSDARG00000089244	U5
ENSDARG00000089487	U1
ENSDARG00000089699	U1
ENSDARG00000090852	U5
ENSDARG00000091732	U5
ENSDARG00000093486	BX664716.1
ENSDARG00000093486	BX664716.1
ENSDARG00000093486	BX664716.1
ENSDARG00000093486	BX664716.1
ENSDARG00000093873	BX324213.1
ENSDARG00000093977	si:ch211-220f16.1
ENSDARG00000093977	si:ch211-220f16.1
ENSDARG00000093977	si:ch211-220f16.1
ENSDARG00000093977	si:ch211-220f16.1
ENSDARG00000094302	BX296552.1
ENSDARG00000095704	si:dkey-4c15.13
ENSDARG00000095704	si:dkey-4c15.13
ENSDARG00000095704	si:dkey-4c15.13
ENSDARG00000095704	si:dkey-4c15.13
ENSDARG00000096729	CR385078.3
ENSDARG00000096904	si:dkeyp-100a5.4
ENSDARG00000097694	CU137681.5
ENSDARG00000097945	CU137681.6
ENSDARG00000098692	U1
ENSDARG00000099662	U1
ENSDARG00000099818	5S_rRNA

Ensembl Gene ID	Symbol
ENSDARG00000100744	U1
ENSDARG00000100880	5S_rRNA
ENSDARG00000101416	U1
ENSDARG00000102896	jmjd6
ENSDARG00000102896	jmjd6
ENSDARG00000103706	U1
ENSDARG00000104060	U1
ENSDARG00000107406	CU207269.6
ENSDARG00000107406	CU207269.6
ENSDARG00000107967	CU406963.1
ENSDARG00000108003	BX000463.3
ENSDARG00000108462	CU207269.8
ENSDARG00000108462	CU207269.8
ENSDARG00000108462	CU207269.8
ENSDARG00000108503	BX510309.6
ENSDARG00000108696	CABZ01073286.1

I also performed RNA-seq analysis of hematopoietic cells from the kidney marrow with the help of Genewiz and followed it with pathway enrichment analysis. Pathway enrichment analysis of the differentially expressed genes using ReactomePA showed upregulation of multiple DNA repair pathways (Figure 17D), an indication of possible genotoxic stress. The downregulated pathways include various amino-acid metabolic pathways (Figure 17E), downregulation of which is part of the candidate gene signature seen in preleukemic states (L. Li et al., 2011).

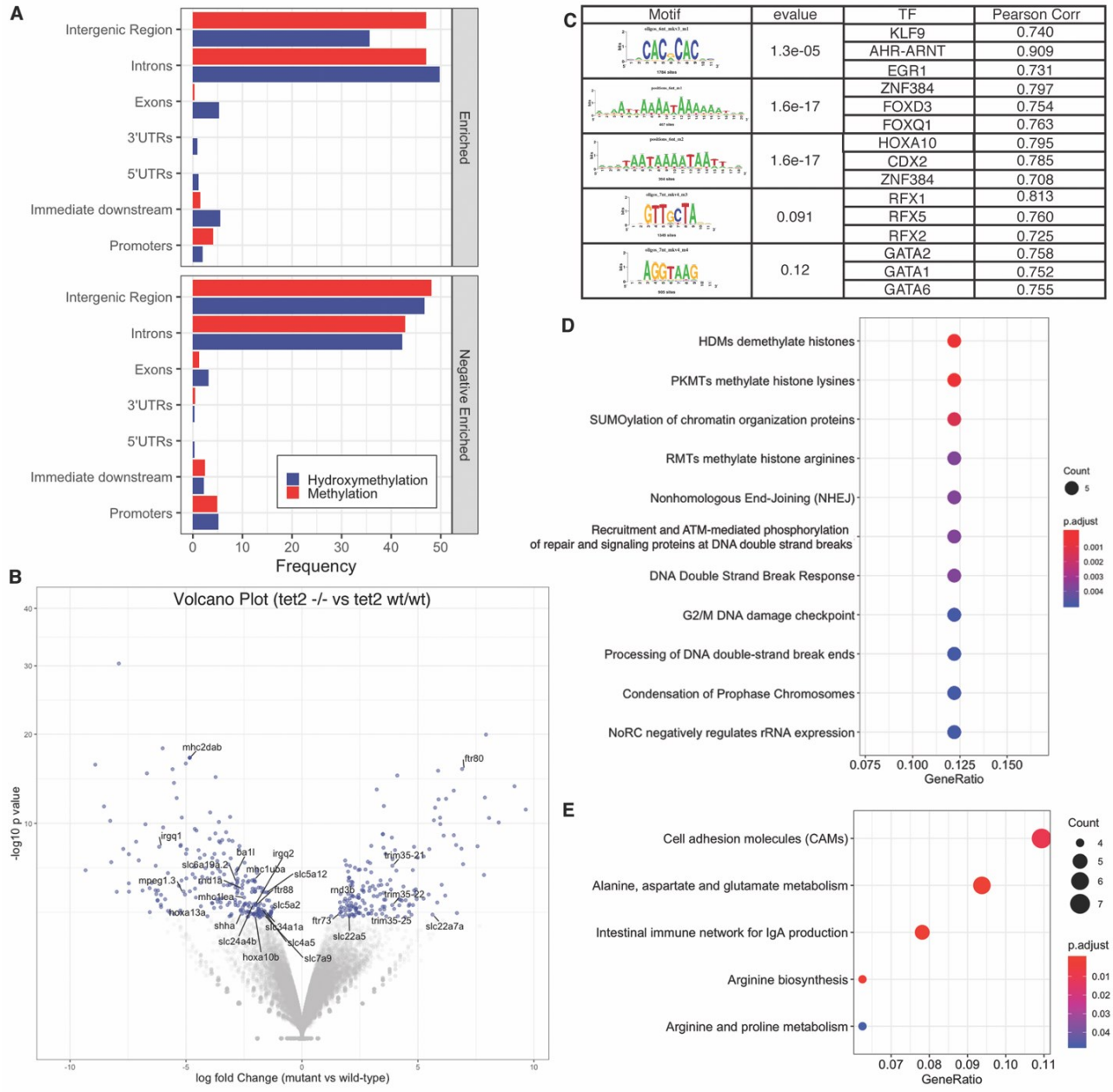

Figure 17: MeDIP/hMeDIP and RNAseq analysis of adult kidney marrow shows that tet2 loss has an impact on hematopoietic differentiation-related genes.

(A) MeDIP and hMeDIP plots were plotted based on the frequency of methylation and hydroxymethylation enrichment respectively. hMEDIP sequencing analysis shows a decrease (positive peaks vs. negative peaks) in the hydroxymethylation profile of *tet2* mutant larvae, which is restricted to the intergenic and promoter regions.

(B) Volcano plot of RNAseq analysis shows downregulation of key hematopoietic genes and upregulation of TRIM family genes (labelled). The genes which are significantly regulated are indicated with a blue dot (FDR>0.05).

(C) The table lists motifs and enriched transcription factor (TF) from TF binding analysis of hypermethylated sequences of *tet2* deficient zebrafish kidney marrow cells.

(D) Pathway enrichment was performed from the list of upregulated genes (p-value cut-off=0.05), showing enrichment of DNA damage repair pathways and pathways regulation rRNA expression.

(E) Kegg pathway enrichment of downregulated genes (p-value cut-off=0.05) shows enrichment of pathways involving amino acid metabolism and cell-to-cell adhesion.

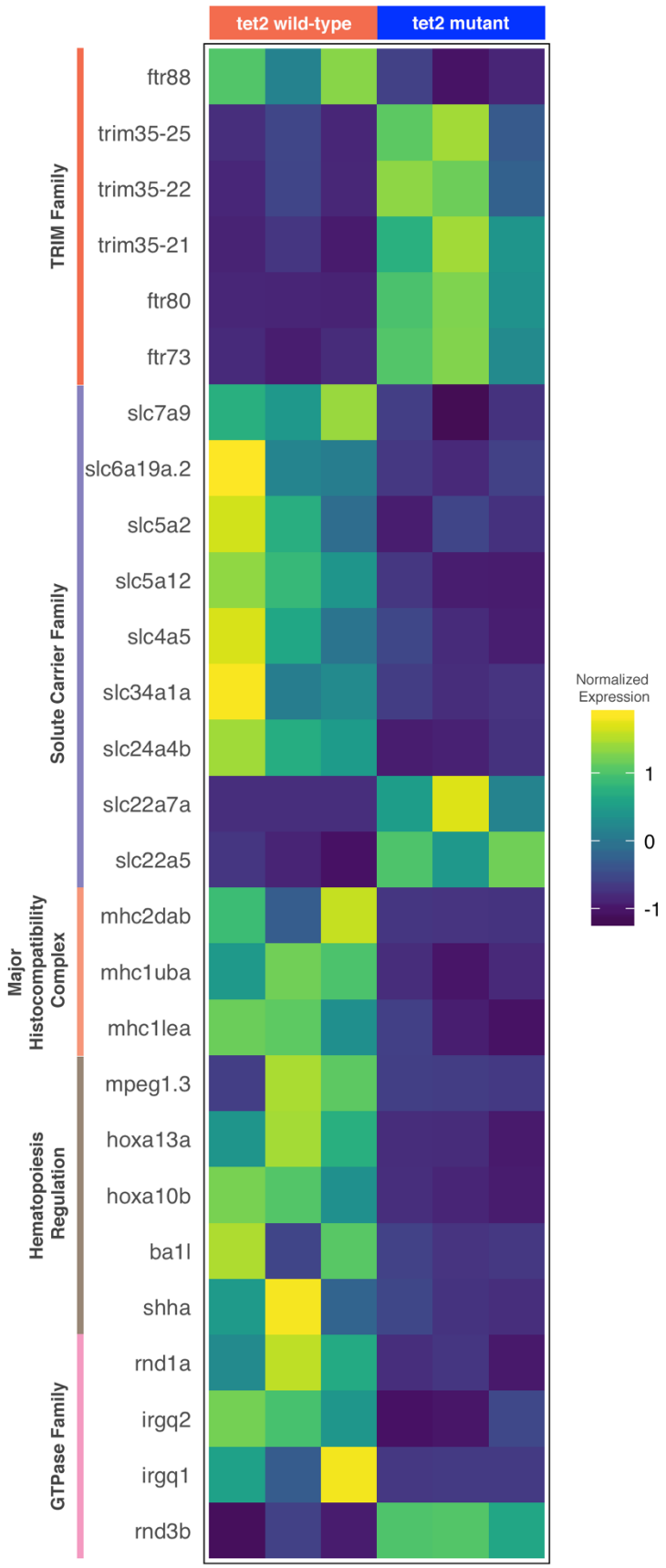

Figure 18: Heatmap of selected differentially upregulated and downregulated genes from RNAseq.

A heatmap was generated for the normalized data for genes clusters based on functions. The normalized data was further normalized across the list of selected genes in order to obtain normalized expression for heatmap analysis. Genes belonging to the TRIM family, solute carrier family, MHC, hematopoietic regulation and GTPase activity were significantly regulated.

4.6 Negative regulation of 5s ribosomal RNA expression in tet2 mutants increases p53

Our results from methylation sequencing showed increased methylation of the 5srRNA promoter in the *tet2* mutant. When we analyzed the RNA-seq results from the kidney marrow and performed pathway enrichment, we saw upregulation of pathways specific to negative epigenetic regulation of rRNA genes (Figure 17D & Figure 19A). Previous literature suggests that mice lacking *60s Ribosomal protein L29* (*Rpl29)* showed global growth defects; a finding in keeping with the reduced size observed in *tet2* mutant larvae (Figure 12D).

I was curious to know if *tet2* zebrafish mutants develop ribosomopathy-like features seen in various preleukemic conditions. One feature observed in ribosomopathies is the upregulation of p53 at the protein level, due to blockade of MDM2 and the MDMX axis (Dror, 2002). Also, previous literature suggests differential expression of rRNA is known to impact p53 expression, so I wanted to see if p53 was differentially regulated in the *tet2* mutants. I found increased p53 protein expression in *tet2* mutants compared to *wild-type* controls (Figure 19 B&C). I next wanted to see if this increase in p53 correlated to an increase in p53-dependent transcripts like p21 (*cdkn1a*) and *bax*. However, paradoxically, levels of p21 and *bax* gene expression were lower in *tet2* mutant larvae compared to *wild type* following treatment with gamma irradiation (Figure 19 D).

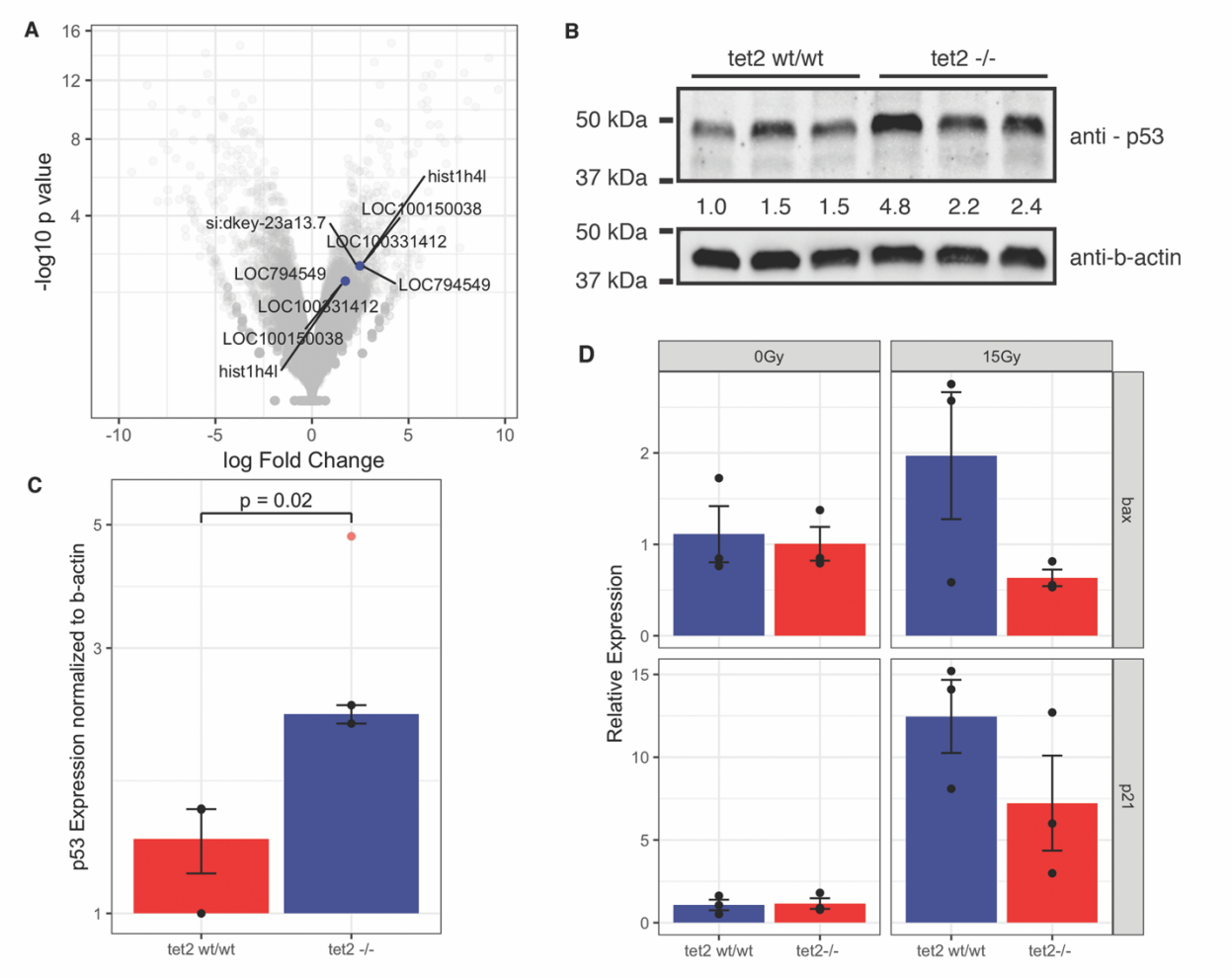

Figure 19: Absence of tet2 leads to upregulation of genes involved in transcriptional repression of rRNA that may contribute to increased p53 levels.

(A) Volcano plot of RNAseq analysis. Genes indicated with blue dots are genes that contribute to the negative regulation and epigenetic repression of rRNA transcription as found in Fig. 16D.

(B) Immunoblotting shows increased levels of p53 in 24-hour post-fertilization (hpf) embryos that lack *tet2* compared to age-matched wild-type embryos.

(C) Quantification of immunoblot relative to beta-actin shows a trend towards increased p53 expression in embryos that lack *tet2* (p=0.16).

(D) Lack of *tet2* leads to no change in *p21* and *bax* levels in uninduced conditions, but unlike in wild-type embryos, *p21* and *bax* levels in *tet2* deficient larvae (54 hpf) decrease in response to gamma irradiation.

4.7 Emergency granulopoiesis leads to increased immature granulocytes in *tet2* mutants

Previously studies with p21 knock-out mice showed that p21 absence is associated with higher levels of inflammation and neutrophil proliferation during infection (Martin et al., 2016). Therefore, given the lower levels of p21 expression observed upon induction of genotoxic stress, I next asked if the induction of emergency granulopoiesis would lead to a proliferation of immature granulocytes. First, I directly induced emergency granulopoiesis by microinjection of zebrafish granulocyte colony stimulating factor *(gcsf; csf3)* mRNA into one-cell stage zebrafish embryos and looked for cells positive for *cebp1*. *cebp1* is a zebrafish homologue of CEBP1-epsilon (CEBP1ε) expressed in humans, which marks proliferating granulocytes and progenitors (Figure 20A). I detected an almost 2-fold increase in *cebp1*+ cells in the *tet2* mutant larvae injected with *gcsf* mRNA compared to similarly treated wild-type larvae (Figure 20B & 20C). Next, I repeated this experiment using PAM3CSK4 (PAM), a Toll like receptor 2 (TLR2) agonist that closely mimics bacterial infection and induces expression of proinflammatory cytokines similar to bacterial response. PAM was injected into the circulation of 48 hpf larvae, and at two days-post-injection (2dpi) I again observed a 1.7-fold increase in *cebp1+* cells in the *tet2* mutant larvae injected with PAM compared to wild-type controls (Figure 20D & 20E).

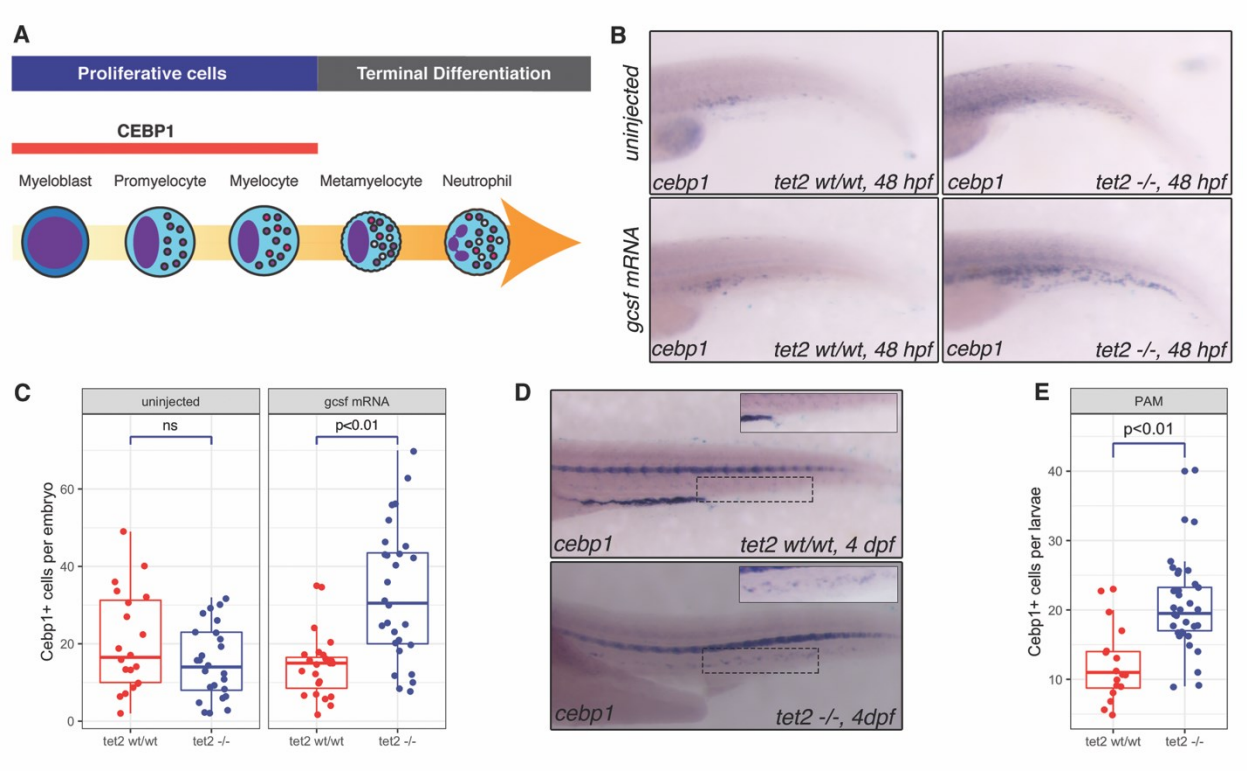

Figure 20: Stress-induced granulopoiesis leads to an increase in immature cells in tet2 deficient larvae.

(A) Graphical representation showing normal granulopoiesis and the time-point of *CCAAT/enhancer-binding protein 1 (cebp1)* expression during the process.

(B) Representative 48-hour post-fertilization (hpf) whole-*mount in situ* hybridization images of wild-type and *tet2* deficient embryos injected with zebrafish *gcsf* mRNA at the single-cell stage. The images show an increase in cebp1+ cells in *tet2* deficient embryos in comparison to wild type *gcsf* injected larvae.

(C) Quantification of cebp1+ cells in wild-type and *tet2* deficient embryos shows no difference in the uninjected condition, but upon gcsf induction, tet2 lacking embryos exhibit a ~2-fold increase in cebp1+ cell numbers compared to wild-type larvae ($p<0.01$).

(D) Representative whole-mount *in situ* hybridization images of wild-type and *tet2* deficient embryos injected with PAM3CSK4 (PAM), a TLR2 agonist at 48 hpf. The images show an increase in cebp1+ cells in PAM injected embryos lacking tet2 in comparison to wild-type injected embryos. (E) Quantification of cebp1+ cells in wild-type and *tet2* deficient embryos show a 1.7-fold increase in cebp1+ cell numbers compared to wild-type cells ($p<0.01$).

4.8 Exposure of *TET2* mutant cells to cytokines increase proliferation during differentiation

I then asked if emergency hematopoiesis induction specific to other hematopoietic lineages would result in similar findings and if this would be true in a human context. I immunomagnetically enriched hematopoietic stem and progenitor cells (HSPCs) derived from human umbilical cord blood cells and targeted *TET2* using hit and run CRISPR methodology (Figure 21A). I used a sgRNA targeting the human *TET2* gene for this experiment, and cells targeted only with HiFi Cas9 was used as control. Four days following gene editing, a sample was collected for amplicon sequencing, and the HSPCs were allowed to differentiate into erythroid cells in a serum-free composition containing recombinant interleukin 3 (IL3), stem cell factor (SCF), and erythropoietin (EPO). EPO and IL3 are inducers of stress hematopoiesis (Vemula et al., 2012; J. L. Zhao & Baltimore, 2015). We collected another sample for amplicon sequencing at Day 14 of differentiation. Upon analyses of amplicon sequencing results across multiple samples, I saw that the TET2 mutant cells that were initially less than 5% of the sample at Day 0 increased to more than 50% at the end of Day 14 (Figure 21B). This result clearly shows that TET2 loss confers growth and proliferative advantages to HSPCs. Flow cytometry analysis showed an increase in CD45 dim, CD117+ and CD71+ cells (CFU-E) and proerythrocyte populations (Figure 22). The increase in proerythrocytes were almost 2-fold higher in the *TET2* mutant cells compared to mock-transfected controls when controlling for the number of live cells (Figure 21C). The observed results are consistent with the results we observed in *tet2* mutant zebrafish, where there was an increase in *cebp1*+ proliferating myeloid cells.

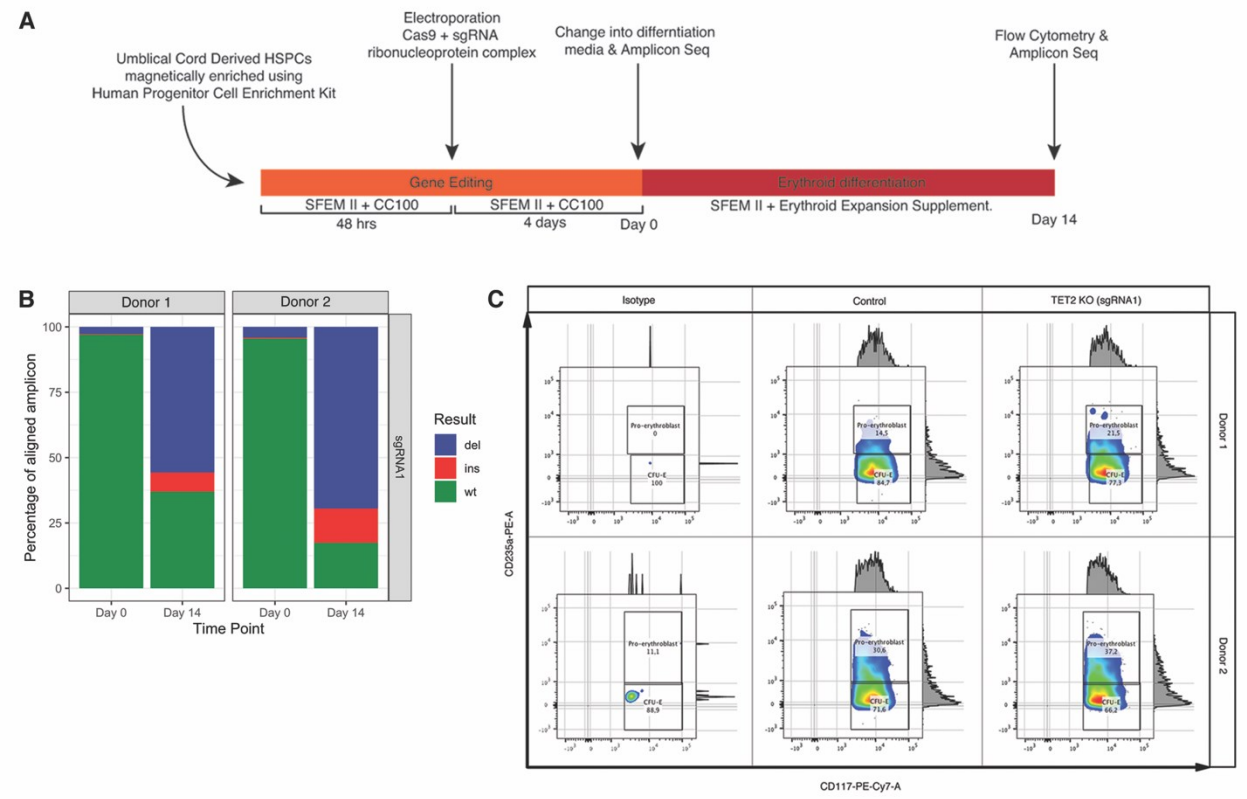

Figure 21: Differentiation induction under high cytokine conditions increases BFU-E and proerythrocyte population in human HSPCs lacking TET2.

(A) Graphical overview of the experimental strategy.

(B) Amplicon sequencing of CRISPR mutated human cord-blood derived human stem and progenitor cells (HSPCs) before differentiation and after differentiation suggests a clonal advantage of *tet2* mutant cells.

(C) Flow cytometry profile of *tet2* mutant HSPCs at 14 days of differentiation from two biological donors shows an increase in the proerythrocyte population compared to mock-transfected cells.

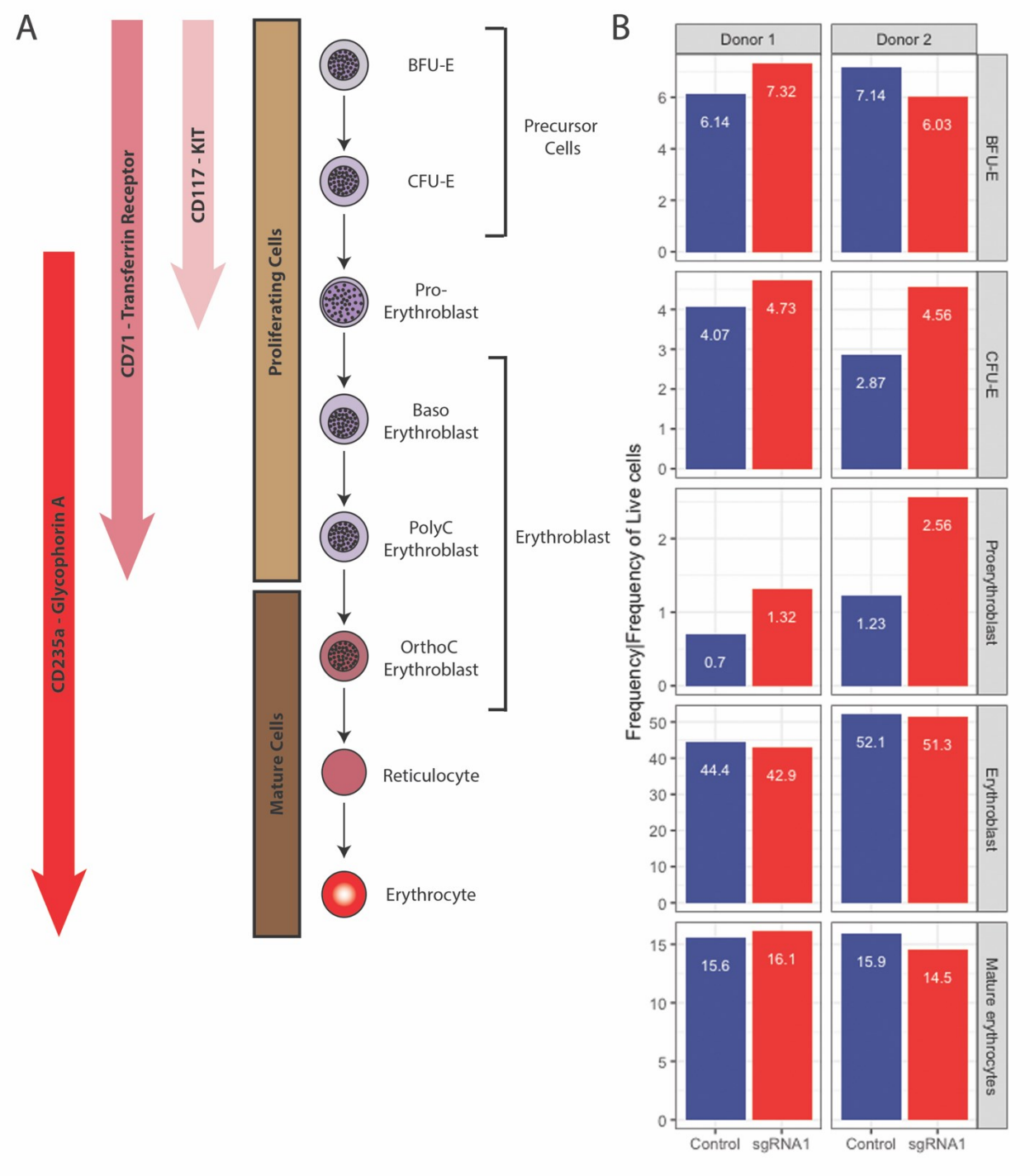

Figure 22: Flow cytometry analysis of human erythrocytes in erythroid expansion media showed an increase in CFU-E and proerythroblasts.

A) Human erythroid culture was classified into 5 subsets based on CD71, CD117 and CD235a expression.

B) Frequency of each of the subset was obtained with respect to the frequency of live cells. The frequency values are specified within the box plot.

4.9 Discussion

Human aging leads to aberrations in hematopoiesis that include an age-associated bias to produce more myeloid cells and an increased mutational load in the HSPC compartment, providing a growth advantage to the mutated clone and leading to myeloid malignancies. Clonal hematopoiesis is rare in younger individuals (less than 50 years of age), but an error-corrected sequencing study revealed that 95% of healthy individuals between 50-60 years of age exhibited clonal hematopoiesis (A. L. Young et al., 2016). A study involving whole-exome sequencing of 12,380 persons highlighted *DNMT3A, TET2, ASXL1, PPM1D,* and *JAK2* as the most common somatic mutations seen in individuals with clonal hematopoiesis (Genovese et al., 2014). A mutation in *TET2* leads to a variety of hematologic conditions, including MDS, myeloproliferative neoplasms, mastocytosis, polycythemia vera, and leukemia involving multiple lineages. For example, the presence of a *TET2* mutation in polycythemia vera is associated with a poor prognosis and increases the tendency to leukemic transformation (Lundberg et al., 2014).

Prior to the current zebrafish model presented here, there have been two other published zebrafish *tet2* mutants (Ge et al., 2014; Gjini et al., 2015a; Gjini et al., 2015b). One employed an antisense oligonucleotide called a morpholino and the second was a zinc finger-induced loss-of-function mutant. While the mutant model showed no embryonic phenotype, the *tet2* "morphant" zebrafish embryos displayed pancytopenia, including a reduction in the number of cells in the HSC compartment; a phenotype reminiscent of aplastic anemia. In contrast, we did not see any decrease in the HSC compartment, but there was a decrease in progenitor and mature cells across myeloid and erythroid lineages. My data was most consistent with the *tet2*

morphant data but significantly varied from that of the previous mutant. This difference in phenotype may be due to the location of mutation (N-terminal versus catalytic domain) or genetic compensation. It has been previously shown in mice that *Tet2* deficiency leads to a delayed and restricted differentiation of HSCs (Ko et al., 2011). My data showing a decrease in multi-lineage differentiation and no change at the HSC level corroborates the murine findings. Hemoglobin staining showed that despite decreased *gata1* expression, which marks erythroid progenitors and globin gene expression, there was no deficiency in hemoglobin, and furthermore the mutants survive to adulthood.

When I analyzed the MEDIP-seq data, I saw an enrichment in domains specific to differentiation-mediating factors like HOX. A domain search using InterPro and Pfam algorithms on the downregulated RNAseq genes as input returned similar results. These data support the fact that there is a differentiation block.

I also saw an increase in 5s rRNA promoter methylation and RNAseq showed subsequent downregulation of 5s rRNA regulating genes. Usually, p53 is stabilized upon abrogation of translational machinery through either the MDM2 or MDMX locus, and our results showed an increase in p53 at the protein level in *tet2* mutant larvae. Upregulation of p53 should lead to an increase in p21 following induction, but I surprisingly noticed a decrease in p21 levels in *tet2* mutant larvae compared to WT. When I performed TF enrichment from our RNAseq results I saw an increased representation of histone methyltransferase, *enhancer of zeste homolog 2* (EZH2). EZH2 is a part of the *polycomb repressor complex 2* (PRC2) and a known transcriptional repressor

of tumor suppressor genes (Odd-ratio- 3.3). EZH2 activity is known to directly downregulate the expression of p21 in cancers (Ohuchi et al., 2018) through recruitment to the p21 promoter along with H3K27me3. EZH2 is transcriptionally known to repress p21 (Xin et al., 2019). Recently, much emphasis has been put on p21 dynamics and how that determines cell fate (Hsu, Altschuler, & Wu, 2019). Both low and high levels of p21 leads to cellular apoptosis and cell cycle arrest, but when p21 is expressed in an intermediate level it leads to a proliferative state. In this context, the decrease in p21 expression observed here might push p21 levels into the so-called "p21 Goldilocks zone" leading to proliferation. Validation of this will require a much more complex experimental set-up in a single cell level with time-lapse imaging and reporter system.

Taking into consideration the above evidence, we thought the block of differentiation seen in *tet2* mutants might represent a proactive effect taken by the cell to guard against genetic perturbations. Activation of proinflammatory cytokine in TET2 loss will lead to a proliferative phenotype; in this context, evidence from the literature suggest that most commonly occurring CHIP mutations lead to coronary atherosclerotic plagues. TET2, in particular, is known to increase the risk of coronary heart disease in an age-independent way. The hypercholesterolemic-mouse model showed an increased size of aortic-plaques when transplanted with bone marrow from *Tet2* deficient mouse compared to the mouse that received bone marrow from WT controls; further expression analysis of the *Tet2* deficient macrophages revealed increased cytokines, chemokines and receptors (Jaiswal et al., 2017). Low-density lipoprotein is toxic and contributes to tissue damage leading to inflammatory response; the above study associated larger plaque formation in the context of TET2 loss may be due to the induction of pro-inflammatory cytokine

interleukin-1β. We saw an overexpression of TRIM family members in our RNAseq data. This protein family is involved in the regulation of cytokine secretion and activation of immune signaling. TRIM35 was upregulated in our dataset and it is known to negatively regulate interferon signaling (Huang et al., 2017; Y. Wang et al., 2015). Thus, I hypothesized a cytokine storm induced by a bacterial infection or other external stimuli could help overcome this impasse pushing the cells towards a proliferation phenotype. With this in mind, I employed two complementary approaches using either G-CSF or the TLR2 agonist, PAM, to mimic bacterial infection. Both these approaches increased numbers of immature proliferating myeloblasts.

Acute erythroid leukemia or MDS with erythroid dysplasia has been reported in cases of individuals with β-thalassemia (Ahlstedt, Wang, & Fang, 2017). β-thalassemia is a disease characterized by ineffective erythropoiesis leading to decreased mature erythroid cells due to increased erythroid-cell death and/or decreased red blood cell terminal differentiation. In these patients, the body compensates for the lack of mature erythroid cells by overproducing EPO (Ponnikorn et al., 2019), a scenario that is very similar to the trends I uncovered in granulocytosis in the context of TET2 deficiency. Thus, I decided to test the capacity for emergency erythropoiesis in human TET2 deficient blood cells. Like previous publications, I saw that the *TET2* mutation provides human cells a clonal advantage as observed by the increased frequency of TET2 mutant cells at a later time point. Similar to my observation during emergency granulopoiesis, there was an increase in proliferating erythroid cells (proerythrocytes) observed.

Overall, I have determined that initiation of emergency hematopoiesis may play a crucial role in the transition of clonal hematopoiesis into MDS and subsequently into leukemia in the absence of TET2. Currently, therapeutic options for MDS include the use of human growth factors, differentiation-inducing agents, immunomodulators, and cytotoxic chemotherapy. Therapy using human hematopoietic growth factors like G-CSF, GM-CSF, and EPO are used frequently in hematological disorders, including various causes of neutropenia, refractory anemia, and low-risk MDS. A prospective study suggested the use of hematopoietic growth factors in such cases leads to better overall responses, event-free survival, and lower side-effects compared to other therapeutic options (Golshayan et al., 2007). In my work, I show that an increase in inflammatory cytokines in the context of TET2 deficiency may actually lead to disease progression. Others have shown that a Tet2 deficiency in mice seems to increase microbial load, and a fraction of these mice develop pre-leukemic myeloproliferation (Meisel et al., 2018).

Together, this work has revealed a conserved mechanism whereby loss of TET function results in a hematopoietic differentiation block that following exposure to an emergency hematopoiesis stimulant (growth factor, infection) results in immature myeloid cell proliferation, providing a mechanistic basis for the selective progression to leukemia in a subset of TET2 mutant individuals.

Chapter 5 – KIT D816V mutation leads to downstream signalling independent of KIT ligand and receptor dimerization

5.1 Introduction

TET2 loss-of-function has a high statistical correlation for co-occurrence with the *KIT* D816V mutation and the biological reason for this correlation is currently unknown (Nangalia et al., 2013). As suggested in the Chapter 1, KIT D816V mutation is both seen as initiating and secondary mutation. KIT signals downstream by phosphorylating downstream targets.

Protein phosphorylation and dephosphorylation are two post-translational modifications used by biological systems to regulate complex processes like signal transduction. Phosphorylation and dephosphorylation are effected by protein kinases and phosphatases, respectively. The process is tightly controlled, and aberrations may lead to various disorders, including cancer. Receptor tyrosine kinases are cell surface receptors capable of stimulating downstream signals through phosphorylation, leading to proliferation during development and cancer progression. KIT (CD117, SCFR, C-KIT) is a membrane-bound type III tyrosine kinase receptor and is activated by binding of bivalent stem cell factor (SCF, Steel Factor) extracellularly (Lemmon, Pinchasi, Zhou, Lax, & Schlessinger, 1997; Philo et al., 1996). KIT activation involves a ligand-driven dimerization step, followed by intermolecular tyrosine auto-phosphorylation. This process leads to the relaxation of the juxtamembrane domain, facilitating the binding of other cytoplasmic protein tyrosine kinases (PTK) and activating downstream signalling through phosphorylation of cytoplasmic PTKs. The phenotypic cellular consequence following the activation of this signalling pathway is the promotion of proliferation, migration and survival (Linnekin, 1999). A molecular

event resulting from activation is that the receptor is internalized and ubiquitinated leading to lysosomal degradation and receptor recycling (Broudy et al., 1999; Gommerman, Rottapel, & Berger, 1997; Jahn et al., 2002).

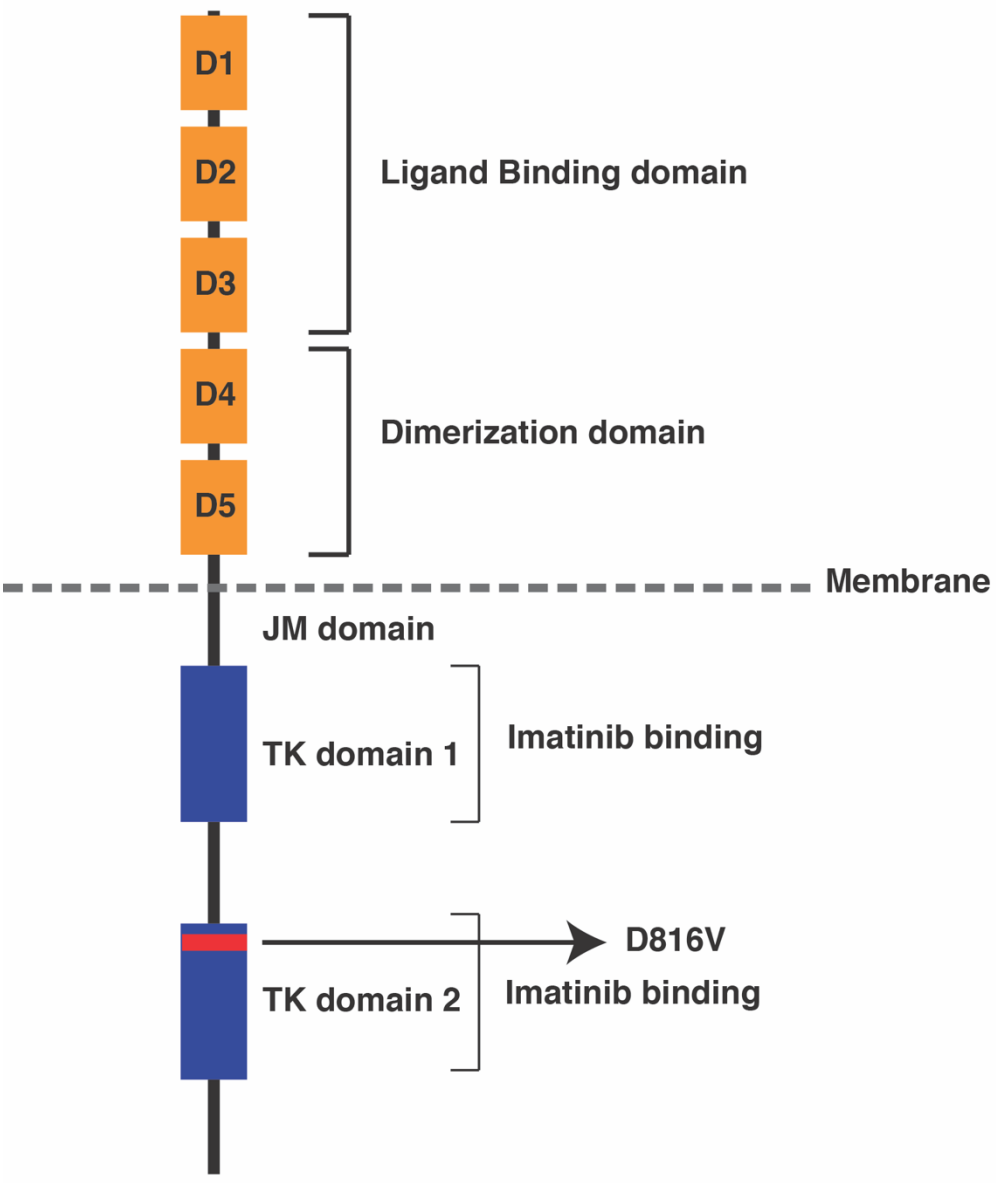

Figure 23: Summary of biochemical domains of KIT receptor

A graphical overview of KIT receptor highlighting various domains and mutational hotspot. Imatinib binds only to inactive confirmation of KIT receptor and does not bind to the D816V mutant. JM: Juxtamembrane; TK: Tyrosine kinase.

The KIT protein contains various domains, an extracellular domain (ectodomain) that consists of five Ig-like domains (D1-D5), transmembrane and juxtamembrane (JM) domains, and two intracellular kinase domains. The D1, D2 and D3 components of the ectodomain are important for KIT ligand binding, while D4 and D5 interact with D4 and D5 of another KIT molecule during SCF binding-mediated homodimerization (Yuzawa et al., 2007) (Figure 23). The D4 and D5 domains were recently targeted using a monoclonal antibody that inhibit KIT dimerization and thereby, activation (Reshetnyak et al., 2013). The juxtamembrane (JM) domain has the potential to maintain KIT in an inactive conformation by functioning as an auto-inhibitory loop (Mol et al., 2004). This process is overcome by trans-phosphorylation of several amino acid residues that stabilize an active conformation or by gain-of-function mutations in the JM or kinase domains. Mutations of the JM domain are implicated in gastrointestinal cancers and effectively targeted with tyrosine kinase inhibitors (de SILVA & Reid, 2003; DeMatteo, 2002). The kinase domain of KIT is unique compared to other tyrosine kinases, as it contains an 80 amino acid insert, effectively splitting the kinase domain into two.

Copy number aberrations and gain-of-function mutations of the KIT receptor are implicated in various malignancies and haematological disorders like AML (Care et al., 2003; Ikeda et al., 1991), mast cell leukemia (Beghini, Larizza, Cairoli, & Morra, 1998), mastocytosis (Bodemer et al., 2010; Garcia-Montero et al., 2006; Longley et al., 1999) and sinonasal T-cell lymphomas (Longley, Reguera, & Ma, 2001). The aspartate to valine substitution occurring in codon 816 of *KIT* is the most frequent *KIT* mutation detected in patients with a condition characterized by hyperproliferation of mast cell called as systemic mastocytosis and is also reported in patients

with gastrointestinal stromal tumours (GISTs) and germ cell tumours (Valent et al., 2007). The KIT D816V mutation is found in approximately 90% of patients with systemic mastocytosis (Garcia-Montero et al., 2006). Tyrosine kinase inhibitors can bind to KIT only in an inactive conformation (Mol et al., 2004a; Mol et al., 2004b). KIT-related disorders are treated using tyrosine kinase inhibitors, which are usually effective against KIT mutants in JM domain, but tyrosine kinase domain mutants are usually resistant to most of these inhibitors (Ma et al., 2002). A tyrosine kinase mutated KIT protein usually exists only in an active conformation, explaining the mechanism behind resistance to tyrosine kinase inhibitors like imatinib and sunitinib that bind only to the inactive conformation (Schindler et al., 2000). By contrast, dasatinib, a tyrosine kinase inhibitor targeting the active conformation, is effective against KIT kinase domain mutants (Shah et al., 2006).

KIT D816V is ligand-independent and constitutively phosphorylate to activate downstream signalling. Unlike wild-type KIT, KIT D816V exhibits intracellular localization and is localized primarily within the Golgi apparatus (Xiang, Kreisel, Cain, Colson, & Tomasson, 2007). It is generally thought that KIT D816V undergoes dimerization similar to KIT WT, but to date, this mechanism has not been sufficiently examined experimentally. One study, employing the membrane-impermeable chemical cross-linker BS^3, concluded that KIT D816V does not dimerize (Kitayama et al., 1995). Subsequent commentaries attributed this finding to the intracellular nature of mutant KIT and maintained that KIT D816V would still dimerize intracellularly (Lennartsson & Rönnstrand, 2012). A computational analysis predicted that KIT D816V differed in dimerization properties from its WT counterpart and proposed that the kinase domain mutant undergoes intracellular dimerization (Laine, de Beauchêne, Perahia, Auclair, & Tchertanov, 2011).

I was interested in determining the importance of KIT D816V dimerization in the pursuit of developing inhibitors of this process as a novel therapeutic strategy in malignancies harbouring this mutation and resistant to most tyrosine kinase inhibitors. Here, I provide direct evidence from cell biological and biochemical assays that definitively reveal that KIT D816V does not form homodimers irrespective of the presence of SCF. While this finding eliminates inhibiting dimerization as a worthy treatment modality, it has helped resolve the discrepancy in the literature regarding the conformational function KIT D816V. In addition, I have identified ways the mutant KIT activates downstream signalling, providing new insights into molecular targets for KIT mutant diseases.

5.2 Mutant KIT does not dimerize

Previous literature has established that the D4-D5 domain is crucial for dimerization in KIT WT (Yuzawa et al., 2007), but these publications predict that KIT D816V undergoes intracellular dimerization without the aid of the extracellular D4-D5 domain (Laine, de Beauchêne, et al., 2011). To verify this, I designed a mammalian two-hybrid assay, where I cloned in the intracellular domains of KIT WT, KIT D816V and a deletion mutant that lacks the mutational hotspot region (Δ816-822), similar to that which was previously reported to make platelet-derived Growth Factor Receptor α (PDGFRα Δ845-848) constitutively active. PDGFRα-related GIST (Heinrich et al., 2003) is similar to the KIT D816V mutation in that this mutation was also reported to be insensitive to imatinib (Corless et al., 2005). The results of the mammalian two-hybrid assay (Figure 24) suggest that none of the KIT intracellular domains constitutively dimerize, a

conclusion that contradicts previous bioinformatics-based assumptions that suggested that the intracellular domains of the mutant may lead to constitutive dimerization and activation.

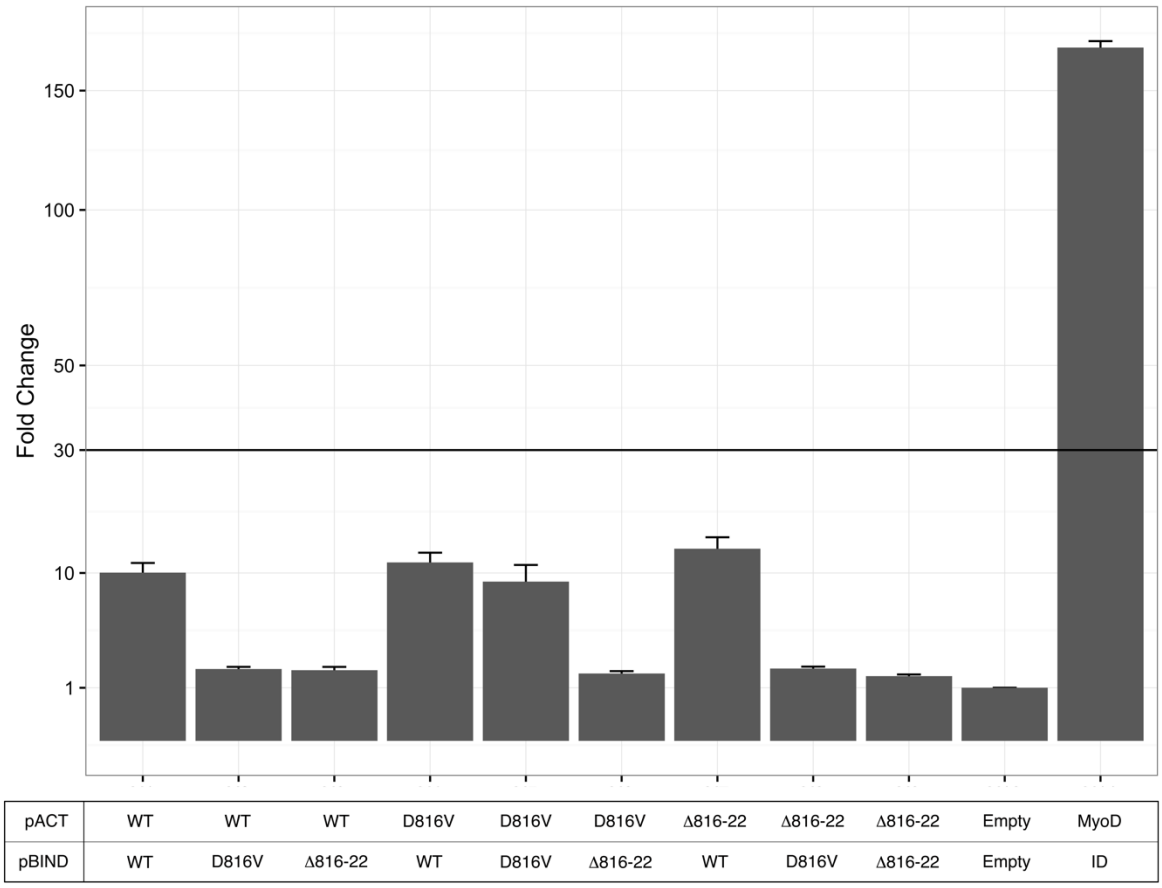

Figure 24: Mammalian 2 hybrid shows no signs of dimerization independent of the extracellular domain.

Plasmids pACT and pBIND containing wild type and the mutant version of the KIT receptor as tabulated were transfected. MyoD and ID were used as control. A fold-change of 30 was considered as a cut-off for dimerization.

5.3 KIT D816V does not have to dimerize to be constitutively activated

After concluding that KIT D816V did not undergo intracellular dimerization from the mammalian two-hybrid assay, I thought it would be important to evaluate the dimerization potential of KIT D816V using a full-length KIT protein because at least in wild-type condition we know that the extracellular domain plays an important role in dimerization. For this experiment, I performed a BiFC assay using the iSplit BiFC constructs, wherein the iRFP713 protein is split into two domains namely PAS and GAFm and are fused with full-length *KIT* WT or D816V mutant. These constructs were each stably transduced into an SC macrophage cell line. Samples were subjected to flow cytometry analysis and baseline was established by gating on live cells and the change in iRFP713 fluorescence was measured. While KIT WT underwent dimerization following exposure to SCF, KIT D816V did not undergo constitutive or SCF-induced dimerization (Figure 25A). As KIT D816V undergoes rapid degradation and recycling through ubiquitination and endocytosis, I performed the same experiment in the presence of MG132, a ubiquitination inhibitor, and observed similar results (Figure 25B). Together, these studies provide evidence that KIT D816V does not undergo constitutive dimerization even in the presence of SCF. This latter finding is consistent with the intracellular localization of the mutated receptor, making it inaccessible to its cognate ligand.

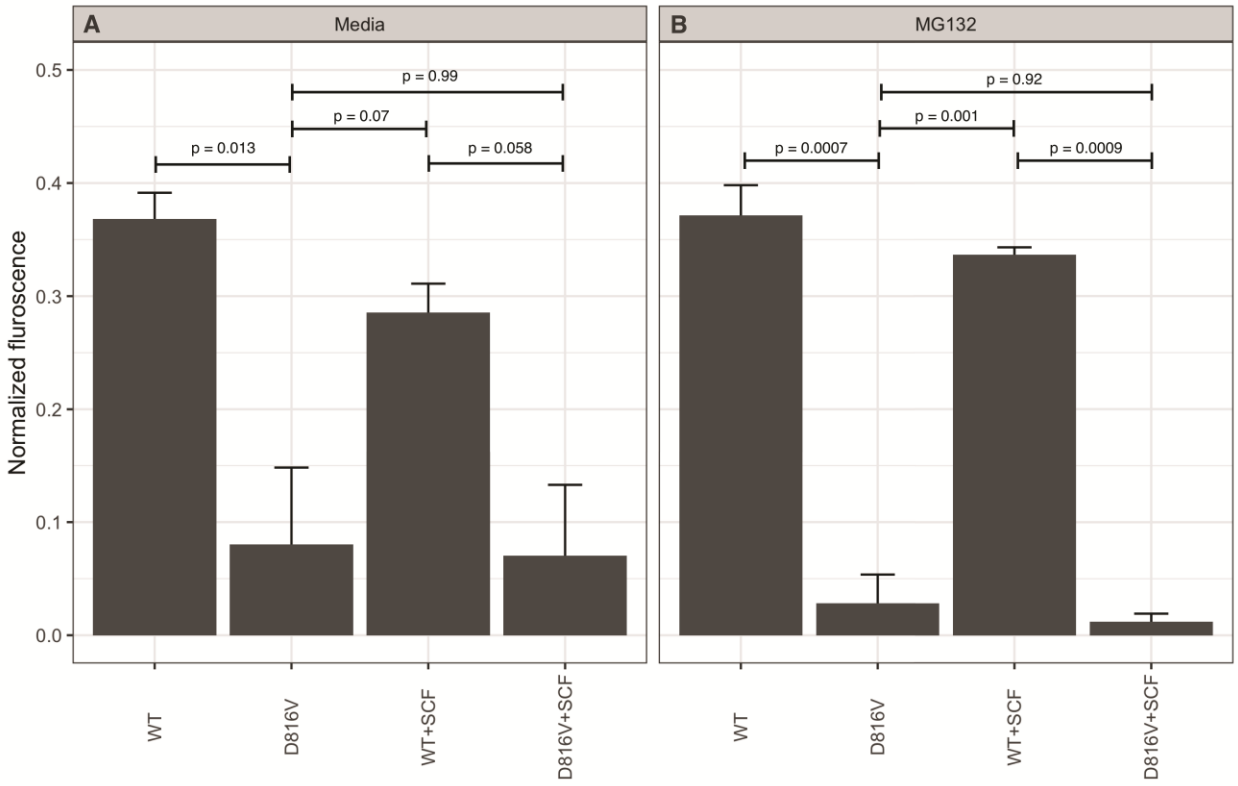

Figure 25: Bimolecular fluorescence complementation shows that KIT D816V does not dimerize
Human 293T cells were co-transfected with a plasmid containing wild-type and D816V mutant KIT receptor. The cells were maintained in serum depleted media and treated with KIT ligand, SCF, overnight. The cells were maintained in two conditions: A) serum depleted media and B) serum depleted media and proteasomal degradation blocker, MG132.

5.4 KITD816V leads to decrease in alpha-helical propensity in the neighbouring polypeptide chain

Previously it was found that EGFR constitutive dimerization was due to a decrease in stability conferred by the mutation in the region surrounding the mutation (Shan et al., 2012). Therefore, I next asked if *KIT* D816V structurally changes the stability of the local region surrounding the mutation. In collaboration with the Rainey lab, I mapped the Far Ultraviolet Circular Dichroism spectra of three 30AA synthetic peptides (KIT WT, KITD816V and KIT Δ816-822) the peptide include the 816th amino acid along with neighbouring amino acid moieties. My initial analysis with sodium phosphate buffer at 37C did show a disordered structure (Figure 24A). Since this particular region contains several long-range interactions with a distant region of the protein, I repeated this experiment in the presence of 1,1,3,3,3-hexafluoro-2-proponal (HFIP), an efficient hydrogen-bond donor that helps stimulate some of this long-range interaction. In HFIP solution, KIT WT showed an increased propensity to form a stable-alpha helix compared to the two mutants (Figure 26B). Even though this is preliminary data and would require sophisticated techniques like Nuclear magnetic resonance (NMR) to evaluate, this finding suggested that structural changes might contribute to the constitutive dimerization of ligand-bound WT KIT.

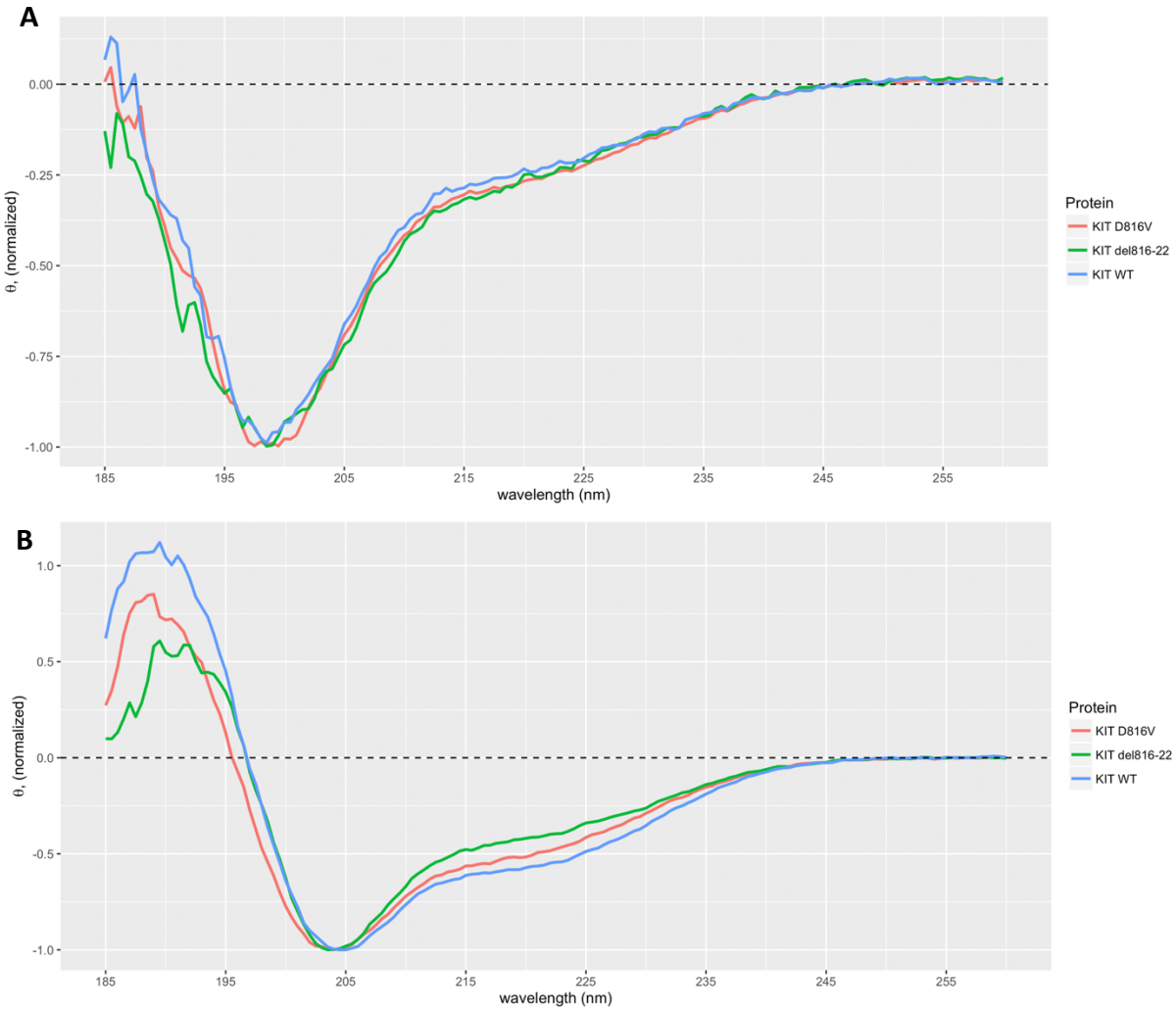

Figure 26: KIT D816V reduces the stability of the polypeptide surrounding the mutational hotspot.

(A) Circular dichroism spectropolarimetry of peptides around the mutational hotspot from wild-type, D816V and Δ816-822 was performed in a sodium-phosphate buffer at 37°C.

(B) Circular dichroism spectropolarimetry of peptides around the mutational hotspot from KIT wild-type, D816V and Δ816-822 were performed in 1,1,3,3,3-hexafluoro-2-proponal at 37°C.

5.5 Kinase specific enrichment analysis of phosphoproteome data reveals increased MAPK and mTOR signalling in KIT D816V

Since there were stability-related changes identified in KIT D816V, I hypothesized that KIT D816V would have different binding partners compared to WT, and thus could activate novel pathways that could potentially be targeted therapeutically. In order to identify novel pathways and due to the fact that KIT signals through phosphorylation, I focused on a phosphoproteome-based approach and compared the phosphorylation pattern between cells containing uninduced KIT, KIT induced with SCF and KIT D816V. I found a total of 1273 mono- and poly-phosphorylated residues from the analysis. In order to find if the activity of a particular kinase was highly regulated, I performed a kinase enrichment analysis. I found differential kinase enrichment patterns between the three groups (Figure 27A). Even though SCF induced KIT and KIT D816V phosphorylated similar residues, the intensity of phosphorylation was higher in KIT D816V; specifically, there was an increase in ERK (MAPK) signalling and mTOR signalling in the mutant compared to SCF induced KIT WT (Figure 27B). Kinase enrichment analysis also showed that KIT D816V tends to enhance cell cycle progression through specific cyclin-dependent kinases (CDK1 and CDK7) in contrast to the activated WT KIT (CDK2 and CDK4) (Figure 25B).

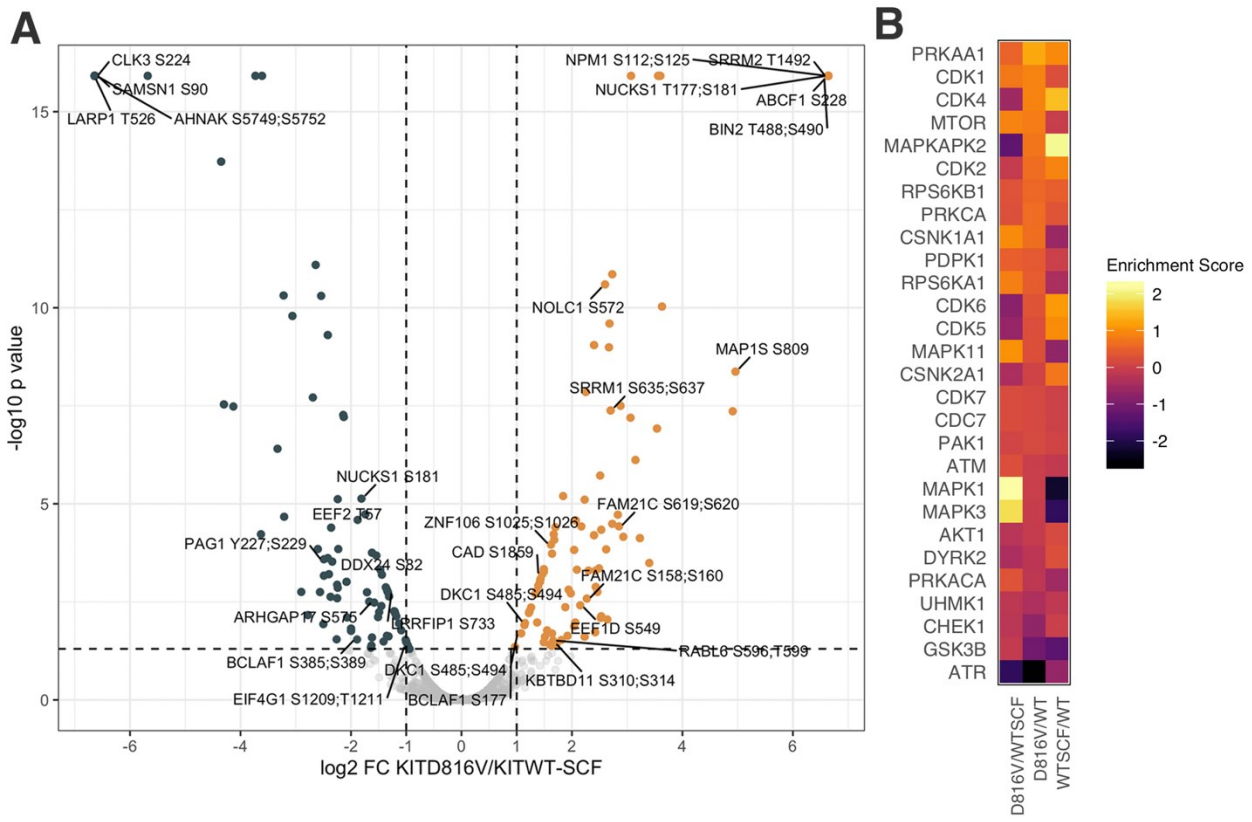

Figure 27: KITD816V increases the level of mTOR and MAPK signaling

A) Volcano plot of phosphoproteome data comparing KIT D816V to KIT WT.
B) Kinase Specific Enrichment Analysis (KSEA) of regulated phosphoproteome from KIT D816V vs KIT WT SCF, KIT D816V vs WT, KIT WT – SCF vs WT

5.6 KIT D816V increases RPS6 mediated protein translation initiation

I further examined the specific actions of KIT D816V. As observed above, I noticed a specific upregulation of mTOR signalling. Specifically, the critical component of mTOR, RAPTOR, whose phosphorylation activates mTORC1 was differentially phosphorylated at S722, S863 and T865 (Figure 28). I further investigated if this change perturbed downstream signalling. I observed phosphorylation activity of both the RPS6 kinases (RPS6KA1 and RPS6KB1) in the KIT D816V sample compared to only RPS6B1 in KIT WT induced with SCF (Figure 27B). Further, components

of the translation initiation complex, EIF3B, EIF3CL and EIF5B were only phosphorylated with the presence of KIT D816V. Pathway enrichment for upregulated genes from total proteome analysis complemented these results, suggesting an increase in downstream signalling related to the eukaryotic translation initiation, ribosomal scanning and start codon recognition (Figure 29A). In particular, components of the ribosome assembly complex, including RPL19, RPL23, RPL24 and RPL30 were upregulated significantly in KIT D816V in comparison to induced KIT WT.

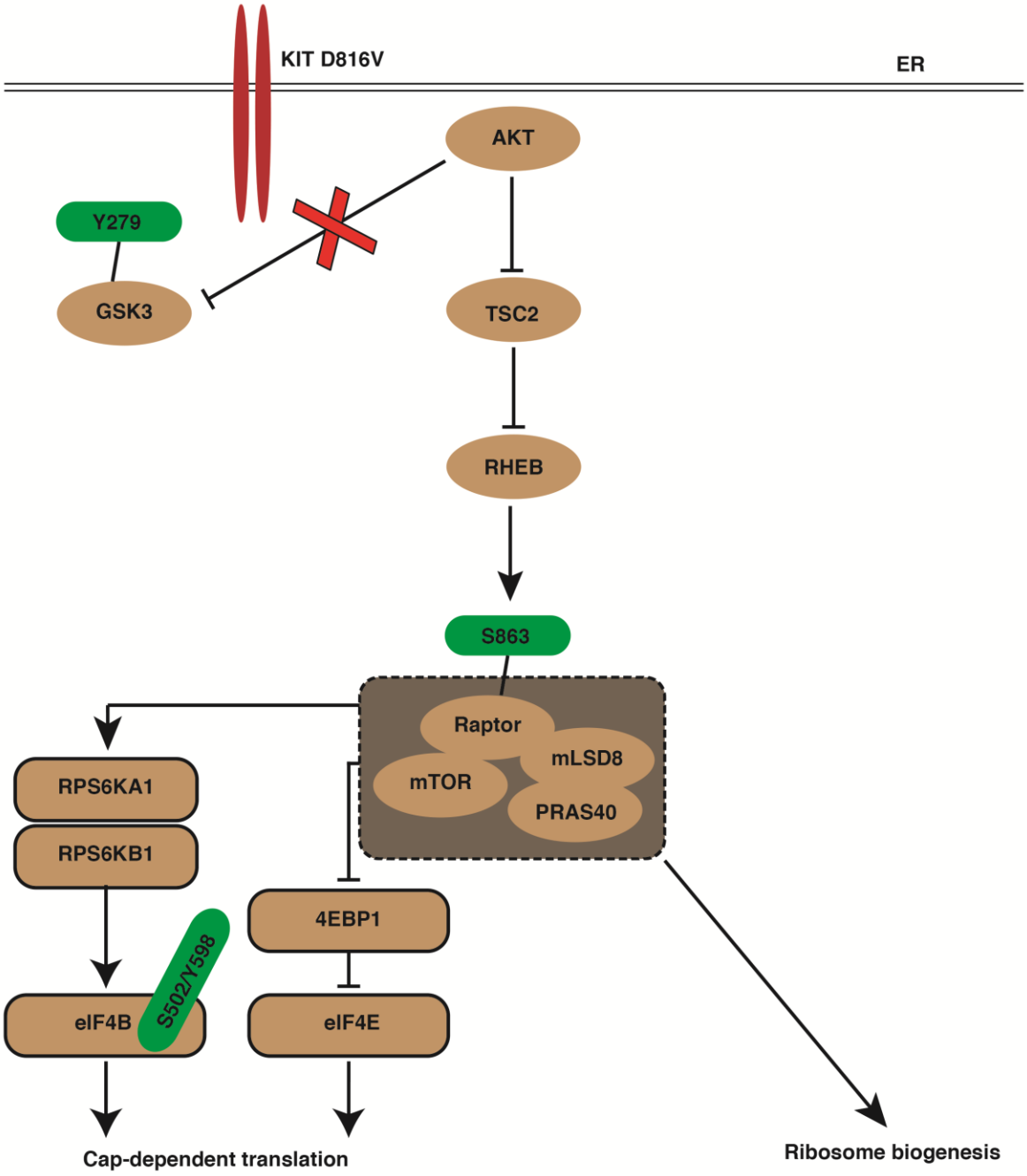

Figure 28: Schematic of KIT D816V induced protein translation initiation
Graphical representation of the molecular mechanism of KIT D816V derived from a combination of phosphoproteome, total proteome and Kinase Specific Enrichment Assay data. Briefly, constitutively active KIT D816V phosphorylates mTOR1 and activates RPS6KA1 and B2, and blocks 4EBP1 to aid cap-dependent translation.

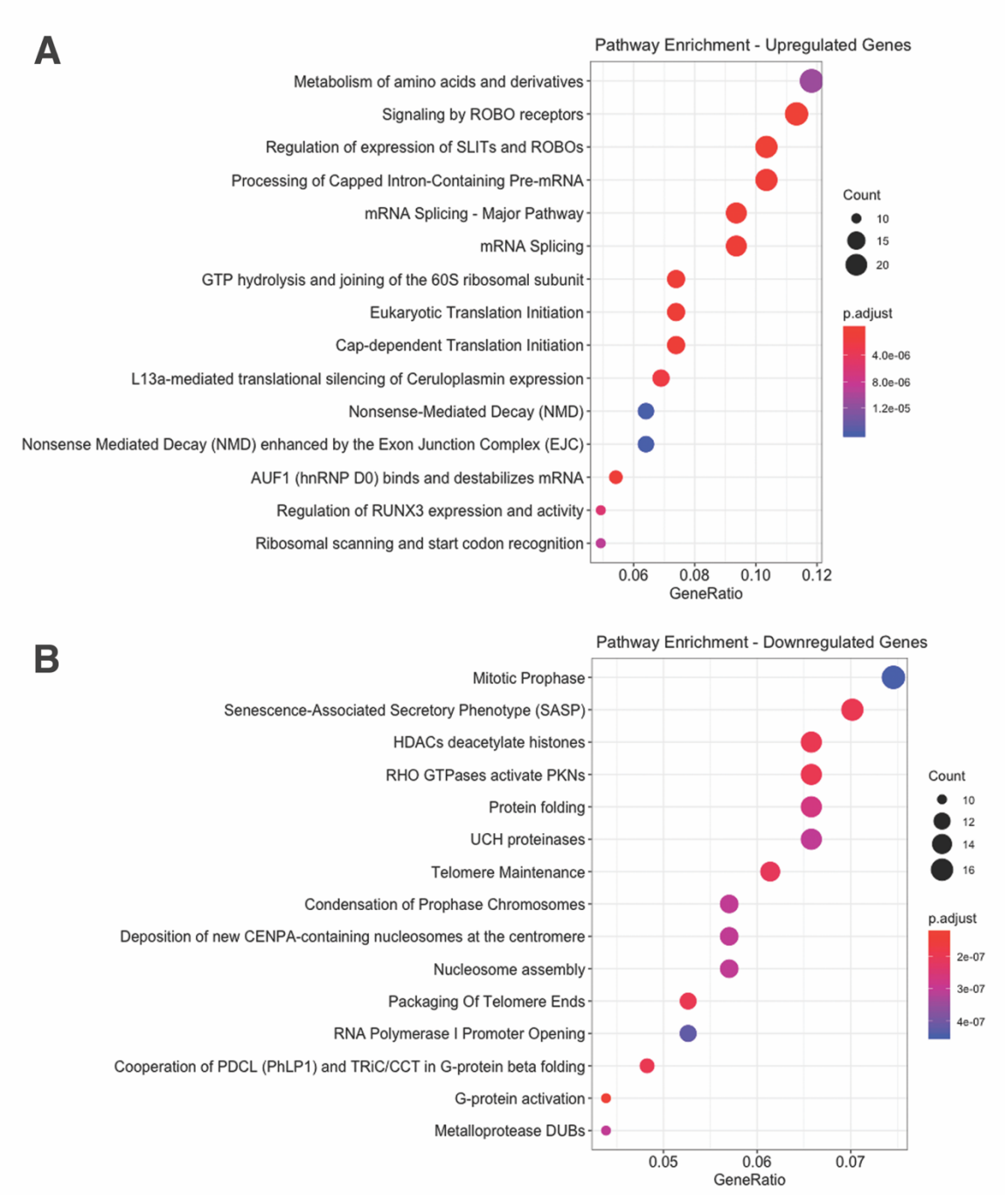

Figure 29: Pathway enrichment of upregulated and down-regulated proteins in KIT D816V

Regulated proteins from total protein analysis was used for pathway enrichment analysis A) upregulated genes and B) down-regulated genes.

5.7 KIT D816V blocks the pathway leading to cell cycle arrest and apoptosis through multiple mechanisms

In KIT WT induced with SCF, an active AKT1 maintains phosphorylation of GSK3, leading to cell cycle arrest; this event counters the activation of cyclin dependent kinases (CDKs) in the WT context. However, I observed that AKT1 phosphorylation of GSK3B (phospho S9) was reduced as observed by the increased kinase activity of GSK3B through KSEA in the KIT D816V mutant. Further, GSK3A also exhibited an elevated level of Y279 phosphorylation, resulting in maximal phosphotransferase activity and nuclear localization of GSK3A (Hughes, Nikolakaki, Plyte, Totty, & Woodgett, 1993), highlighting the elevated signalling activity of GSK3 compared to induced KIT WT. KSEA also showed a decrease in ATR and CHEK1 kinase activity, specifically in KIT D816V (Figure 27B). ATR responds to DNA damage signalling in a CHEK1-dependant manner, causing apoptosis and cell cycle arrest (Flynn & Zou, 2011). Downregulation of this pathway also suggests that KIT D816V+ cells evade apoptosis in an ATR-CHEK1 dependent manner.

5.8 Discussion

KIT D816V is a common genomic perturbation seen in mastocytosis. This mutation is also seen in AML and Mast cell leukemia (Care et al., 2003; Ikeda et al., 1991). The KIT D816V mutation sometimes plays the role of an initiation mutation and can acquire other mutations like the *TET2* loss-of-function to evolve into leukemia. There is enormous information available about the activity of KIT D816V mutation in a biochemical and biophysical context.

First, we know that KIT D816V confers biological activity of the receptor in a ligand-independent manner and that KIT D816V also has intracellular localization. However, previous experimental and molecular dynamic (MD) stimulations experiments have yielded questionable results regarding KIT D816V receptor dimerization (Laine, Chauvot de Beauchêne, Perahia, Auclair, & Tchertanov, 2011). My results through two independent approaches have confirmed that KIT D816V indeed is constitutively active independent of dimerization. Pioneering work has previously highlighted a global structural change post-ligand binding and shift to an active conformation (Yuzawa et al., 2007). KIT D816V always remains in an active conformation (Schindler et al., 2000). I investigated and confirmed that amino acids around the site of mutation referred to as "mutational hotspot" show a decrease in stability and may result in increased capacity to accommodate promiscuous binding of partner proteins without need to dimerize.

A phosphoproteome approach was employed to see if this stability change results in an aberrant signalling pattern, but it did not result in any different signalling events. However, my observations strongly suggest that the intensity of signalling is increased by multiple fold in the KIT D816V mutation. Notably, I found changes in mitogen signalling and apoptosis-related signalling events, suggesting that the KIT D816V mutation confers a proliferative and survival advantage compared to the ligand stimulated condition.

Total proteome analysis also revealed that KIT D816V down-regulates the DNA packing complex and upregulates the spliceosome complex through an unknown mechanism. This data suggests that mitogenic activation of KIT D816V occurs at diverse levels, including epigenetic,

transcriptional, translational and post-translational. Activation of the ubiquitous mTOR pathway helps in survival mechanism by evading apoptosis and also creates in a proliferative state, similarly MAPK pathway also leads to proliferative effect. The use of rapamycin and its analogues that targets mTOR will thus be a potential therapeutic option that can help in reducing the survival advantage of this cell.

Chapter 6: Discussion

Preleukemia is a term given to multiple complex disorders that arise before leukemic progression. Some preleukemic conditions contains bona fide leukemic progression capability like the genomic instability inherent in Fanconi anemia that will lead to leukemic progression in nearly all individuals (Shimamura & Alter, 2010). However, in scenarios where not all individuals progress to develop complete leukemia, therapeutics and even preventative methods can be implemented if the mechanism of progression is known.

Currently, modelling of preleukemic genetic perturbations is in its infancy. Mouse xenografts, the gold standard of the leukemic xenograft assays, have only recently been modified to support the survival of preleukemic cells (Song et al., 2019). The mouse xenograft platform lacks the ability to perform high throughput drug and biomarker screening workflows. Preleukemic samples derived from patients have fewer initiating cells compared to leukemia samples, and therefore the success rate in these experiments is low. In genetic models, the process of generating the precise mutant is quite laborious, and most of the mutants do exhibit an exaggerated phenotype or conversely present with a form fruste due to germline mutation compensation.

Secondly, some of these preleukemic conditions do have pan-hematopoietic system effects and can lead to the leukemia of diverse hematological lineages, which can depend on the time point of the initiating mutation and the permissive microenvironment (Rowe et al., 2019). All this makes the system very complex involving multiple lineages of cells along with a complex cell-cell communication network.

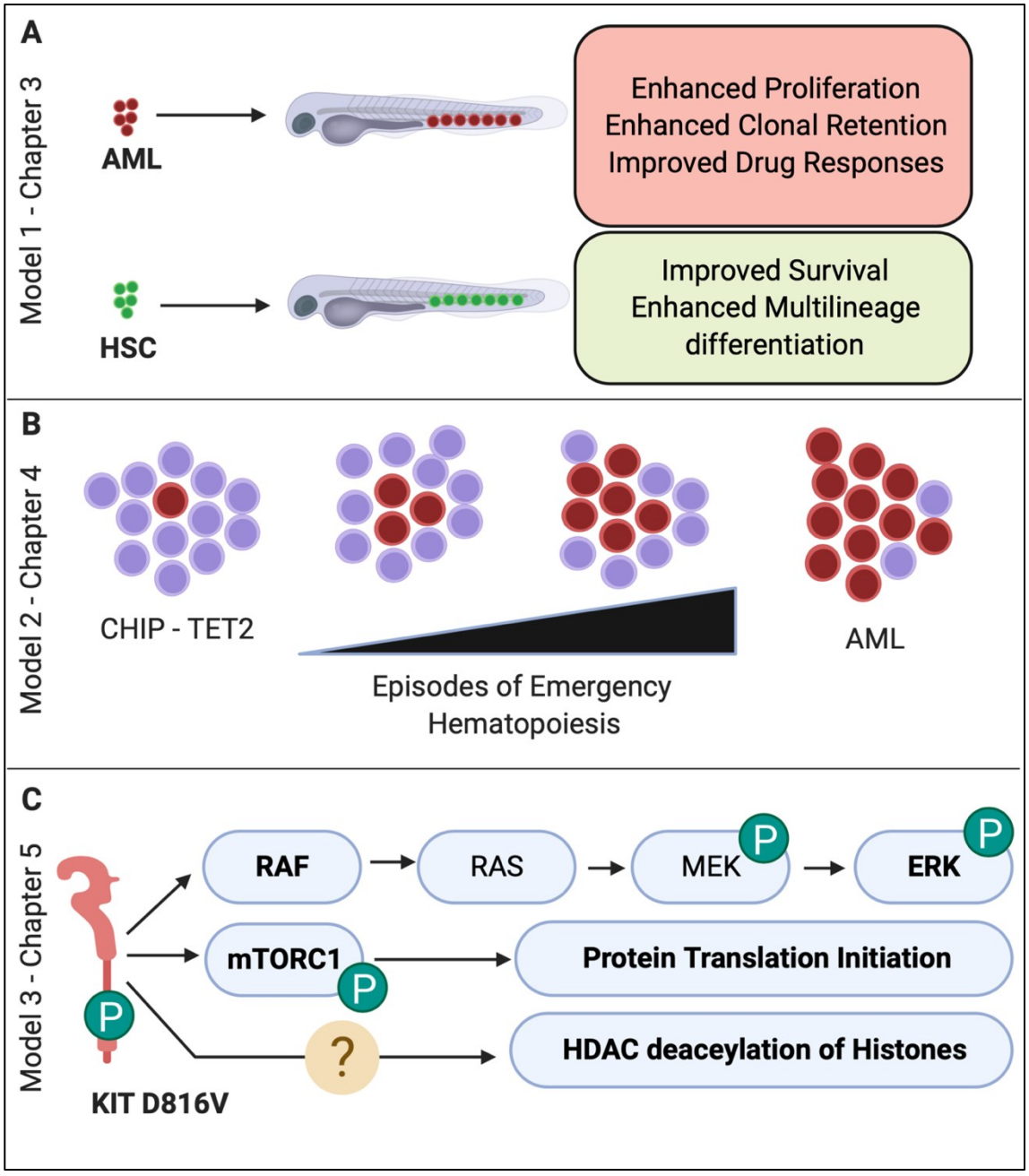

Figure 30: Graphical Overview of the thesis

A. An overview of the human cytokine expressing transgenic xenograft model discussed in Chapter 3.
B. An overview of the TET2 model discussed in Chapter 4.
C. An overview of the KIT D816V model discussed in Chapter 5.

Through this thesis, I have made attempts to address this problem. In Chapter 3 (Figure 30 A), I created a transgenic humanized zebrafish model taking lessons from the current trends in mouse xenograft models. The human cytokine expressing zebrafish model that I developed did show improved engraftment of hematopoietic stem cells, the most primitive blood cells. Patient-derived leukemia xenografts in this model showed an increase in retention of multiple clonal populations. The humanized zebrafish model actually outperformed the mouse xenograft data on clonal retention (Klco et al., 2014); though a head-to-head comparison of these two models with the sample biological sample will be more informative about the robustness of the current model that I developed.

In Chapter 4 (Figure 30 B), I created a tet2-loss-of-function zebrafish model in order to mimic a preleukemic genetic aberrancy that increases the probability of progression to leukemia or atherosclerosis. Many individuals with this mutation remain healthy throughout their life (A. L. Young et al., 2016), which might be partly due to the age at which the mutation occurs (chances of an individual acquiring *TET2* mutation below 50 years of age is small). TET2-related leukemia is one example where an individual harboring that mutation can develop leukemia of different lineages and also other complications like atherosclerosis (Jaiswal & Libby, 2019). When I initially phenotyped the *tet2* mutant, I found a very restrictive environment in the fish characterized by reduced blood cells of multiple lineages as well as stunted growth. For the very first time, I carried out both methylation and hypermethylation and RNAseq from blood cells extracted from the kidney marrow of these zebrafish. The extensive dataset generated from this analysis showed a very restrictive process in the organism. This led me to hypothesize and successfully elucidate

that emergency hematopoiesis initiation leads to a proliferative advantage. Interestingly, these results also show why a patient with a *TET2* mutation has increased risk of atherosclerosis; higher levels of low-density lipoproteins are inflammatory as they damage tissues leading to secretion of pro-inflammatory cytokines (Maiolino et al., 2013). The inflammatory cytokines increase granulocytic differentiation leading to atherosclerotic plaques. In a tet2 deficient condition, the presence of pro-inflammatory cytokines provides these cells with a proliferative advantage and thus clinically *TET2* mutant patients can develop a sizeable atherosclerotic plaque.

To further understand a complex biological system like that involving TET2, I should use sophisticated technology that can generate high throughput data at a single cell level. A single-cell RNAseq experiment would improve our understanding of my *tet2* mutant, particularly since we have somewhat limited understanding of the intermediate cell types generated during hematopoietic differentiation. There has been some evidence from my RNAseq data analysis that lack of tet2, at least at the germline level, will suppress NF-kB. This is indirect evidence from transcription factor analysis data, however, and will need to be complemented with ATAC-Seq or additional functional experimental verification. My findings using the *tet2* mutant also has therapeutic implications. Currently patients with low-risk MDS receive treatment with recombinant human growth factors like GCSF, erythropoietin and thrombopoietin, and a subset of low-risk MDS patients respond to this therapy. My experiments clearly show that human growth factor treatment given to patients whose leukemia harbours a *TET2* mutation could be detrimental and could also increase the risk of atherosclerosis, one potential therapeutic option would be to use lenalidomide on patients with TET2 loss-of-function. Lenalidomide is an anti-

proliferative drug, currently approved both by FDA & Health Canada for treatment of adult MDS with 5q- even though there is no data available about the TET2 status of the treated patients. The mechanism of lenalidomide to reduce proinflammatory signaling by suppressing tumor necrosis factor and interferon signaling could represent a potential option currently available for patients with TET2 mutation (Kotla et al., 2009).

Finally, in chapter 5 (Figure 30 C), I studied another preleukemic lesion (*KIT* D816V) commonly seen in mastocytosis and which increasingly has been found to co-occur with the *TET2* mutation. KIT D816V has been studied for a long time, but there has been some questionable interpretation regarding dimerization of the KIT D816V mutant that has led to certain conclusions in the field. During the start of my thesis, BLU 285, the potent selective KIT D816V inhibitor was not available (DeAngelo et al., 2017), and we envisioned that understanding this mechanism will lead to improvement of clinically available KIT inhibitors. I found that KIT D816V does not constitutively dimerize but can activate downstream signalling independent of a dimerization event. Analyzing downstream pathways using a home-built phosphoproteome workflow led to the understanding that KIT D816V is potent to increase the strength of KIT signalling compared to ligand activation; the increase in phosphorylation lead to downstream signalling activation resulting in a proliferative and survival advantage. Further, for the first time, I discovered the involvement of KIT D816V in epigenetic signalling through downregulation of multiple histones that are involved in histone packing thus leading to an open histone conformation through an unknown mechanism.

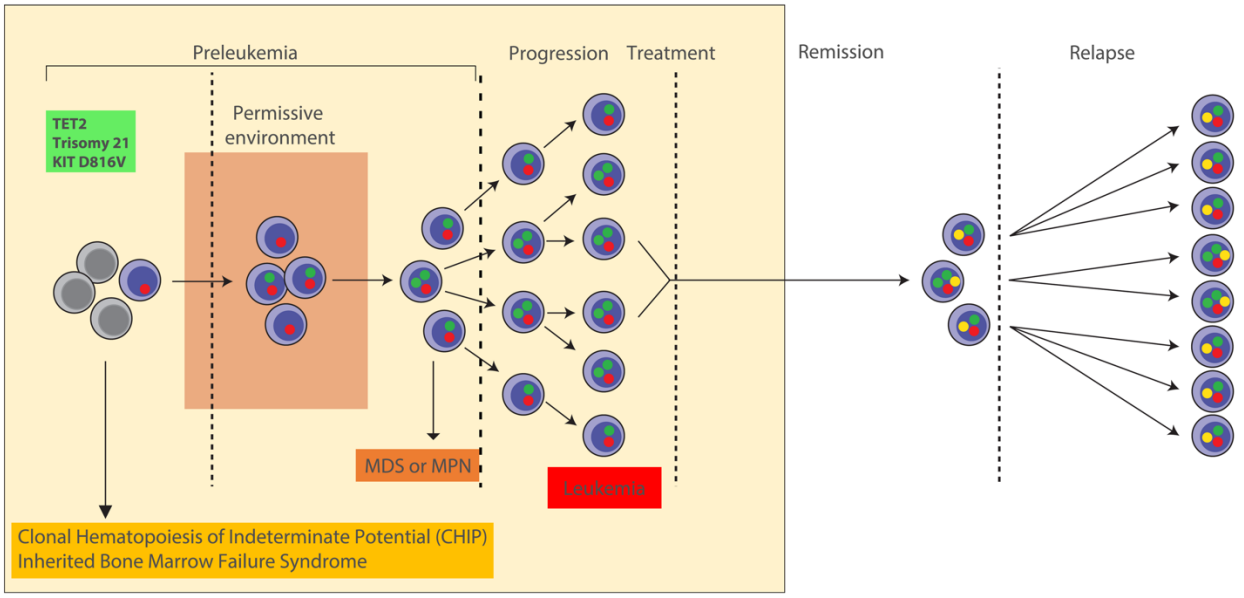

Figure 31: Model of Preleukemia to Leukemia transformation
Preleukemia begins when a clone acquires an initiating genomic lesion and continues to evolve with time. The clone with the genomic perturbations is aided by a permissive microenvironment that occurs either due to developmental states or other external factors like an infection. This permissive microenvironment helps in leukemic progression. MDS: Myelodysplastic Syndrome; MPN: Myeloproliferative Neoplasm.

Together, my current work is a significant step towards the understanding of preleukemia (Figure 31). Secondary mutations are recognized contributors to leukemic progression, though the influence of the surrounding leukemic niche in aiding in the acquisition of these secondary mutations and survival of the clone harboring initiating mutation, is less appreciated. This work, in particular, elucidates the niche or microenvironmental contribution to leukemic progression. Recently, leukemic mutations have been discovered in leukemic bone marrow mesenchymal stem cells. underlining the importance of the microenvironment (Blau et al., 2011). A consortium wide effort to screen cells from the bone marrow microenvironment for mutations and gene expression will provide further enlightenment on the contribution of microenvironment on disease development, progression and relapse.

Limitations

Modelling human diseases in another model is far from ideal, but this prototype provides useful information that can be used to improve health condition and treat diseases. The models that have been investigated have certain limitations, and they are as follows:

The zebrafish expressing human cytokines is an improvement to the models available in the zebrafish xenotransplantation research. However, this model is still in its infancy. Despite, rigorous experimental strategies, we were still not able to reproducibly rescue the human cells transplanted into the zebrafish using flow cytometry because of antibody cross-reactivity. The expression of GM-CSF and SCF under a tetracycline-inducible promoter is advantageous compared to expressing them under a strong ubiquitous promoter, but a knock-in zebrafish will provide much more robust experimentation.

The tet2 loss-of-function model also provides a very detailed insight into how the tet2 mutation helps in leukemic progression. However, some of the results might be exaggerated or understated because the current mutant has a germline mutation, but the patients only have a somatic mutation.

The major drawback of the KIT model is the fact that it is a cell line model. The BiFC assay currently was done using a transfection protocol and under a powerful promoter; this makes the assay at least in the case of wild-type less dependable. A knock-in assay or transduction protocol with one integration and a less powerful promoter like *elongation factor 1a (ef1a)* could

potentially help to overcome this deficiency. The phosphorylation signals are highly time-dependent, and a time-course experiment will throw more light into nuances of KIT D816V signalling; the home-build phosphoproteome approach even though robust is less amenable to high-throughput experiments and also expensive to perform a time-course experiment.

Contributions

Part of this thesis is under different stage of reviews in different journals. Individual contributions are as follows: Nicole Melong and Benjamin King: assisted with the xenograft experiments in Chapter 3; Spencer Tong, Wing Wong Hing and Dr Todd Druley (University of Washington, St. Louis) assisted in performing RNA-error corrected sequencing in Chapter 3; Rachel Woodside: assisted with *in situ* experiments for initial phenotyping in Chapter 4; Michelle Moksha and Dr. Martin Hirst assisted with meDIP/hmeDIP sequencing in Chapter 4; Annaick Charles assisted in initial mapping and normalization of meDIP/hmeDIP data in Chapter 4. Dr. Sergey Prykhozhij assisted with experimental design in Chapter 5. Drs. Aditya Pandey and Jan Rainey assisted with the Circular Dichroism experiment in Chapter 6. Dr. Jason Berman assisted with experimental conceptualization and editing of the text.

Reference

Ahlstedt, J., Wang, Y., & Fang, Y. (2017). A Rare Case of Myelodysplastic Syndrome with Ring Sideroblasts, SF3B1 and TET2 Mutations in a Patient with Beta Thalassemia Trait. *North American Journal of Medicine and Science, 10*(1), 32-35.

Al-Drees, M. A., Yeo, J. H., Boumelhem, B. B., Antas, V. I., Brigden, K. W., Colonne, C. K., & Fraser, S. T. (2015). Making blood: the haematopoietic niche throughout ontogeny. *Stem cells international, 2015*.

Amaya, E. (2013). The hemangioblast: a state of competence. *Blood, 122*(24), 3853-3854.

Ara, T., Tokoyoda, K., Sugiyama, T., Egawa, T., Kawabata, K., & Nagasawa, T. (2003). Long-Term Hematopoietic Stem Cells Require Stromal Cell-Derived Factor-1 for Colonizing Bone Marrow during Ontogeny. *Immunity, 19*(2), 257-267. doi:10.1016/S1074-7613(03)00201-2

Arai, A., Jin, A., Yan, W., Mizuchi, D., Yamamoto, K., Nanki, T., & Miura, O. (2005). SDF-1 synergistically enhances IL-3-induced activation of the Raf-1/MEK/Erk signaling pathway through activation of Rac and its effector Pak kinases to promote hematopoiesis and chemotaxis. *Cellular Signalling, 17*(4), 497-506. doi:https://doi.org/10.1016/j.cellsig.2004.09.007

Auerbach, A. D., & Allen, R. G. (1991). Leukemia and preleukemia in Fanconi anemia patients: A review of the literature and report of the International Fanconi Anemia Registry. *Cancer Genetics and Cytogenetics, 51*(1), 1-12. doi:https://doi.org/10.1016/0165-4608(91)90002-C

Austin, K. M., Gupta, M. L., Coats, S. A., Tulpule, A., Mostoslavsky, G., Balazs, A. B., . . . Shimamura, A. (2008). Mitotic spindle destabilization and genomic instability in Shwachman-Diamond syndrome. *The Journal of clinical investigation, 118*(4), 1511-1518.

Barker, J. (1997). Early transplantation to a normal microenvironment prevents the development of Steel hematopoietic stem cell defects. *Experimental Hematology, 25*(6), 542-547.

Barretina, J., Caponigro, G., Stransky, N., Venkatesan, K., Margolin, A. A., Kim, S., . . . Sonkin, D. J. N. (2012). The Cancer Cell Line Encyclopedia enables predictive modelling of anticancer drug sensitivity. *Nature, 483*(7391), 603.

Becker, A. J., McCulloch, E. A., & Till, J. E. (1963). Cytological demonstration of the clonal nature of spleen colonies derived from transplanted mouse marrow cells.

Beghini, A., Larizza, L., Cairoli, R., & Morra, E. (1998). c-Kit activating mutations and mast cell proliferation in human leukemia. *Blood, 92*(2), 701-703.

Bennett, C. M., Kanki, J. P., Rhodes, J., Liu, T. X., Paw, B. H., Kieran, M. W., . . . Look, A. T. (2001). Myelopoiesis in the zebrafish, *Danio rerio*. *Blood, 98*(3), 643-651. doi:10.1182/blood.V98.3.643 %J Blood

Bentley, V. L., Veinotte, C. J., Corkery, D. P., Pinder, J. B., LeBlanc, M. A., Bedard, K., . . . Dellaire, G. (2014). Focused chemical genomics using zebrafish xenotransplantation as a preclinical therapeutic platform for T-cell acute lymphoblastic leukemia. *Haematologica*, haematol. 2014.110742.

Bentley, V. L., Veinotte, C. J., Corkery, D. P., Pinder, J. B., LeBlanc, M. A., Bedard, K., . . . Dellaire, G. (2015). Focused chemical genomics using zebrafish xenotransplantation as a pre-clinical therapeutic platform for T-cell acute lymphoblastic leukemia. *haematologica, 100*(1), 70-76.

Bhatnagar, N., Nizery, L., Tunstall, O., Vyas, P., & Roberts, I. (2016). Transient abnormal myelopoiesis and AML in Down syndrome: an update. *Current hematologic malignancy reports, 11*(5), 333-341.

Blau, O., Baldus, C. D., Hofmann, W.-K., Thiel, G., Nolte, F., Burmeister, T., . . . Blau, I. W. (2011). Mesenchymal stromal cells of myelodysplastic syndrome and acute myeloid leukemia patients have distinct genetic abnormalities compared with leukemic blasts. *Blood, 118*(20), 5583-5592. doi:10.1182/blood-2011-03-343467

Block, M., Jacobson, L. O., & Bethard, W. F. (1953). Preleukemic acute human leukemia. *Journal of the American Medical Association, 152*(11), 1018-1028.

Bodemer, C., Hermine, O., Palmérini, F., Yang, Y., Grandpeix-Guyodo, C., Leventhal, P. S., . . . Cohen-Akenine, A. (2010). Pediatric mastocytosis is a clonal disease associated with D 816 V and other activating c-KIT mutations. *Journal of Investigative Dermatology, 130*(3), 804-815.

Bonnet, D., & Dick, J. E. (1997a). Human acute myeloid leukemia is organized as a hierarchy that originates from a primitive hematopoietic cell. *Nature Medicine, 3*(7), 730-737. doi:10.1038/nm0797-730

Bonnet, D., & Dick, J. E. (1997b). Human acute myeloid leukemia is organized as a hierarchy that originates from a primitive hematopoietic cell. *Nature Medicine, 3*, 730. doi:10.1038/nm0797-730

Boocock, G. R. B., Morrison, J. A., Popovic, M., Richards, N., Ellis, L., Durie, P. R., & Rommens, J. M. (2003). Mutations in SBDS are associated with Shwachman–Diamond syndrome. *Nature genetics, 33*(1), 97-101. doi:10.1038/ng1062

Boulais, P. E., & Frenette, P. S. (2015). Making sense of hematopoietic stem cell niches. *Blood, 125*(17), 2621-2629. doi:10.1182/blood-2014-09-570192

Brocker, C., Thompson, D., Matsumoto, A., Nebert, D. W., & Vasiliou, V. (2010). Evolutionary divergence and functions of the human interleukin (IL) gene family. *Human Genomics, 5*(1), 30. doi:10.1186/1479-7364-5-1-30

Brouard, N., Jost, C., Matthias, N., Albrecht, C., Egard, S., Gandhi, P., . . . Simmons, P. J. (2017). A unique microenvironment in the developing liver supports the expansion of megakaryocyte progenitors. *Blood advances, 1*(21), 1854-1866.

Broudy, V. C., Lin, N. L., Liles, W. C., Corey, S. J., O'Laughlin, B., Mou, S., & Linnekin, D. (1999). Signaling via Src family kinases is required for normal internalization of the receptor c-Kit. *Blood, 94*(6), 1979-1986.

Brown, J. A., & Boussiotis, V. A. (2008). Umbilical cord blood transplantation: Basic biology and clinical challenges to immune reconstitution. *Clinical Immunology, 127*(3), 286-297. doi:https://doi.org/10.1016/j.clim.2008.02.008

Bryce, P. J., Falahati, R., Kenney, L. L., Leung, J., Bebbington, C., Tomasevic, N., . . . Brehm, M. A. (2016a). Humanized mouse model of mast cell mediated passive cutaneous anaphylaxis and passive systemic anaphylaxis. *Journal of Allergy and Clinical Immunology, 138*(3), 769-779. doi:10.1016/j.jaci.2016.01.049

Bryce, P. J., Falahati, R., Kenney, L. L., Leung, J., Bebbington, C., Tomasevic, N., . . . Brehm, M. A. (2016b). Humanized mouse model of mast cell–mediated passive cutaneous anaphylaxis

and passive systemic anaphylaxis. *Journal of Allergy and Clinical Immunology, 138*(3), 769-779. doi:https://doi.org/10.1016/j.jaci.2016.01.049

Care, R. S., Valk, P. J., Goodeve, A. C., Abu-Duhier, F. M., Geertsma-Kleinekoort, W., Wilson, G. A., . . . Reilly, J. T. (2003). Incidence and prognosis of c-KIT and FLT3 mutations in core binding factor (CBF) acute myeloid leukaemias. *British journal of haematology, 121*(5), 775-777.

Ceasar, S. A., Rajan, V., Prykhozhij, S. V., Berman, J. N., & Ignacimuthu, S. (2016). Insert, remove or replace: A highly advanced genome editing system using CRISPR/Cas9. *Biochimica et Biophysica Acta (BBA) - Molecular Cell Research, 1863*(9), 2333-2344. doi:https://doi.org/10.1016/j.bbamcr.2016.06.009

Chagraoui, J., Gareau, Y., Gingras, S., Rjean, R., Csaszar, E., Cohen, S., . . . Sauvageau, G. (2013). UM171 Is a Novel and Potent Agonist Of Human Hematopoietic Stem Cell Renewal. *Blood, 122*(21), 798-798.

Chatterjee, A., Ghosh, J., & Kapur, R. (2015). Mastocytosis: a mutated KIT receptor induced myeloproliferative disorder. *Oncotarget, 6*(21), 18250.

Chen, L.-L., Lin, H.-P., Zhou, W.-J., He, C.-X., Zhang, Z.-Y., Cheng, Z.-L., . . . Guan, K.-L. (2018). SNIP1 Recruits TET2 to Regulate c-MYC Target Genes and Cellular DNA Damage Response. *Cell Reports, 25*(6), 1485-1500.e1484. doi:10.1016/j.celrep.2018.10.028

Chen, M. J., Li, Y., De Obaldia, M. E., Yang, Q., Yzaguirre, A. D., Yamada-Inagawa, T., . . . Speck, N. A. (2011). Erythroid/myeloid progenitors and hematopoietic stem cells originate from distinct populations of endothelial cells. *Cell stem cell, 9*(6), 541-552.

Chiu, P. P. L., Jiang, H., & Dick, J. E. (2010). Leukemia-initiating cells in human T-lymphoblastic leukemia exhibit glucocorticoid resistance. *Blood, 116*(24), 5268-5279. doi:10.1182/blood-2010-06-292300

Choi, K., Kennedy, M., Kazarov, A., Papadimitriou, J. C., & Keller, G. (1998). A common precursor for hematopoietic and endothelial cells. *Development, 125*(4), 725-732.

Chou, S., & Lodish, H. F. (2010). Fetal liver hepatic progenitors are supportive stromal cells for hematopoietic stem cells. *Proceedings of the National Academy of Sciences, 107*(17), 7799-7804. doi:10.1073/pnas.1003586107

Chou, W.-C., Chou, S.-C., Liu, C.-Y., Chen, C.-Y., Hou, H.-A., Kuo, Y.-Y., . . . Tien, H.-F. (2011). TET2 mutation is an unfavorable prognostic factor in acute myeloid leukemia patients with intermediate-risk cytogenetics. *Blood, 118*(14), 3803-3810. doi:10.1182/blood-2011-02-339747 %J Blood

Christensen, J. L., Wright, D. E., Wagers, A. J., & Weissman, I. L. (2004). Circulation and Chemotaxis of Fetal Hematopoietic Stem Cells. *PLOS Biology, 2*(3), e75. doi:10.1371/journal.pbio.0020075

Ciganda, M., & Williams, N. (2011). Eukaryotic 5S rRNA biogenesis. *Wiley Interdisciplinary Reviews: RNA, 2*(4), 523-533.

Constantinou, C., Elia, A., & Clemens, M. J. (2008). Activation of p53 stimulates proteasome-dependent truncation of eIF4E-binding protein 1 (4E-BP1). *Biology of the Cell, 100*(5), 279-289.

Corces, M. R., Chang, H. Y., & Majeti, R. (2017). Preleukemic Hematopoietic Stem Cells in Human Acute Myeloid Leukemia. *Frontiers in Oncology, 7*(263). doi:10.3389/fonc.2017.00263

Corkery, D. P., Dellaire, G., & Berman, J. N. (2011). Leukaemia xenotransplantation in zebrafish–chemotherapy response assay in vivo. *British journal of haematology, 153*(6), 786-789.

Corless, C. L., Schroeder, A., Griffith, D., Town, A., McGreevey, L., Harrell, P., . . . Heinrich, M. C. (2005). PDGFRA mutations in gastrointestinal stromal tumors: frequency, spectrum and in vitro sensitivity to imatinib. *Journal of clinical oncology, 23*(23), 5357-5364.

Coughlan, A. M., Harmon, C., Whelan, S., O'Brien, E. C., O'Reilly, V. P., Crotty, P., . . . Little, M. A. (2016). Myeloid Engraftment in Humanized Mice: Impact of Granulocyte-Colony Stimulating Factor Treatment and Transgenic Mouse Strain. *Stem Cells and Development, 25*(7), 530-541. doi:10.1089/scd.2015.0289

Crane, G. M., Jeffery, E., & Morrison, S. J. (2017). Adult haematopoietic stem cell niches. *Nature Reviews Immunology, 17*, 573. doi:10.1038/nri.2017.53

Cutler, C., Multani, P., Robbins, D., Kim, H. T., Le, T., Hoggatt, J., . . . Rezner, B. (2013). Prostaglandin-modulated umbilical cord blood hematopoietic stem cell transplantation. *Blood, 122*(17), 3074-3081.

Davidson, A. J., & Zon, L. I. (2004). The 'definitive' (and 'primitive') guide to zebrafish hematopoiesis. *Oncogene, 23*(43), 7233-7246. doi:10.1038/sj.onc.1207943

de Pater, E., Kaimakis, P., Vink, C. S., Yokomizo, T., Yamada-Inagawa, T., van der Linden, R., . . . Dzierzak, E. (2013). Gata2 is required for HSC generation and survival. *The Journal of Experimental Medicine, 210*(13), 2843-2850. doi:10.1084/jem.20130751 %J The Journal of Experimental Medicine

de Paula Ayres-Silva, J., de Abreu Manso, P. P., da Cunha Madeira, M. R., Pelajo-Machado, M., & Lenzi, H. L. (2011). Sequential morphological characteristics of murine fetal liver hematopoietic microenvironment in Swiss Webster mice. *Cell and tissue research, 344*(3), 455.

de SILVA, M. C., & Reid, R. (2003). Gastrointestinal stromal tumors (GIST): C-kit mutations, CD117 expression, differential diagnosis and targeted cancer therapy with Imatinib. *Pathology Oncology Research, 9*(1), 13-19.

DeAngelo, D. J., Quiery, A. T., Radia, D., Drummond, M. W., Gotlib, J., Robinson, W. A., . . . Alvarez-Diez, T. (2017). Clinical activity in a phase 1 study of Blu-285, a potent, highly-selective inhibitor of KIT D816V in advanced systemic mastocytosis (AdvSM). In: Am Soc Hematology.

DeMatteo, R. P. (2002). The GIST of targeted cancer therapy: a tumor (gastrointestinal stromal tumor), a mutated gene (c-kit), and a molecular inhibitor (STI571). *Annals of Surgical Oncology, 9*(9), 831-839.

Donadieu, J., Leblanc, T., Meunier, B. B., Barkaoui, M., Fenneteau, O., Bertrand, Y., . . . Phillipe, N. (2005). Analysis of risk factors for myelodysplasias, leukemias and death from infection among patients with congenital neutropenia. Experience of the French Severe Chronic Neutropenia Study Group. *haematologica, 90*(1), 45-53.

Dooley, K. A., Davidson, A. J., & Zon, L. I. (2005). Zebrafish scl functions independently in hematopoietic and endothelial development. *Developmental Biology, 277*(2), 522-536. doi:https://doi.org/10.1016/j.ydbio.2004.09.004

Drexler, H. G., Dirks, W. G., & MacLeod, R. A. F. (2009). Many are called MDS cell lines: One is chosen. *Leukemia research, 33*(8), 1011-1016. doi:https://doi.org/10.1016/j.leukres.2009.03.005

Dror, Y. (2002). p53 Protein Overexpression in Shwachman-Diamond Syndrome. *Archives of Pathology & Laboratory Medicine, 126*(10), 1157-1158. doi:10.1043/1543-2165(2002)126<1157b:PPOISS>2.0.CO;2

Eilken, H. M., Nishikawa, S.-I., & Schroeder, T. (2009). Continuous single-cell imaging of blood generation from haemogenic endothelium. *Nature, 457*(7231), 896.

El-Brolosy, M. A., Kontarakis, Z., Rossi, A., Kuenne, C., Günther, S., Fukuda, N., . . . Stainier, D. Y. R. (2019). Genetic compensation triggered by mutant mRNA degradation. *Nature, 568*(7751), 193-197. doi:10.1038/s41586-019-1064-z

Elghetany, M. T., & Alter, B. P. (2002). p53 Protein Overexpression in Bone Marrow Biopsies of Patients With Shwachman-Diamond Syndrome Has a Prevalence Similar to That of Patients With Refractory Anemia. *Archives of Pathology & Laboratory Medicine, 126*(4), 452-455. doi:10.1043/0003-9985(2002)126<0452:Ppoibm>2.0.Co;2

Fiegl, M. (2016). Epidemiology, pathogenesis, and etiology of acute leukemia. In W. Hiddemann (Ed.), *Handbook of Acute Leukemia* (pp. 3-13). Cham: Springer International Publishing.

Flores-Figueroa, E., Gutiérrez-Espíndola, G., Montesinos, J. J., Arana-Trejo, R. M. a., & Mayani, H. (2002). In vitro characterization of hematopoietic microenvironment cells from patients with myelodysplastic syndrome. *Leukemia research, 26*(7), 677-686.

Flynn, R. L., & Zou, L. (2011). ATR: a master conductor of cellular responses to DNA replication stress. *Trends in Biochemical Sciences, 36*(3), 133-140. doi:10.1016/j.tibs.2010.09.005

Fukumoto, T. (1992). Possible developmental interactions of hematopoietic cells and hepatocytes in fetal rat liver. *Biomedical Research, 13*(6), 385-413.

Gamis, A. S., Alonzo, T. A., Gerbing, R. B., Hilden, J. M., Sorrell, A. D., Sharma, M., . . . Doyle, J. (2011). Natural history of transient myeloproliferative disorder clinically diagnosed in Down syndrome neonates: a report from the Children's Oncology Group Study A2971. *Blood, 118*(26), 6752-6759.

Garcia-Montero, A. C., Jara-Acevedo, M., Teodosio, C., Sanchez, M. L., Nunez, R., Prados, A., . . . Orfao, A. (2006). KIT mutation in mast cells and other bone marrow hematopoietic cell lineages in systemic mast cell disorders: a prospective study of the Spanish Network on

Mastocytosis (REMA) in a series of 113 patients. *Blood, 108*(7), 2366-2372. doi:10.1182/blood-2006-04-015545

Gatti, R., Meuwissen, H., Allen, H., Hong, R., & Good, R. (1968). Immunological reconstitution of sex-linked lymphopenic immunological deficiency. *The Lancet, 292*(7583), 1366-1369.

Ge, L., Zhang, R.-p., Wan, F., Guo, D.-y., Wang, P., Xiang, L.-x., & Shao, J.-z. (2014). TET2 plays an essential role in erythropoiesis by regulating lineage-specific genes via DNA oxidative demethylation in a zebrafish model. *Molecular and cellular biology, 34*(6), 989-1002.

Genovese, G., Kähler, A. K., Handsaker, R. E., Lindberg, J., Rose, S. A., Bakhoum, S. F., . . . McCarroll, S. A. (2014). Clonal Hematopoiesis and Blood-Cancer Risk Inferred from Blood DNA Sequence. *New England Journal of Medicine, 371*(26), 2477-2487. doi:10.1056/NEJMoa1409405

Giovanella, B., Yim, S., Stehlin, J., & Williams Jr, L. (1972). Development of invasive tumors in the "nude" mouse after injection of cultured human melanoma cells. *Journal of the National Cancer Institute, 48*(5), 1531-1533.

Gjini, E., Mansour, M. R., Sander, J. D., Moritz, N., Nguyen, A. T., Kesarsing, M., . . . Look, A. T. (2015a). A Zebrafish Model of Myelodysplastic Syndrome Produced through *tet2* Genomic Editing. *Molecular and Cellular Biology, 35*(5), 789-804. doi:10.1128/mcb.00971-14

Gjini, E., Mansour, M. R., Sander, J. D., Moritz, N., Nguyen, A. T., Kesarsing, M., . . . Look, A. T. (2015b). A zebrafish model of myelodysplastic syndrome produced through tet2 genomic editing. *Molecular and cellular biology, 35*(5), 789-804.

Glass, T. J., Lund, T. C., Patrinostro, X., Tolar, J., Bowman, T. V., Zon, L. I., & Blazar, B. R. (2011). Stromal cell–derived factor-1 and hematopoietic cell homing in an adult zebrafish model of hematopoietic cell transplantation. *Blood, 118*(3), 766-774. doi:10.1182/blood-2011-01-328476 %J Blood

Glaubach, T., Robinson, L. J., & Corey, S. J. (2014). Pediatric myelodysplastic syndromes: they do exist! *Journal of pediatric hematology/oncology, 36*(1), 1-7.

Golshayan, A.-R., Jin, T., Maciejewski, J., Fu, A. Z., Bershadsky, B., Kattan, M. W., . . . Sekeres, M. A. (2007). Efficacy of growth factors compared to other therapies for low-risk

myelodysplastic syndromes. *British Journal of Haematology, 137*(2), 125-132. doi:10.1111/j.1365-2141.2007.06546.x

Golub, R., & Cumano, A. (2013). Embryonic hematopoiesis. *Blood Cells, Molecules, and Diseases, 51*(4), 226-231. doi:https://doi.org/10.1016/j.bcmd.2013.08.004

Gommerman, J. L., Rottapel, R., & Berger, S. A. (1997). Phosphatidylinositol 3-kinase and Ca2+ influx dependence for ligand-stimulated internalization of the c-Kit receptor. *Journal of Biological Chemistry, 272*(48), 30519-30525.

Goyama, S., Wunderlich, M., & Mulloy, J. C. (2015). Xenograft models for normal and malignant stem cells. *Blood, 125*(17), 2630-2640.

Greenbaum, A., Hsu, Y.-M. S., Day, R. B., Schuettpelz, L. G., Christopher, M. J., Borgerding, J. N., . . . Link, D. C. (2013). CXCL12 in early mesenchymal progenitors is required for haematopoietic stem-cell maintenance. *Nature, 495*, 227. doi:10.1038/nature11926 https://www.nature.com/articles/nature11926#supplementary-information

Haferlach, T., Nagata, Y., Grossmann, V., Okuno, Y., Bacher, U., Nagae, G., . . . Ogawa, S. (2013). Landscape of genetic lesions in 944 patients with myelodysplastic syndromes. *Leukemia, 28*, 241. doi:10.1038/leu.2013.336 https://www.nature.com/articles/leu2013336#supplementary-information

Haldi, M., Ton, C., Seng, W. L., & McGrath, P. (2006). Human melanoma cells transplanted into zebrafish proliferate, migrate, produce melanin, form masses and stimulate angiogenesis in zebrafish. *Angiogenesis, 9*(3), 139-151.

Hasle, H., Clemmensen, I. H., & Mikkelsen, M. (2000). Risks of leukaemia and solid tumours in individuals with Down's syndrome. *The Lancet, 355*(9199), 165-169.

Hatakeyama, S. (2017). TRIM Family Proteins: Roles in Autophagy, Immunity, and Carcinogenesis. *Trends in Biochemical Sciences, 42*(4), 297-311. doi:https://doi.org/10.1016/j.tibs.2017.01.002

Heinrich, M. C., Corless, C. L., Duensing, A., McGreevey, L., Chen, C.-J., Joseph, N., . . . Town, A. (2003). PDGFRA activating mutations in gastrointestinal stromal tumors. *Science, 299*(5607), 708-710.

Hidalgo, M., Amant, F., Biankin, A. V., Budinská, E., Byrne, A. T., Caldas, C., . . . Villanueva, A. (2014). Patient-Derived Xenograft Models: An Emerging Platform for Translational Cancer Research. *Cancer discovery, 4*(9), 998-1013. doi:10.1158/2159-8290.CD-14-0001 %J Cancer Discovery

Ho, Y.-H., del Toro, R., Rivera-Torres, J., Rak, J., Korn, C., García-García, A., . . . Mendez-Ferrer, S. (2018). Aging of Bone Marrow Microenvironment Promotes Myeloid Bias of Hematopoietic Progenitors and Is a Target in Age-Related Myeloproliferative Neoplasms. *Blood, 132*(Suppl 1), 3842-3842. doi:10.1182/blood-2018-99-116015

Horny, H., Akin, C., Metcalfe, D., Escribano, L., Bennett, J., Valent, P., & Bain, B. (2008). Mastocytosis (mast cell disease): World Health Organization (WHO) classification of tumors: pathology and genetics. *Tumours of Haematopoietic and Lymphoid Tissues*, 54-63.

Howe, K., Clark, M. D., Torroja, C. F., Torrance, J., Berthelot, C., Muffato, M., . . . Stemple, D. L. (2013). The zebrafish reference genome sequence and its relationship to the human genome. *Nature, 496*, 498. doi:10.1038/nature12111 https://www.nature.com/articles/nature12111#supplementary-information

Hsu, C.-H., Altschuler, S. J., & Wu, L. F. (2019). Patterns of Early p21 Dynamics Determine Proliferation-Senescence Cell Fate after Chemotherapy. *Cell, 178*(2), 361-373.e312. doi:https://doi.org/10.1016/j.cell.2019.05.041

Huang, Y., Zhang, J., Liu, J., Hu, Y., Ni, S., Yang, Y., . . . Qin, Q. (2017). Fish TRIM35 negatively regulates the interferon signaling pathway in response to grouper nodavirus infection. *Fish & Shellfish Immunology, 69*, 142-152. doi:https://doi.org/10.1016/j.fsi.2017.08.019

Huber, T. L., Kouskoff, V., Joerg Fehling, H., Palis, J., & Keller, G. (2004). Haemangioblast commitment is initiated in the primitive streak of the mouse embryo. *Nature, 432*(7017), 625-630. doi:10.1038/nature03122

Hughes, K., Nikolakaki, E., Plyte, S. E., Totty, N. F., & Woodgett, J. R. (1993). Modulation of the glycogen synthase kinase-3 family by tyrosine phosphorylation. *The EMBO journal, 12*(2), 803-808.

Ihle, J. N. (1995). Cytokine receptor signalling. *Nature, 377*, 591. doi:10.1038/377591a0

Ikeda, H., Kanakura, Y., Tamaki, T., Kuriu, A., Kitayama, H., Ishikawa, J., . . . Griffin, J. (1991). Expression and functional role of the proto-oncogene c-kit in acute myeloblastic leukemia cells. *Blood, 78*(11), 2962-2968.

Isern, J., He, Z., Fraser, S. T., Nowotschin, S., Ferrer-Vaquer, A., Moore, R., . . . Baron, M. H. (2011). Single-lineage transcriptome analysis reveals key regulatory pathways in primitive erythroid progenitors in the mouse embryo. *Blood, 117*(18), 4924-4934. doi:10.1182/blood-2010-10-313676

Jahn, T., Seipel, P., Coutinho, S., Urschel, S., Schwarz, K., Miething, C., . . . Duyster, J. (2002). Analysing c-kit internalization using a functional c-kit-EGFP chimera containing the fluorochrome within the extracellular domain. *Oncogene, 21*(29), 4508-4520.

Jaiswal, S., & Libby, P. (2019). Clonal haematopoiesis: connecting ageing and inflammation in cardiovascular disease. *Nature Reviews Cardiology*. doi:10.1038/s41569-019-0247-5

Jaiswal, S., Natarajan, P., Silver, A. J., Gibson, C. J., Bick, A. G., Shvartz, E., . . . Ebert, B. L. (2017). Clonal Hematopoiesis and Risk of Atherosclerotic Cardiovascular Disease. *New England Journal of Medicine, 377*(2), 111-121. doi:10.1056/NEJMoa1701719

Jan, M., Snyder, T. M., Corces-Zimmerman, M. R., Vyas, P., Weissman, I. L., Quake, S. R., & Majeti, R. (2012). Clonal evolution of preleukemic hematopoietic stem cells precedes human acute myeloid leukemia. *Science translational medicine, 4*(149), 149ra118-149ra118.

Jawhar, M., Kreil, S., Schwaab, J., Shoumariyeh, K., Span, L. L. F., Fuhrmann, S., . . . Reiter, A. (2017). Systemic Mastocytosis with Associated Acute Myeloid Leukemia (SM-AML): a Poor-Risk Multi-Mutated Disease That Follows a Distinct Diagnostic Algorithm and Requires High-Dose Stem Cell-Targeting Therapy. *Blood, 130*(Suppl 1), 2916-2916.

Joenje, H., & Patel, K. J. (2001). The emerging genetic and molecular basis of Fanconi anaemia. *Nature Reviews Genetics, 2*, 446. doi:10.1038/35076590
https://www.nature.com/articles/35076590#supplementary-information

Kitayama, H., Kanakura, Y., Furitsu, T., Tsujimura, T., Oritani, K., Ikeda, H., . . . Kitamura, Y. (1995). Constitutively activating mutations of c-kit receptor tyrosine kinase confer factor-independent growth and tumorigenicity of factor-dependent hematopoietic cell lines. *Blood, 85*(3), 790-798.

Klco, Jeffery M., Spencer, David H., Miller, Christopher A., Griffith, M., Lamprecht, Tamara L., O'Laughlin, M., . . . Ley, Timothy J. (2014). Functional Heterogeneity of Genetically Defined Subclones in Acute Myeloid Leukemia. *Cancer Cell, 25*(3), 379-392. doi:https://doi.org/10.1016/j.ccr.2014.01.031

Klusmann, J.-H., Creutzig, U., Zimmermann, M., Dworzak, M., Jorch, N., Langebrake, C., . . . Reinhardt, D. (2008). Treatment and prognostic impact of transient leukemia in neonates with Down syndrome. *Blood, 111*(6), 2991-2998.

Ko, M., Bandukwala, H. S., An, J., Lamperti, E. D., Thompson, E. C., Hastie, R., . . . Rao, A. (2011). Ten-Eleven-Translocation 2 (TET2) negatively regulates homeostasis and differentiation of hematopoietic stem cells in mice. *Proceedings of the National Academy of Sciences, 108*(35), 14566-14571. doi:10.1073/pnas.1112317108

Koeffler, H., & Leong, G. (2017). Preleukemia: one name, many meanings. *Leukemia, 31*(3), 534.

Kotla, V., Goel, S., Nischal, S., Heuck, C., Vivek, K., Das, B., & Verma, A. (2009). Mechanism of action of lenalidomide in hematological malignancies. *Journal of Hematology & Oncology, 2*(1), 36. doi:10.1186/1756-8722-2-36

Krivtsov, A. V., Twomey, D., Feng, Z., Stubbs, M. C., Wang, Y., Faber, J., . . . Gilliland, D. G. (2006). Transformation from committed progenitor to leukaemia stem cell initiated by MLL–AF9. *Nature, 442*(7104), 818.

Kulkeaw, K., & Sugiyama, D. (2012). Zebrafish erythropoiesis and the utility of fish as models of anemia. *Stem Cell Research & Therapy, 3*(6), 55. doi:10.1186/scrt146

Kumar, S., & Hedges, S. B. (1998). A molecular timescale for vertebrate evolution. *Nature, 392*(6679), 917-920. doi:10.1038/31927

Kurahashi, H., Hara, J., Yumura-Yagi, K., Murayama, N., Inoue, M., Ishihara, S., . . . Kawa-Ha, K. (1991). Monoclonal nature of transient abnormal myelopoiesis in Down's syndrome. *Blood, 77*(6), 1161-1163.

Kwok, J., O'Shea, M., Hume, D. A., & Lengeling, A. (2017). Jmjd6, a JmjC dioxygenase with many interaction partners and pleiotropic functions. *Frontiers in genetics, 8*, 32.

Labuhn, M., Perkins, K., Papaemmanuil, E., Garnett, C., Matzk, S., Amstislavskiy, V., . . . Vyas, P. (2018). Modelling the Progression of a Preleukemic Stage to Overt Leukemia in Children with Down Syndrome. *Blood, 132*(Suppl 1), 543-543. doi:10.1182/blood-2018-99-116661 %J Blood

Lacaud, G., & Kouskoff, V. (2017). Hemangioblast, hemogenic endothelium, and primitive versus definitive hematopoiesis. *Experimental Hematology, 49*, 19-24. doi:https://doi.org/10.1016/j.exphem.2016.12.009

Laine, E., Chauvot de Beauchêne, I., Perahia, D., Auclair, C., & Tchertanov, L. (2011). Mutation D816V Alters the Internal Structure and Dynamics of c-KIT Receptor Cytoplasmic Region: Implications for Dimerization and Activation Mechanisms. *PLOS Computational Biology, 7*(6), e1002068. doi:10.1371/journal.pcbi.1002068

Laine, E., de Beauchêne, I. C., Perahia, D., Auclair, C., & Tchertanov, L. (2011). Mutation D816V alters the internal structure and dynamics of c-KIT receptor cytoplasmic region: implications for dimerization and activation mechanisms. *PLoS Comput Biol, 7*(6), e1002068.

Lam, S., Chua, H., Gong, Z., Lam, T., & Sin, Y. (2004). Development and maturation of the immune system in zebrafish, Danio rerio: a gene expression profiling, in situ hybridization and immunological study. *Developmental & Comparative Immunology, 28*(1), 9-28.

Lange, B. J., Kobrinsky, N., Barnard, D. R., Arthur, D. C., Buckley, J. D., Howells, W. B., . . . Smith, F. O. (1998). Distinctive demography, biology, and outcome of acute myeloid leukemia and myelodysplastic syndrome in children with Down syndrome: Children's Cancer Group Studies 2861 and 2891. *Blood, 91*(2), 608-615.

Lapidot, T., Pflumio, F., Doedens, M., Murdoch, B., Williams, D. E., & Dick, J. E. (1992). Cytokine stimulation of multilineage hematopoiesis from immature human cells engrafted in SCID mice. *Science, 255*(5048), 1137-1141.

Lapidot, T., Sirard, C., Vormoor, J., Murdoch, B., Hoang, T., Caceres-Cortes, J., . . . Dick, J. E. (1994). A cell initiating human acute myeloid leukaemia after transplantation into SCID mice. *Nature, 367*(6464), 645-648. doi:10.1038/367645a0

Larochelle, A., Vormoor, J., Hanenberg, H., Wang, J. C. Y., Bhatia, M., Lapidot, T., . . . Dick, J. E. (1996). Identification of primitive human hematopoietic cells capable of repopulating

NOD/SCID mouse bone marrow: Implications for gene therapy. *Nature Medicine, 2*(12), 1329-1337. doi:10.1038/nm1296-1329

Lauter, G., Söll, I., & Hauptmann, G. (2011). Two-color fluorescent in situ hybridization in the embryonic zebrafish brain using differential detection systems. *BMC Developmental Biology, 11*(1), 43. doi:10.1186/1471-213X-11-43

Le Guyader, D., Redd, M. J., Colucci-Guyon, E., Murayama, E., Kissa, K., Briolat, V., . . . Herbomel, P. (2008). Origins and unconventional behavior of neutrophils in developing zebrafish. *Blood, 111*(1), 132-141. doi:10.1182/blood-2007-06-095398

Lee, L. M. J., Seftor, E. A., Bonde, G., Cornell, R. A., & Hendrix, M. J. C. (2005). The fate of human malignant melanoma cells transplanted into zebrafish embryos: Assessment of migration and cell division in the absence of tumor formation. *Developmental Dynamics, 233*(4), 1560-1570. doi:10.1002/dvdy.20471

Lemmon, M. A., Pinchasi, D., Zhou, M., Lax, I., & Schlessinger, J. (1997). Kit receptor dimerization is driven by bivalent binding of stem cell factor. *Journal of Biological Chemistry, 272*(10), 6311-6317.

Lennartsson, J., & Rönnstrand, L. (2012). Stem cell factor receptor/c-Kit: from basic science to clinical implications. *Physiological reviews, 92*(4), 1619-1649.

Li, C., Lan, Y., Schwartz-Orbach, L., Korol, E., Tahiliani, M., Evans, T., & Goll, M. G. (2015). Overlapping requirements for Tet2 and Tet3 in normal development and hematopoietic stem cell emergence. *Cell reports, 12*(7), 1133-1143.

Li, L., Li, M., Sun, C., Francisco, L., Chakraborty, S., Sabado, M., . . . Bhatia, R. (2011). Altered Hematopoietic Cell Gene Expression Precedes Development of Therapy-Related Myelodysplasia/Acute Myeloid Leukemia and Identifies Patients at Risk. *Cancer Cell, 20*(5), 591-605. doi:10.1016/j.ccr.2011.09.011

Li, Z., Cai, X., Cai, C.-L., Wang, J., Zhang, W., Petersen, B. E., . . . Xu, M. (2011). Deletion of *Tet2* in mice leads to dysregulated hematopoietic stem cells and subsequent development of myeloid malignancies. *Blood, 118*(17), 4509-4518. doi:10.1182/blood-2010-12-325241

Lim, K.-H., Tefferi, A., Lasho, T. L., Finke, C., Patnaik, M., Butterfield, J. H., . . . Pardanani, A. (2009). Systemic mastocytosis in 342 consecutive adults: survival studies and prognostic factors. *Blood, 113*(23), 5727-5736.

Lin, C. S., Lim, S. K., D'Agati, V., & Costantini, F. (1996). Differential effects of an erythropoietin receptor gene disruption on primitive and definitive erythropoiesis. *Genes & Development, 10*(2), 154-164. doi:10.1101/gad.10.2.154

Linnekin, D. (1999). Early signaling pathways activated by c-Kit in hematopoietic cells. *The international journal of biochemistry & cell biology, 31*(10), 1053-1074.

Lipton, J. M., & Ellis, S. R. (2009). Diamond-Blackfan Anemia: Diagnosis, Treatment, and Molecular Pathogenesis. *Hematology/Oncology Clinics of North America, 23*(2), 261-282. doi:https://doi.org/10.1016/j.hoc.2009.01.004

Liu, Y., Asnani, A., Zou, L., Bentley, V. L., Yu, M., Wang, Y., . . . Peterson, R. T. (2014). Visnagin protects against doxorubicin-induced cardiomyopathy through modulation of mitochondrial malate dehydrogenase. *Science Translational Medicine, 6*(266), 266ra170-266ra170. doi:10.1126/scitranslmed.3010189

Longley, B. J., Metcalfe, D. D., Tharp, M., Wang, X., Tyrrell, L., Lu, S.-z., . . . Ma, Y. (1999). Activating and dominant inactivating c-KIT catalytic domain mutations in distinct clinical forms of human mastocytosis. *Proceedings of the National Academy of Sciences, 96*(4), 1609-1614.

Longley, B. J., Reguera, M. J., & Ma, Y. (2001). Classes of c-KIT activating mutations: proposed mechanisms of action and implications for disease classification and therapy. *Leukemia research, 25*(7), 571-576.

Lundberg, P., Karow, A., Nienhold, R., Looser, R., Hao-Shen, H., Nissen, I., . . . Skoda, R. C. (2014). Clonal evolution and clinical correlates of somatic mutations in myeloproliferative neoplasms. *Blood, 123*(14), 2220-2228. doi:10.1182/blood-2013-11-537167

Ma, Y., Zeng, S., Metcalfe, D. D., Akin, C., Dimitrijevic, S., Butterfield, J. H., . . . Longley, B. J. (2002). The c-KIT mutation causing human mastocytosis is resistant to STI571 and other KIT kinase inhibitors; kinases with enzymatic site mutations show different inhibitor sensitivity profiles than wild-type kinases and those with regulatory-type mutations. *Blood, 99*(5), 1741-1744.

Magnusson, M., Brun, A. C. M., Miyake, N., Larsson, J., Ehinger, M., Bjornsson, J. M., . . . Karlsson, S. (2007). HOXA10 is a critical regulator for hematopoietic stem cells and erythroid/megakaryocyte development. *Blood, 109*(9), 3687-3696. doi:10.1182/blood-2006-10-054676

Maiolino, G., Rossitto, G., Caielli, P., Bisogni, V., Rossi, G. P., & Calò, L. A. (2013). The role of oxidized low-density lipoproteins in atherosclerosis: the myths and the facts. *Mediators of inflammation, 2013*.

Mandal, L., Banerjee, U., & Hartenstein, V. (2004). Evidence for a fruit fly hemangioblast and similarities between lymph-gland hematopoiesis in fruit fly and mammal aorta-gonadal-mesonephros mesoderm. *Nature genetics, 36*(9), 1019.

Manz, M. G. (2007). Human-Hemato-Lymphoid-System Mice: Opportunities and Challenges. *Immunity, 26*(5), 537-541. doi:10.1016/j.immuni.2007.05.001

Marcondes, A. M., Mhyre, A. J., Stirewalt, D. L., Kim, S.-H., Dinarello, C. A., & Deeg, H. J. (2008). Dysregulation of IL-32 in myelodysplastic syndrome and chronic myelomonocytic leukemia modulates apoptosis and impairs NK function. *Proceedings of the National Academy of Sciences, 105*(8), 2865-2870.

Martin, C., Ohayon, D., Alkan, M., Mocek, J., Pederzoli-Ribeil, M., Candalh, C., . . . Witko-Sarsat, V. (2016). Neutrophil-Expressed p21/waf1 Favors Inflammation Resolution in Pseudomonas aeruginosa Infection. *American Journal of Respiratory Cell and Molecular Biology, 54*(5), 740-750. doi:10.1165/rcmb.2015-0047OC

Massey, G. V., Zipursky, A., Chang, M. N., Doyle, J. J., Nasim, S., Taub, J. W., . . . Weinstein, H. J. (2006). A prospective study of the natural history of transient leukemia (TL) in neonates with Down syndrome (DS): Children's Oncology Group (COG) study POG-9481. *Blood, 107*(12), 4606-4613.

Medyouf, H., Mossner, M., Jann, J.-C., Nolte, F., Raffel, S., Herrmann, C., . . . Nowak, D. (2014). Myelodysplastic Cells in Patients Reprogram Mesenchymal Stromal Cells to Establish a Transplantable Stem Cell Niche Disease Unit. *Cell stem cell, 14*(6), 824-837. doi:https://doi.org/10.1016/j.stem.2014.02.014

Meisel, M., Hinterleitner, R., Pacis, A., Chen, L., Earley, Z. M., Mayassi, T., . . . Jabri, B. (2018). Microbial signals drive pre-leukaemic myeloproliferation in a Tet2-deficient host. *Nature, 557*(7706), 580-584. doi:10.1038/s41586-018-0125-z

Melong, N., Steele, S., MacDonald, M., Holly, A., Collins, C. C., Zoubeidi, A., . . . Dellaire, G. (2017). Enzalutamide inhibits testosterone-induced growth of human prostate cancer xenografts in zebrafish and can induce bradycardia. *Scientific Reports, 7*(1), 14698. doi:10.1038/s41598-017-14413-w

Metelo, A. M., Noonan, H. R., Li, X., Jin, Y., Baker, R., Kamentsky, L., . . . Iliopoulos, O. (2015). Pharmacological HIF2α inhibition improves VHL disease–associated phenotypes in zebrafish model. *The Journal of Clinical Investigation, 125*(5), 1987-1997. doi:10.1172/JCI73665

Miyashita, T., Asada, M., Fujimoto, J., Inaba, T., Takihara, Y., Sugita, K., . . . Mizutani, S. (1991). Clonal analysis of transient myeloproliferative disorder in Down's syndrome. *Leukemia, 5*(1), 56-59.

Mol, C. D., Dougan, D. R., Schneider, T. R., Skene, R. J., Kraus, M. L., Scheibe, D. N., . . . Wilson, K. P. (2004). Structural basis for the autoinhibition and STI-571 inhibition of c-Kit tyrosine kinase. *Journal of Biological Chemistry, 279*(30), 31655-31663.

Moore, J. C., Tang, Q., Yordán, N. T., Moore, F. E., Garcia, E. G., Lobbardi, R., . . . Sadreyev, R. I. (2016). Single-cell imaging of normal and malignant cell engraftment into optically clear prkdc-null SCID zebrafish. *Journal of Experimental Medicine, 213*(12), 2575-2589.

Moran-Crusio, K., Reavie, L., Shih, A., Abdel-Wahab, O., Ndiaye-Lobry, D., Lobry, C., . . . Levine, Ross L. (2011). Tet2 Loss Leads to Increased Hematopoietic Stem Cell Self-Renewal and Myeloid Transformation. *Cancer Cell, 20*(1), 11-24. doi:https://doi.org/10.1016/j.ccr.2011.06.001

Morrison, S. J., Hemmati, H. D., Wandycz, A. M., & Weissman, I. L. (1995). The purification and characterization of fetal liver hematopoietic stem cells. *Proceedings of the National Academy of Sciences, 92*(22), 10302-10306.

Morrison, S. J., & Scadden, D. T. (2014). The bone marrow niche for haematopoietic stem cells. *Nature, 505*, 327. doi:10.1038/nature12984

Morton, J. J., Bird, G., Keysar, S. B., Astling, D. P., Lyons, T. R., Anderson, R. T., . . . Jimeno, A. (2015). XactMice: humanizing mouse bone marrow enables microenvironment reconstitution in a patient-derived xenograft model of head and neck cancer. *Oncogene, 35*, 290. doi:10.1038/onc.2015.94
https://www.nature.com/articles/onc201594#supplementary-information

Murayama, E., Kissa, K., Zapata, A., Mordelet, E., Briolat, V., Lin, H.-F., . . . Herbomel, P. (2006). Tracing Hematopoietic Precursor Migration to Successive Hematopoietic Organs during Zebrafish Development. *Immunity, 25*(6), 963-975. doi:10.1016/j.immuni.2006.10.015

Murphy, W. J., Pringle, T. H., Crider, T. A., Springer, M. S., & Miller, W. (2007). Using genomic data to unravel the root of the placental mammal phylogeny. *Genome research, 17*(4), 413-421.

Myers, C. T., & Krieg, P. A. (2013). BMP-mediated specification of the erythroid lineage suppresses endothelial development in blood island precursors. *Blood, 122*(24), 3929-3939.

Myers, K. C., Furutani, E. M., Siegele, B., Fleming, M. D., Elghetany, M. T., Arsenault, V., . . . Shimamura, A. (2017). MDS and AML in Shwachman-Diamond Syndrome: Clinical Features and Outcomes. *Blood, 130*(Suppl 1), 1177-1177.

Nagasawa, T., Hirota, S., Tachibana, K., Takakura, N., Nishikawa, S.-i., Kitamura, Y., . . . Kishimoto, T. (1996). Defects of B-cell lymphopoiesis and bone-marrow myelopoiesis in mice lacking the CXC chemokine PBSF/SDF-1. *Nature, 382*(6592), 635-638. doi:10.1038/382635a0

Nangalia, J., Massie, C. E., Baxter, E. J., Nice, F. L., Gundem, G., Wedge, D. C., . . . Kent, D. G. (2013). Somatic CALR mutations in myeloproliferative neoplasms with nonmutated JAK2. *New England Journal of Medicine, 369*(25), 2391-2405.

Narla, A., & Ebert, B. L. (2010). Ribosomopathies: human disorders of ribosome dysfunction. *Blood, 115*(16), 3196-3205. doi:10.1182/blood-2009-10-178129

Nick, H. J., Kim, H.-G., Chang, C.-W., Harris, K. W., Reddy, V., & Klug, C. A. (2012). Distinct classes of c-Kit–activating mutations differ in their ability to promote RUNX1-ETO–associated acute myeloid leukemia. *Blood, 119*(6), 1522-1531.

Nicolini, F. E., Cashman, J. D., Hogge, D. E., Humphries, R. K., & Eaves, C. J. (2003). NOD/SCID mice engineered to express human IL-3, GM-CSF and Steel factor constitutively mobilize engrafted human progenitors and compromise human stem cell regeneration. *Leukemia, 18*, 341. doi:10.1038/sj.leu.2403222

Nicolini, F. E., Cashman, J. D., Hogge, D. E., Humphries, R. K., & Eaves, C. J. (2004). NOD/SCID mice engineered to express human IL-3, GM-CSF and Steel factor constitutively mobilize engrafted human progenitors and compromise human stem cell regeneration. *Leukemia, 18*(2), 341-347. doi:10.1038/sj.leu.2403222

Nishikawa, T., Ota, T., & Isogai, T. (2000). Prediction whether a human cDNA sequence contains initiation codon by combining statistical information and similarity with protein sequences. *Bioinformatics, 16*(11), 960-967. doi:10.1093/bioinformatics/16.11.960

North, T. E., Goessling, W., Walkley, C. R., Lengerke, C., Kopani, K. R., Lord, A. M., . . . Zon, L. I. (2007). Prostaglandin E2 regulates vertebrate haematopoietic stem cell homeostasis. *Nature, 447*, 1007. doi:10.1038/nature05883
https://www.nature.com/articles/nature05883#supplementary-information

Ohneda, O., Fennie, C., Zheng, Z., Donahue, C., La, H., Villacorta, R., . . . Lasky, L. A. (1998). Hematopoietic Stem Cell Maintenance and Differentiation Are Supported by Embryonic Aorta-Gonad-Mesonephros Region–Derived Endothelium. *Blood, 92*(3), 908-919. Retrieved from http://www.bloodjournal.org/content/bloodjournal/92/3/908.full.pdf

Ohuchi, M., Sakamoto, Y., Tokunaga, R., Kiyozumi, Y., Nakamura, K., Izumi, D., . . . Iwatsuki, M. (2018). Increased EZH2 expression during the adenoma-carcinoma sequence in colorectal cancer. *Oncology letters, 16*(4), 5275-5281.

Oostendorp, R. A., Robin, C., Steinhoff, C., Marz, S., Bräuer, R., Nuber, U. A., . . . Peschel, C. (2005). Long-term maintenance of hematopoietic stem cells does not require contact with embryo-derived stromal cells in cocultures. *Stem Cells, 23*(6), 842-851.

Orkin, S. H., & Zon, L. I. (2008). Hematopoiesis: an evolving paradigm for stem cell biology. *Cell, 132*(4), 631-644.

Paget, S. (1889). The Distribution of Secondary Growths in Cancer of the Breast. *The Lancet, 133*(3421), 571-573. doi:https://doi.org/10.1016/S0140-6736(00)49915-0

Palis, J., Robertson, S., Kennedy, M., Wall, C., & Keller, G. (1999). Development of erythroid and myeloid progenitors in the yolk sac and embryo proper of the mouse. *Development, 126*(22), 5073-5084.

Papaemmanuil, E., Gerstung, M., Bullinger, L., Gaidzik, V. I., Paschka, P., Roberts, N. D., . . . Campbell, P. J. (2016). Genomic Classification and Prognosis in Acute Myeloid Leukemia. *New England Journal of Medicine, 374*(23), 2209-2221. doi:10.1056/NEJMoa1516192

Passaro, D., Irigoyen, M., Catherinet, C., Gachet, S., Da Costa De Jesus, C., Lasgi, C., . . . Ghysdael, J. (2015). CXCR4 Is Required for Leukemia-Initiating Cell Activity in T Cell Acute Lymphoblastic Leukemia. *Cancer Cell, 27*(6), 769-779. doi:10.1016/j.ccell.2015.05.003

Payushina, O. V. (2012). Hematopoietic microenvironment in the fetal liver: roles of different cell populations. *ISRN Cell Biology, 2012*.

Peled, A., Kollet, O., Ponomaryov, T., Petit, I., Franitza, S., Grabovsky, V., . . . Lapidot, T. (2000). The chemokine SDF-1 activates the integrins LFA-1, VLA-4, and VLA-5 on immature human CD34+ cells: role in transendothelial/stromal migration and engraftment of NOD/SCID mice. *Blood, 95*(11), 3289-3296. Retrieved from http://www.bloodjournal.org/content/bloodjournal/95/11/3289.full.pdf

Perdiguero, E. G., & Geissmann, F. (2015). The development and maintenance of resident macrophages. *Nature Immunology, 17*, 2. doi:10.1038/ni.3341

Philo, J. S., Wen, J., Wypych, J., Schwartz, M. G., Mendiaz, E. A., & Langley, K. E. (1996). Human stem cell factor dimer forms a complex with two molecules of the extracellular domain of its receptor, Kit. *Journal of Biological Chemistry, 271*(12), 6895-6902.

Ponnikorn, S., Kong, S. P., Thitivirachawat, S., Tanjasiri, C., Tungpradabkul, S., & Hongeng, S. (2019). Proteomic Analysis of β-Thalassemia/HbE: A Perspective from Hematopoietic Stem Cells (HSCs). In *Proteomics Technologies and Applications*: IntechOpen.

Ponomaryov, T., Peled, A., Petit, I., Taichman, R. S., Habler, L., Sandbank, J., . . . Lapidot, T. (2000). Induction of the chemokine stromal-derived factor-1 following DNA damage improves human stem cell function. *The Journal of Clinical Investigation, 106*(11), 1331-1339. doi:10.1172/JCI10329

Pruvot, B., Jacquel, A., Droin, N., Auberger, P., Bouscary, D., Tamburini, J., . . . Solary, E. (2011a). Leukemic cell xenograft in zebrafish embryo for investigating drug efficacy. *Haematologica*, haematol. 2010.031401.

Pruvot, B., Jacquel, A., Droin, N., Auberger, P., Bouscary, D., Tamburini, J., . . . Solary, E. (2011b). Leukemic cell xenograft in zebrafish embryo for investigating drug efficacy. *haematologica, 96*(4), 612-616.

Prykhozhij, S. V., Fuller, C., Steele, S. L., Veinotte, C. J., Razaghi, B., Robitaille, J. M., . . . Berman, J. N. (2018). Optimized knock-in of point mutations in zebrafish using CRISPR/Cas9. *Nucleic Acids Research, 46*(17), e102-e102. doi:10.1093/nar/gky512

Quivoron, C., Couronné, L., Della Valle, V., Lopez, C. K., Plo, I., Wagner-Ballon, O., . . . Stern, M.-H. (2011). TET2 inactivation results in pleiotropic hematopoietic abnormalities in mouse and is a recurrent event during human lymphomagenesis. *Cancer Cell, 20*(1), 25-38.

Raaijmakers, M. H. G. P., Mukherjee, S., Guo, S., Zhang, S., Kobayashi, T., Schoonmaker, J. A., . . . Scadden, D. T. (2010). Bone progenitor dysfunction induces myelodysplasia and secondary leukaemia. *Nature, 464*, 852. doi:10.1038/nature08851
https://www.nature.com/articles/nature08851#supplementary-information

Rajan, V., Dellaire, G., & Berman, J. N. (2016). Modeling Leukemogenesis in the Zebrafish Using Genetic and Xenograft Models. *Zebrafish: Methods and Protocols*, 171-189.

Rasmussen, K. D., Berest, I., Keβler, S., Nishimura, K., Simón-Carrasco, L., Vassiliou, G. S., . . . Helin, K. (2019). TET2 binding to enhancers facilitates transcription factor recruitment in hematopoietic cells. *Genome Research, 29*(4), 564-575. doi:10.1101/gr.239277.118

Reshetnyak, A. V., Nelson, B., Shi, X., Boggon, T. J., Pavlenco, A., Mandel-Bausch, E. M., . . . Lax, I. (2013). Structural basis for KIT receptor tyrosine kinase inhibition by antibodies targeting the D4 membrane-proximal region. *Proceedings of the National Academy of Sciences, 110*(44), 17832-17837.

Rongvaux, A., Takizawa, H., Strowig, T., Willinger, T., Eynon, E. E., Flavell, R. A., & Manz, M. G. (2013). Human hemato-lymphoid system mice: current use and future potential for medicine. *Annual review of immunology, 31*, 635-674.

Rongvaux, A., Willinger, T., Martinek, J., Strowig, T., Gearty, S. V., Teichmann, L. L., . . . Flavell, R. A. (2014). Development and function of human innate immune cells in a humanized mouse model. *Nature Biotechnology, 32*, 364. doi:10.1038/nbt.2858
https://www.nature.com/articles/nbt.2858#supplementary-information

Rongvaux, A., Willinger, T., Takizawa, H., Rathinam, C., Auerbach, W., Murphy, A. J., . . . Stevens, S. (2011). Human thrombopoietin knockin mice efficiently support human hematopoiesis in vivo. *Proceedings of the National Academy of Sciences, 108*(6), 2378-2383.

Rongvaux, A., Willinger, T., Takizawa, H., Rathinam, C., Auerbach, W., Murphy, A. J., . . . Flavell, R. A. (2011). Human thrombopoietin knockin mice efficiently support human hematopoiesis in vivo. *Proceedings of the National Academy of Sciences, 108*(6), 2378-2383. doi:10.1073/pnas.1019524108

Rosenberg, P. S., Greene, M. H., & Alter, B. P. (2003). Cancer incidence in persons with Fanconi anemia. *Blood, 101*(3), 822-826. doi:10.1182/blood-2002-05-1498

Rossjohn, J., McKinstry, W. J., Woodcock, J. M., McClure, B. J., Hercus, T. R., Parker, M. W., . . . Bagley, C. J. (2000). Structure of the activation domain of the GM-CSF/IL-3/IL-5 receptor common β-chain bound to an antagonist. *95*(8), 2491-2498. Retrieved from http://www.bloodjournal.org/content/bloodjournal/95/8/2491.full.pdf

Rowe, R. G., Lummertz da Rocha, E., Sousa, P., Missios, P., Morse, M., Marion, W., . . . Daley, G. Q. (2019). The developmental stage of the hematopoietic niche regulates lineage in MLL-rearranged leukemia. *The Journal of Experimental Medicine, 216*(3), 527-538. doi:10.1084/jem.20181765

Roy, A., Cowan, G., Mead, A. J., Filippi, S., Bohn, G., Chaidos, A., . . . Roberts, I. (2012). Perturbation of fetal liver hematopoietic stem and progenitor cell development by trisomy 21. *Proceedings of the National Academy of Sciences, 109*(43), 17579-17584. doi:10.1073/pnas.1211405109

Rygaard, J., & Poulsen, C. O. (1969). Heterotransplantation of a human malignant tumour to "Nude" mice. *Acta Pathologica Microbiologica Scandinavica, 77*(4), 758-760.

Sacco, A., Roccaro, A. M., Ma, D., Shi, J., Mishima, Y., Moschetta, M., . . . Ghobrial, I. M. (2016). Cancer Cell Dissemination and Homing to the Bone Marrow in a Zebrafish Model. *76*(2), 463-471. doi:10.1158/0008-5472.CAN-15-1926 %J Cancer Research

Sánchez, M.-J., Holmes, A., Miles, C., & Dzierzak, E. (1996). Characterization of the first definitive hematopoietic stem cells in the AGM and liver of the mouse embryo. *Immunity, 5*(6), 513-525.

Sankaran, V. G., & Orkin, S. H. (2013). The Switch from Fetal to Adult Hemoglobin. *Cold Spring Harbor Perspectives in Medicine, 3*(1). doi:10.1101/cshperspect.a011643

Santamaría, C., Muntión, S., Rosón, B., Blanco, B., López-Villar, O., Carrancio, S., . . . Sarasquete, M. E. (2012). Impaired expression of DICER, DROSHA, SBDS and some microRNAs in mesenchymal stromal cells from myelodysplastic syndrome patients. *haematologica, 97*(8), 1218-1224.

Schindler, T., Bornmann, W., Pellicena, P., Miller, W. T., Clarkson, B., & Kuriyan, J. (2000). Structural mechanism for STI-571 inhibition of abelson tyrosine kinase. *Science, 289*(5486), 1938-1942.

Shah, N. P., Lee, F. Y., Luo, R., Jiang, Y., Donker, M., & Akin, C. (2006). Dasatinib (BMS-354825) inhibits KITD816V, an imatinib-resistant activating mutation that triggers neoplastic growth in most patients with systemic mastocytosis. *Blood, 108*(1), 286-291.

Shan, Y., Eastwood, M. P., Zhang, X., Kim, E. T., Arkhipov, A., Dror, R. O., . . . Shaw, D. E. (2012). Oncogenic mutations counteract intrinsic disorder in the EGFR kinase and promote receptor dimerization. *Cell, 149*(4), 860-870.

Shen, Q., Zhang, Q., Shi, Y., Shi, Q., Jiang, Y., Gu, Y., . . . Cao, X. (2018). Tet2 promotes pathogen infection-induced myelopoiesis through mRNA oxidation. *Nature, 554*, 123. doi:10.1038/nature25434
https://www.nature.com/articles/nature25434#supplementary-information

Shimamura, A., & Alter, B. P. (2010). Pathophysiology and management of inherited bone marrow failure syndromes. *Blood Reviews, 24*(3), 101-122. doi:https://doi.org/10.1016/j.blre.2010.03.002

Shlush, L. I., Zandi, S., Mitchell, A., Chen, W. C., Brandwein, J. M., Gupta, V., . . . Dick, J. E. (2014). Identification of pre-leukaemic haematopoietic stem cells in acute leukaemia. *Nature, 506*, 328. doi:10.1038/nature13038
https://www.nature.com/articles/nature13038#supplementary-information

Siminovitch, L., McCulloch, E. A., & Till, J. E. (1963). The distribution of colony-forming cells among spleen colonies. *Journal of Cellular and Comparative Physiology, 62*(3), 327-336.

Siolas, D., & Hannon, G. J. (2013). Patient Derived Tumor Xenografts: transforming clinical samples into mouse models. *J Cancer Research*, canres.1069.2013. doi:10.1158/0008-5472.CAN-13-1069 %J Cancer Research

Song, Y., Rongvaux, A., Taylor, A., Jiang, T., Tebaldi, T., Balasubramanian, K., . . . Halene, S. (2019). A highly efficient and faithful MDS patient-derived xenotransplantation model for pre-clinical studies. *Nature Communications, 10*(1), 366. doi:10.1038/s41467-018-08166-x

Spits, H. (2014). New models of human immunity. *Nature Biotechnology, 32*, 335. doi:10.1038/nbt.2871

Stachura, D. L., Svoboda, O., Campbell, C. A., Espín-Palazón, R., Lau, R. P., Zon, L. I., . . . Traver, D. (2013). The zebrafish granulocyte colony stimulating factors (Gcsfs): two paralogous cytokines and their roles in hematopoietic development and maintenance. *Blood*, blood-2012-2012-475392.

Stoletov, K., Montel, V., Lester, R. D., Gonias, S. L., & Klemke, R. (2007). High-resolution imaging of the dynamic tumor cell–vascular interface in transparent zebrafish. *Proceedings of the National Academy of Sciences, 104*(44), 17406-17411. doi:10.1073/pnas.0703446104

Sugiyama, T., Kohara, H., Noda, M., & Nagasawa, T. (2006). Maintenance of the Hematopoietic Stem Cell Pool by CXCL12-CXCR4 Chemokine Signaling in Bone Marrow Stromal Cell Niches. *Immunity, 25*(6), 977-988. doi:10.1016/j.immuni.2006.10.016

Sun, Z., & Williams, G. M. (2016). Chapter 18 - Skin Wound Healing: Skin Regeneration With Pharmacological Mobilized Stem Cells. In S. J. Lee, J. J. Yoo, & A. Atala (Eds.), *In Situ Tissue Regeneration* (pp. 345-368). Boston: Academic Press.

Tamplin, O. J., Durand, E. M., Carr, L. A., Childs, S. J., Hagedorn, E. J., Li, P., . . . Zon, L. I. (2015). Hematopoietic stem cell arrival triggers dynamic remodeling of the perivascular niche. *Cell, 160*(1-2), 241-252.

Tamplin, Owen J., Durand, Ellen M., Carr, Logan A., Childs, Sarah J., Hagedorn, Elliott J., Li, P., . . . Zon, Leonard I. (2015). Hematopoietic Stem Cell Arrival Triggers Dynamic Remodeling of the Perivascular Niche. *Cell, 160*(1), 241-252. doi:10.1016/j.cell.2014.12.032

Tamura, H., Ogata, K., Dong, H., & Chen, L. (2003). Immunology of B7-H1 and its roles in human diseases. *International journal of hematology, 78*(4), 321-328.

Tang, Q., Abdelfattah, N. S., Blackburn, J. S., Moore, J. C., Martinez, S. A., Moore, F. E., . . . Berman, J. N. (2014). Optimized cell transplantation using adult rag2 mutant zebrafish. *Nature methods, 11*(8), 821.

Taub, J. W., Mundschau, G., Ge, Y., Poulik, J. M., Qureshi, F., Jensen, T., . . . Crispino, J. D. (2004). Prenatal origin of GATA1 mutations may be an initiating step in the development of megakaryocytic leukemia in Down syndrome. *Blood, 104*(5), 1588-1589.

Taussig, D. C., Vargaftig, J., Miraki-Moud, F., Griessinger, E., Sharrock, K., Luke, T., . . . Bonnet, D. (2010). Leukemia-initiating cells from some acute myeloid leukemia patients with mutated nucleophosmin reside in the CD34[−] fraction. *Blood, 115*(10), 1976-1984. doi:10.1182/blood-2009-02-206565

Tefferi, A., Levine, R. L., Lim, K. H., Abdel-Wahab, O., Lasho, T. L., Patel, J., . . . Gilliland, D. G. (2009). Frequent TET2 mutations in systemic mastocytosis: clinical, KITD816V and FIP1L1-PDGFRA correlates. *Leukemia, 23*, 900. doi:10.1038/leu.2009.37

Tefferi, A., Pardanani, A., Lim, K. H., Abdel-Wahab, O., Lasho, T. L., Patel, J., . . . Levine, R. L. (2009). TET2 mutations and their clinical correlates in polycythemia vera, essential thrombocythemia and myelofibrosis. *Leukemia, 23*, 905. doi:10.1038/leu.2009.47

Tennant, G., Walsh, V., Truran, L., Edwards, P., Mills, K., & Burnett, A. (2000). Abnormalities of adherent layers grown from bone marrow of patients with myelodysplasia. *British journal of haematology, 111*(3), 853-862.

Theodore, L. N., Lundin, V., Wrighton, P. J., Cox, A. G., Sousa, P., Goessling, W., . . . North, T. E. (2017). YAP Regulates Hematopoietic Stem Cell Formation in Response to the Biophysical Forces of Blood Flow. *130*(Suppl 1), 1147-1147.

Thomas-Chollier, M., Darbo, E., Herrmann, C., Defrance, M., Thieffry, D., & van Helden, J. (2012). A complete workflow for the analysis of full-size ChIP-seq (and similar) data sets using peak-motifs. *Nature Protocols, 7*, 1551. doi:10.1038/nprot.2012.088
https://www.nature.com/articles/nprot.2012.088#supplementary-information

Till, J. E., & McCulloch, E. A. (1961). A direct measurement of the radiation sensitivity of normal mouse bone marrow cells. *Radiation research, 14*(2), 213-222.

Traggiai, E., Chicha, L., Mazzucchelli, L., Bronz, L., Piffaretti, J.-C., Lanzavecchia, A., & Manz, M. G. (2004). Development of a Human Adaptive Immune System in Cord Blood Cell-Transplanted Mice. *Science, 304*(5667), 104. Retrieved from http://science.sciencemag.org/content/304/5667/104.abstract

Traina, F., Visconte, V., Jankowska, A. M., Makishima, H., O'Keefe, C. L., Elson, P., . . . Tiu, R. V. (2012). Single Nucleotide Polymorphism Array Lesions, TET2, DNMT3A, ASXL1 and CBL Mutations Are Present in Systemic Mastocytosis. *PLOS ONE, 7*(8), e43090. doi:10.1371/journal.pone.0043090

Traver, D., Paw, B. H., Poss, K. D., Penberthy, W. T., Lin, S., & Zon, L. I. (2003). Transplantation and in vivo imaging of multilineage engraftment in zebrafish bloodless mutants. *Nature Immunology, 4*(12), 1238-1246. doi:10.1038/ni1007

Travnickova, J., Tran Chau, V., Julien, E., Mateos-Langerak, J., Gonzalez, C., Lelièvre, E., . . . Kissa, K. (2015). Primitive macrophages control HSPC mobilization and definitive haematopoiesis. *Nature Communications, 6*, 6227. doi:10.1038/ncomms7227 https://www.nature.com/articles/ncomms7227#supplementary-information

Tulotta, C., Stefanescu, C., Beletkaia, E., Bussmann, J., Tarbashevich, K., Schmidt, T., & Snaar-Jagalska, B. E. (2016). Inhibition of signaling between human CXCR4 and zebrafish ligands by the small molecule IT1t impairs the formation of triple-negative breast cancer early metastases in a zebrafish xenograft model. *9*(2), 141-153. doi:10.1242/dmm.023275 %J Disease Models & Mechanisms

Valent, P., Akin, C., Escribano, L., Födinger, M., Hartmann, K., Brockow, K., . . . Metcalfe, D. D. (2007). Standards and standardization in mastocytosis: Consensus Statements on Diagnostics, Treatment Recommendations and Response Criteria. *European Journal of Clinical Investigation, 37*(6), 435-453. doi:10.1111/j.1365-2362.2007.01807.x

Veinotte, C. J., Dellaire, G., & Berman, J. N. (2014). Hooking the big one: the potential of zebrafish xenotransplantation to reform cancer drug screening in the genomic era. *Disease Models & Mechanisms, 7*(7), 745-754. doi:10.1242/dmm.015784

Vemula, S., Shi, J., Mali, R. S., Ma, P., Liu, Y., Hanneman, P., . . . Kapur, R. (2012). ROCK1 functions as a critical regulator of stress erythropoiesis and survival by regulating p53. *Blood, 120*(14), 2868-2878.

Vlachos, A., Rosenberg, P. S., Atsidaftos, E., Alter, B. P., & Lipton, J. M. (2012). Incidence of neoplasia in Diamond Blackfan anemia: a report from the Diamond Blackfan Anemia Registry. *Blood, 119*(16), 3815-3819. doi:10.1182/blood-2011-08-375972

Vogeli, K. M., Jin, S.-W., Martin, G. R., & Stainier, D. Y. R. (2006). A common progenitor for haematopoietic and endothelial lineages in the zebrafish gastrula. *Nature, 443*(7109), 337-339. doi:10.1038/nature05045

Voskoglou-Nomikos, T., Pater, J. L., & Seymour, L. (2003). Clinical Predictive Value of the in Vitro Cell Line, Human Xenograft, and Mouse Allograft Preclinical Cancer Models. *Clinical Cancer Research, 9*(11), 4227-4239. Retrieved from http://clincancerres.aacrjournals.org/content/clincanres/9/11/4227.full.pdf

Voskoglou-Nomikos, T., Pater, J. L., & Seymour, L. (2003). Clinical predictive value of the in vitro cell line, human xenograft, and mouse allograft preclinical cancer models. *Clinical Cancer Research, 9*(11), 4227-4239.

Wang, S. A., Hutchinson, L., Tang, G., Chen, S. S., Miron, P. M., Huh, Y. O., . . . Medeiros, L. J. (2013). Systemic mastocytosis with associated clonal hematological non-mast cell lineage disease: Clinical significance and comparison of chomosomal abnormalities in SM and AHNMD components. *American journal of hematology, 88*(3), 219-224.

Wang, Y., Yan, S., Yang, B., Wang, Y., Zhou, H., Lian, Q., & Sun, B. (2015). TRIM35 negatively regulates TLR7- and TLR9-mediated type I interferon production by targeting IRF7. *FEBS Letters, 589*(12), 1322-1330. doi:https://doi.org/10.1016/j.febslet.2015.04.019

Warga, R. M., Kane, D. A., & Ho, R. K. (2009). Fate Mapping Embryonic Blood in Zebrafish: Multi- and Unipotential Lineages Are Segregated at Gastrulation. *Developmental Cell, 16*(5), 744-755. doi:10.1016/j.devcel.2009.04.007

Wechsler, J., Greene, M., McDevitt, M. A., Anastasi, J., Karp, J. E., Le Beau, M. M., & Crispino, J. D. (2002). Acquired mutations in GATA1 in the megakaryoblastic leukemia of Down syndrome. *Nature genetics, 32*(1), 148.

White, R. M., Sessa, A., Burke, C., Bowman, T., LeBlanc, J., Ceol, C., . . . Zon, L. I. (2008). Transparent Adult Zebrafish as a Tool for In Vivo Transplantation Analysis. *Cell Stem Cell, 2*(2), 183-189. doi:10.1016/j.stem.2007.11.002

Willinger, T., Rongvaux, A., Takizawa, H., Yancopoulos, G. D., Valenzuela, D. M., Murphy, A. J., . . . Manz, M. G. (2011). Human IL-3/GM-CSF knock-in mice support human alveolar macrophage development and human immune responses in the lung. *Proceedings of the National Academy of Sciences, 108*(6), 2390-2395.

Wong, W. H., Tong, R. S., Young, A. L., & Druley, T. E. (2018). Rare Event Detection Using Error-corrected DNA and RNA Sequencing. *JoVE*(138), e57509. doi:doi:10.3791/57509

Wu, A. M., Till, J. E., Siminovitch, L., & McCulloch, E. A. (1968). Cytological evidence for a relationship between normal hematopoietic colony-forming cells and cells of the lymphoid system. *Journal of Experimental Medicine, 127*(3), 455-464.

Wu, D., Hu, D., Chen, H., Shi, G., Fetahu, I. S., Wu, F., . . . Shi, Y. G. (2018). Glucose-regulated phosphorylation of TET2 by AMPK reveals a pathway linking diabetes to cancer. *Nature, 559*(7715), 637-641. doi:10.1038/s41586-018-0350-5

Wu, H., & Zhang, Y. (2011). Mechanisms and functions of Tet protein-mediated 5-methylcytosine oxidation. *Genes & Development, 25*(23), 2436-2452. doi:10.1101/gad.179184.111

Wunderlich, M., Chou, F., Link, K. A., Mizukawa, B., Perry, R., Carroll, M., & Mulloy, J. (2010). AML xenograft efficiency is significantly improved in NOD/SCID-IL2RG mice constitutively expressing human SCF, GM-CSF and IL-3. *Leukemia, 24*(10), 1785.

Wunderlich, M., Chou, F.-S., Sexton, C., Presicce, P., Chougnet, C. A., Aliberti, J., & Mulloy, J. C. (2018). Improved multilineage human hematopoietic reconstitution and function in NSGS mice. *PLOS ONE, 13*(12), e0209034. doi:10.1371/journal.pone.0209034

Wunderlich, M., Chou, F. S., Link, K. A., Mizukawa, B., Perry, R. L., Carroll, M., & Mulloy, J. C. (2010). AML xenograft efficiency is significantly improved in NOD/SCID-IL2RG mice constitutively expressing human SCF, GM-CSF and IL-3. *Leukemia, 24*, 1785. doi:10.1038/leu.2010.158

Xiang, Z., Kreisel, F., Cain, J., Colson, A., & Tomasson, M. H. (2007). Neoplasia driven by mutant c-KIT is mediated by intracellular, not plasma membrane, receptor signaling. *Molecular and cellular biology, 27*(1), 267-282.

Xin, M., Minghui, C., Bo, X., Bing, Y., Suryadeep, S., & Bo, Z. (2019). EZH2 Confers Sensitivity of Breast Cancer Cells to Taxol by Attenuating p21 Expression Epigenetically. *DNA and Cell Biology, 38*(7), 651-659. doi:10.1089/dna.2019.4699

Xu, H., Xiao, T., Chen, C.-H., Li, W., Meyer, C. A., Wu, Q., . . . Liu, J. S. (2015). Sequence determinants of improved CRISPR sgRNA design. *J Genome research, 25*(8), 1147-1157.

Xu, L., Li, Y., Sun, H., Li, D., & Hou, T. (2013). Structural basis of the interactions between CXCR4 and CXCL12/SDF-1 revealed by theoretical approaches. *Molecular BioSystems, 9*(8), 2107-2117. doi:10.1039/C3MB70120D

Yan, C., Brunson, D. C., Tang, Q., Do, D., Iftimia, N. A., Moore, J. C., . . . Langenau, D. M. (2019). Visualizing Engrafted Human Cancer and Therapy Responses in Immunodeficient Zebrafish. *Cell, 177*(7), 1903-1914.e1914. doi:https://doi.org/10.1016/j.cell.2019.04.004

Young, A. L., Challen, G. A., Birmann, B. M., & Druley, T. E. (2016). Clonal haematopoiesis harbouring AML-associated mutations is ubiquitous in healthy adults. *Nature Communications, 7*, 12484. doi:10.1038/ncomms12484
https://www.nature.com/articles/ncomms12484#supplementary-information

Young, K., Loberg, M., Eudy, E., Bell, R., & Trowbridge, J. J. (2018). The Middle-Aged Bone Marrow Microenvironment Drives Hematopoietic Stem Cell Aging through Altered Production of Insulin-like Growth Factor-1 (IGF1). *Blood, 132*(Suppl 1), 5091-5091. doi:10.1182/blood-2018-99-111055

Yuzawa, S., Opatowsky, Y., Zhang, Z., Mandiyan, V., Lax, I., & Schlessinger, J. (2007). Structural Basis for Activation of the Receptor Tyrosine Kinase KIT by Stem Cell Factor. *Cell, 130*(2), 323-334. doi:10.1016/j.cell.2007.05.055

Zambetti, Noemi A., Ping, Z., Chen, S., Kenswil, Keane J. G., Mylona, Maria A., Sanders, Mathijs A., . . . Raaijmakers, Marc H. G. P. (2016). Mesenchymal Inflammation Drives Genotoxic Stress in Hematopoietic Stem Cells and Predicts Disease Evolution in Human Pre-leukemia. *Cell stem cell, 19*(5), 613-627. doi:https://doi.org/10.1016/j.stem.2016.08.021

Zhang, Y., Dépond, M., He, L., Foudi, A., Kwarteng, E. O., Lauret, E., . . . Wittner, M. (2016). CXCR4/CXCL12 axis counteracts hematopoietic stem cell exhaustion through selective protection against oxidative stress. *Scientific Reports, 6*, 37827. doi:10.1038/srep37827 https://www.nature.com/articles/srep37827#supplementary-information

Zhang, Y., Liu, T., Meyer, C. A., Eeckhoute, J., Johnson, D. S., Bernstein, B. E., . . . Liu, X. S. (2008). Model-based Analysis of ChIP-Seq (MACS). *Genome Biology, 9*(9), R137. doi:10.1186/gb-2008-9-9-r137

Zhao, J. L., & Baltimore, D. (2015). Regulation of stress-induced hematopoiesis. *Current opinion in hematology, 22*(4), 286.

Zhao, L., Melenhorst, J. J., Alemu, L., Kirby, M., Anderson, S., Kench, M., . . . Gilliland, D. G. (2012). KIT with D816 mutations cooperates with CBFB-MYH11 for leukemogenesis in mice. *Blood, 119*(6), 1511-1521.

Zhu, L. J., Gazin, C., Lawson, N. D., Pagès, H., Lin, S. M., Lapointe, D. S., & Green, M. R. (2010). ChIPpeakAnno: a Bioconductor package to annotate ChIP-seq and ChIP-chip data. *BMC bioinformatics, 11*(1), 237.

Zou, Y.-R., Kottmann, A. H., Kuroda, M., Taniuchi, I., & Littman, D. R. (1998). Function of the chemokine receptor CXCR4 in haematopoiesis and in cerebellar development. *Nature, 393*, 595. doi:10.1038/31269

Appendix – Copy right permission

License – Figure 1A

ELSEVIER LICENSE
TERMS AND CONDITIONS
Dec 12, 2019

This Agreement between Mr. Vinothkumar Rajan ("You") and Elsevier ("Elsevier") consists of your license details and the terms and conditions provided by Elsevier and Copyright Clearance Center.

License Number	4671451144778
License date	Sep 17, 2019
Licensed Content Publisher	Elsevier
Licensed Content Publication	Cell
Licensed Content Title	Hematopoiesis: An Evolving Paradigm for Stem Cell Biology
Licensed Content Author	Stuart H. Orkin,Leonard I. Zon
Licensed Content Date	Feb 22, 2008
Licensed Content Volume	132
Licensed Content Issue	4
Licensed Content Pages	14
Start Page	631
End Page	644
Type of Use	reuse in a thesis/dissertation
Portion	figures/tables/illustrations
Number of figures/tables/illustrations	1
Format	electronic
Are you the author of this Elsevier article?	No
Will you be translating?	No
Original figure numbers	2A
Requestor Location	Mr. Vinothkumar Rajan 1348 Summer St LSRI Halifax, NS B3H4R2

	Canada Attn: Mr. Vinothkumar Rajan
Publisher Tax ID	GB 494 6272 12
Total	0.00 CAD

Terms and Conditions

INTRODUCTION

1. The publisher for this copyrighted material is Elsevier. By clicking "accept" in connection with completing this licensing transaction, you agree that the following terms and conditions apply to this transaction (along with the Billing and Payment terms and conditions established by Copyright Clearance Center, Inc. ("CCC"), at the time that you opened your Rightslink account and that are available at any time at http://myaccount.copyright.com).

GENERAL TERMS

2. Elsevier hereby grants you permission to reproduce the aforementioned material subject to the terms and conditions indicated.

3. Acknowledgement: If any part of the material to be used (for example, figures) has appeared in our publication with credit or acknowledgement to another source, permission must also be sought from that source. If such permission is not obtained then that material may not be included in your publication/copies. Suitable acknowledgement to the source must be made, either as a footnote or in a reference list at the end of your publication, as follows:

"Reprinted from Publication title, Vol /edition number, Author(s), Title of article / title of chapter, Pages No., Copyright (Year), with permission from Elsevier [OR APPLICABLE SOCIETY COPYRIGHT OWNER]." Also Lancet special credit - "Reprinted from The Lancet, Vol. number, Author(s), Title of article, Pages No., Copyright (Year), with permission from Elsevier."

4. Reproduction of this material is confined to the purpose and/or media for which permission is hereby given.

5. Altering/Modifying Material: Not Permitted. However figures and illustrations may be altered/adapted minimally to serve your work. Any other abbreviations, additions, deletions and/or any other alterations shall be made only with prior written authorization of Elsevier Ltd. (Please contact Elsevier at permissions@elsevier.com). No modifications can be made to any Lancet figures/tables and they must be reproduced in full.

6. If the permission fee for the requested use of our material is waived in this instance, please be advised that your future requests for Elsevier materials may attract a fee.

7. Reservation of Rights: Publisher reserves all rights not specifically granted in the combination of (i) the license details provided by you and accepted in the course of this licensing transaction, (ii) these terms and conditions and (iii) CCC's Billing and Payment terms and conditions.

8. License Contingent Upon Payment: While you may exercise the rights licensed immediately upon issuance of the license at the end of the licensing process for the transaction, provided that you have disclosed complete and accurate details of your proposed use, no license is finally effective unless and until full payment is received from you (either by publisher or by CCC) as provided in CCC's Billing and Payment terms and conditions. If full payment is not received on a timely basis, then any license preliminarily

granted shall be deemed automatically revoked and shall be void as if never granted. Further, in the event that you breach any of these terms and conditions or any of CCC's Billing and Payment terms and conditions, the license is automatically revoked and shall be void as if never granted. Use of materials as described in a revoked license, as well as any use of the materials beyond the scope of an unrevoked license, may constitute copyright infringement and publisher reserves the right to take any and all action to protect its copyright in the materials.

9. Warranties: Publisher makes no representations or warranties with respect to the licensed material.

10. Indemnity: You hereby indemnify and agree to hold harmless publisher and CCC, and their respective officers, directors, employees and agents, from and against any and all claims arising out of your use of the licensed material other than as specifically authorized pursuant to this license.

11. No Transfer of License: This license is personal to you and may not be sublicensed, assigned, or transferred by you to any other person without publisher's written permission.

12. No Amendment Except in Writing: This license may not be amended except in a writing signed by both parties (or, in the case of publisher, by CCC on publisher's behalf).

13. Objection to Contrary Terms: Publisher hereby objects to any terms contained in any purchase order, acknowledgment, check endorsement or other writing prepared by you, which terms are inconsistent with these terms and conditions or CCC's Billing and Payment terms and conditions. These terms and conditions, together with CCC's Billing and Payment terms and conditions (which are incorporated herein), comprise the entire agreement between you and publisher (and CCC) concerning this licensing transaction. In the event of any conflict between your obligations established by these terms and conditions and those established by CCC's Billing and Payment terms and conditions, these terms and conditions shall control.

14. Revocation: Elsevier or Copyright Clearance Center may deny the permissions described in this License at their sole discretion, for any reason or no reason, with a full refund payable to you. Notice of such denial will be made using the contact information provided by you. Failure to receive such notice will not alter or invalidate the denial. In no event will Elsevier or Copyright Clearance Center be responsible or liable for any costs, expenses or damage incurred by you as a result of a denial of your permission request, other than a refund of the amount(s) paid by you to Elsevier and/or Copyright Clearance Center for denied permissions.

LIMITED LICENSE

The following terms and conditions apply only to specific license types:

15. **Translation**: This permission is granted for non-exclusive world **English** rights only unless your license was granted for translation rights. If you licensed translation rights you may only translate this content into the languages you requested. A professional translator must perform all translations and reproduce the content word for word preserving the integrity of the article.

16. **Posting licensed content on any Website**: The following terms and conditions apply as follows: Licensing material from an Elsevier journal: All content posted to the web site must maintain the copyright information line on the bottom of each image; A hyper-text must be included to the Homepage of the journal from which you are licensing at http://www.sciencedirect.com/science/journal/xxxxx or the Elsevier homepage for

books at http://www.elsevier.com; Central Storage: This license does not include permission for a scanned version of the material to be stored in a central repository such as that provided by Heron/XanEdu.
Licensing material from an Elsevier book: A hyper-text link must be included to the Elsevier homepage at http://www.elsevier.com . All content posted to the web site must maintain the copyright information line on the bottom of each image.

Posting licensed content on Electronic reserve: In addition to the above the following clauses are applicable: The web site must be password-protected and made available only to bona fide students registered on a relevant course. This permission is granted for 1 year only. You may obtain a new license for future website posting.
17. **For journal authors:** the following clauses are applicable in addition to the above:
Preprints:
A preprint is an author's own write-up of research results and analysis, it has not been peer-reviewed, nor has it had any other value added to it by a publisher (such as formatting, copyright, technical enhancement etc.).
Authors can share their preprints anywhere at any time. Preprints should not be added to or enhanced in any way in order to appear more like, or to substitute for, the final versions of articles however authors can update their preprints on arXiv or RePEc with their Accepted Author Manuscript (see below).
If accepted for publication, we encourage authors to link from the preprint to their formal publication via its DOI. Millions of researchers have access to the formal publications on ScienceDirect, and so links will help users to find, access, cite and use the best available version. Please note that Cell Press, The Lancet and some society-owned have different preprint policies. Information on these policies is available on the journal homepage.
Accepted Author Manuscripts: An accepted author manuscript is the manuscript of an article that has been accepted for publication and which typically includes author-incorporated changes suggested during submission, peer review and editor-author communications.
Authors can share their accepted author manuscript:

- immediately
    - via their non-commercial person homepage or blog
    - by updating a preprint in arXiv or RePEc with the accepted manuscript
    - via their research institute or institutional repository for internal institutional uses or as part of an invitation-only research collaboration work-group
    - directly by providing copies to their students or to research collaborators for their personal use
    - for private scholarly sharing as part of an invitation-only work group on commercial sites with which Elsevier has an agreement
- After the embargo period
    - via non-commercial hosting platforms such as their institutional repository
    - via commercial sites with which Elsevier has an agreement

In all cases accepted manuscripts should:

- link to the formal publication via its DOI
- bear a CC-BY-NC-ND license - this is easy to do
- if aggregated with other manuscripts, for example in a repository or other site, be shared in alignment with our hosting policy not be added to or enhanced in any way to appear more like, or to substitute for, the published journal article.

Published journal article (JPA): A published journal article (PJA) is the definitive final record of published research that appears or will appear in the journal and embodies all value-adding publishing activities including peer review co-ordination, copy-editing, formatting, (if relevant) pagination and online enrichment.
Policies for sharing publishing journal articles differ for subscription and gold open access articles:
Subscription Articles: If you are an author, please share a link to your article rather than the full-text. Millions of researchers have access to the formal publications on ScienceDirect, and so links will help your users to find, access, cite, and use the best available version.
Theses and dissertations which contain embedded PJAs as part of the formal submission can be posted publicly by the awarding institution with DOI links back to the formal publications on ScienceDirect.
If you are affiliated with a library that subscribes to ScienceDirect you have additional private sharing rights for others' research accessed under that agreement. This includes use for classroom teaching and internal training at the institution (including use in course packs and courseware programs), and inclusion of the article for grant funding purposes.
Gold Open Access Articles: May be shared according to the author-selected end-user license and should contain a CrossMark logo, the end user license, and a DOI link to the formal publication on ScienceDirect.
Please refer to Elsevier's posting policy for further information.
18. **For book authors** the following clauses are applicable in addition to the above: Authors are permitted to place a brief summary of their work online only. You are not allowed to download and post the published electronic version of your chapter, nor may you scan the printed edition to create an electronic version. **Posting to a repository:** Authors are permitted to post a summary of their chapter only in their institution's repository.
19. **Thesis/Dissertation**: If your license is for use in a thesis/dissertation your thesis may be submitted to your institution in either print or electronic form. Should your thesis be published commercially, please reapply for permission. These requirements include permission for the Library and Archives of Canada to supply single copies, on demand, of the complete thesis and include permission for Proquest/UMI to supply single copies, on demand, of the complete thesis. Should your thesis be published commercially, please reapply for permission. Theses and dissertations which contain embedded PJAs as part of the formal submission can be posted publicly by the awarding institution with DOI links back to the formal publications on ScienceDirect.

Elsevier Open Access Terms and Conditions

20. **Other Conditions**:

v1.9

Questions? customercare@copyright.com or +1-855-239-3415 (toll free in the US) or +1-978-646-2777.

Appendix II

Dear Vino,

Thank you for your recent Springer Nature permissions enquiry.

This work is licensed under the Creative Commons Attribution 4.0 International License, which permits unrestricted use, distribution, modification, and reproduction in any medium, provided you:

1) give appropriate acknowledgment to the original author(s) including the publication source,
2) provide a link to the Creative Commons license, and indicate if changes were made.

You are not required to obtain permission to reuse this article, but you must follow the above two requirements.

Images or other third party material included in the article are encompassed under the Creative Commons license, unless indicated otherwise in the credit line. If the material is not included under the Creative Commons license, users will need to obtain permission from the license holder to reproduce the material.

To view a copy of the Creative Commons license, please visit http://creativecommons.org/licenses/by/4.0/

If you have any questions or concerns, please feel free to contact me directly.

Kind regards,

Paloma Hammond
Rights Assistant

SpringerNature
The Campus, 4 Crinan Street, London N1 9XW, United Kingdom

E paloma.hammond@springernature.com

https://www.macmillanihe.com/
http://www.nature.com
http://www.springer.com
https://www.palgrave.com/gp/